INFORMATION TO USERS

This manuscript has been reproduced from the microfilm master. UMI films the text directly from the original or copy submitted. Thus, some thesis and dissertation copies are in typewriter face, while others may be from any type of computer printer.

The quality of this reproduction is dependent upon the quality of the copy submitted. Broken or indistinct print, colored or poor quality illustrations and photographs, print bleedthrough, substandard margins, and improper alignment can adversely affect reproduction.

In the unlikely event that the author did not send UMI a complete manuscript and there are missing pages, these will be noted. Also, if unauthorized copyright material had to be removed, a note will indicate the deletion.

Oversize materials (e.g., maps, drawings, charts) are reproduced by sectioning the original, beginning at the upper left-hand corner and continuing from left to right in equal sections with small overlaps.

Photographs included in the original manuscript have been reproduced xerographically in this copy. Higher quality 6" x 9" black and white photographic prints are available for any photographs or illustrations appearing in this copy for an additional charge. Contact UMI directly to order.

Bell & Howell Information and Learning
300 North Zeeb Road, Ann Arbor, MI 48106-1346 USA
800-521-0600

Université d'Ottawa · University of Ottawa

DYNAMIC ANALYSIS OF BRIDGES USING THE FINITE STRIP METHOD

By

Abdulkarim Hassan Ali

A Ph. D. Thesis

submitted to the School of Graduate Studies and Research
in partial fulfilment of the requirements for the
Doctor of Philosophy
in Civil Engineering Degree*

University of Ottawa
Ottawa, Ontario, Canada
January 1999

* The Doctor of Philosophy of Civil Engineering Program
is a joint program with Carleton University
administered by the Ottawa-Carleton
Institute in Civil Engineering

ACKNOWLEDGMENTS

I would like to express my sincere gratitude to my supervisor Dr. M. S. Cheung for his constructive guidance and support throughout the course of this study.

I wish also to express sincere appreciation to Dr. W. Li. for his valuable time and advice in discussing various aspects of this thesis.

Special thanks are also extended to my advisory committee, Dr. D. T. Lau, Dr. M. Saatcioglu, Dr. S. F. Ng and Dr. Tanaka for their suggestions regarding the content of this thesis during presentation of my Thesis Proposal.

I will always be grateful to my wife for her support during my Ph.D. studies and to my wise sister, Fadumo, for her constant inspiration throughout my educational years.

ABSTRACT

The dynamic analysis of highway bridges is very complex because of the interaction between the moving vehicle load and the bridge response. Analytical methods such as beam theory and orthotropic plate theory are applicable only to simple structures and highly simplified moving vehicle load models. The beam theory is applicable only to long and narrow bridges since it neglects the effect of transverse flexibility of the bridge. The orthotropic plate theory is only applicable to slab bridges under simple vehicle load models as complex vehicle models render the differential equation of equilibrium difficult or impossible to solve. The finite element method is a very powerful and versatile technique which can be applied to deal with any specific configuration of bridge structure, supports and vehicle load models. However, the efficiency of the method needs to be improved because the finite element solutions usually require too much computer time, too large core storage and too much data input. In addition to these deficiencies, in order to simulate the local of the moving concentrated wheel loads the finite element mesh should be refined in both directions.

The finite strip method has already proven to be the most efficient numerical technique for the static analysis of bridges. In fact the method is even more efficient for dynamic analysis of bridges. The structure can be divided into a number of finite strips. In each strip the displacement components at any point are expressed in terms of the displacement parameters of

nodal lines by means of simple polynomials in the transverse direction and a continuously differentiable smooth series in the longitudinal direction. Thus, the number of dimensions of the analysis is reduced by one. The minimum number of degrees of freedom along a nodal line in the finite strip method is equal to twice times the number of terms used in the series and this is normally much less than that for finite element method, which requires a minimum of three times the number of nodes along the same line. Hence the size and the bandwidth of the matrices are greatly reduced, and consequently it can be handled by personal computers and solved in much shorter time.

In this study the finite strip method is applied to dynamic analysis of simply supported single span slab bridges, slab-on girder bridges, box girder bridges and multi-span bridges by using various vehicle load models. Harmonic analysis of beams is covered in Chapter Two as an introduction for the finite strip method. A FORTRAN computer program capable of analyzing all the topics covered in this thesis is also developed.

TABLE OF CONTENTS

LIST OF MAIN FIGURES

LIST OF TABLES

Chapter 1

INTRODUCTION

1.1 General

In the past three decades various types of highway bridges have been built in North America as well as in many parts of the world due to the rapid development of highways networks. These modern bridges have usually a large span-to-depth ratio and are subject to the passage of faster and heavier vehicles. The interaction between the bridge and the moving vehicle affects the design, because of the increase in deflections and stresses induced in the bridge compared with those produced under static loading. In addition to this impact effect, the vibrations induced by the dynamic interaction may have psychological and physiological effects on pedestrians using the bridge when human tolerance is exceeded. Therefore, a full dynamic analysis of bridges is indispensable for a satisfactory design. The interaction between the bridge and the vehicle and

the increasing complexity of the geometry of bridges makes the dynamic analysis of bridges very difficult and complex. Therefore, an efficient technique of analysis is indispensable.

Analytical methods such as beam theory and orthotropic plate theory are only applicable to highly simplified structures and vehicle models. The finite element method which has been developed in late 1960's is a very powerful and versatile technique for analysis of bridges. The basic concept of the finite element is the discretization of the domain of the continuum into usually triangular, rectangular, or quadrilateral elements of finite size. The displacement or stress field within each element is expressed in terms of a set of unknown nodal parameters. The minimization of the global potential energy yields either a set of linear equations or nonlinear equations due to either material or geometric non-linearity and the vehicle model used. The method can be applied to deal with any specific configuration of bridge structures and supports. It is suitable for analysis involving all types of static and dynamic loads and all kinds of elastic and inelastic deformation. However the efficiency of the method needs to be improved because the finite element usually requires significant storage capacity, tedious and lengthy input data files. Moreover, bridges are subjected to moving wheel loads, the accuracy of numerical results tends to decrease because of element discretization and the mesh needs to be refined in order to simulate the local effects of the wheel loads. An immediate consequence of this is a change of input data, which becomes a serious drawback for practical applications. The distribution of wheel loads into two directions also reduces the accuracy of the results obtained from finite element methods.

The finite strip method can be considered as a special form of the finite element procedure using the displacement approach. In finite strip method, the domain of the bridge structure is divided

into a number of parallel strips instead of finite elements for its response analysis. In each strip, the displacement components at any point are expressed in terms of the displacement parameters of the nodal lines by means of a series of orthogonal functions in the longitudinal direction, y, and simple polynomials in the transverse direction, x. Thus, the number of dimensions of the analysis is reduced by one. For static analysis of bridge structures, the finite strip method has proven to be the most efficient numerical method. The minimum number of degrees of freedom along a nodal line in the finite strip method is equal to twice (one deflection and one rotation) times the number of terms used in the series and this is normally much less than that for finite element method, which requires a minimum of three times (one deflection and two rotations) the number of nodes along the same line. Hence the size and the bandwidth of the matrices are greatly reduced, and consequently it can be handled by personal computers and solved in much shorter time The method is even more efficient for the case of simply supported strip where a decoupling of the terms of the series occurs and thus reduces the size and the bandwidth of the matrices even more drastically. The wheel load can be simulated by either uniformly distributed load (patch load) acting on an area equal to the tire foot print or by a point load which acts on a nodal line.

In summary the finite strip method has the following advantages over the finite element mrthod:

- easy basic concept that involves no complicated mathematics.
- no need for change of input data.
- less and ease of data input
- reduction in the number of unknowns in the problem.
- elimination of one and two rotational degrees of freedom for plates and shells respectively.
- satisfaction of C_1-continuity for plate bending problem.

- rapid convergence
- ease of implementation
- less computer code and easy to program.

1.2 Development of Finite Strip Method

The finite strip method was first published by Y. K. Cheung [1] for static analysis of simply supported bridge deck structures. The finite strip method for rectangular slab-type bridges was also developed independently by Powell and Ogden [2]. The name "finite strip" was also coined by Cheung in his first paper about the method. Since then, the method has been extensively used for the static analysis, and to some extent , the vibration analysis of various types of bridges. Despite its efficiency, the method has not found its use in dynamic analysis of bridges. As far as my knowledge goes, there exists only one paper in the literature on dynamic analysis of bridges using the finite strip method which was published by J. W. Smith [3] .

Research in bridge analysis carried out during the last two decades includes the following:

- rectangular slabs with general end boundary conditions other than simple supports, [5] in 1968.
- continuous slab bridges, flexibility approach, [8] in 1970.
- slab-type bridges with intermediate column supports using flexibility approach, [7] in 1970.
- simply supported box-girder bridges, [4] in 1971.
- circularly curved slab bridges, [6] in 1971.
- frequency analysis of simple and continuous rectangular slabs, [9] in 1971.

- free vibration analysis, [10] in 1971.
- skewed slab bridges, [11] in 1972.
- dynamic response of slab bridges to moving loads, [3] in 1973.
- continuous box girder bridges with transverse diaphragms, flexibility approach, [12] in 1975.
- continuous slab and box girder bridges with transverse diaphragms, stiffness approach, [13] in 1978.
- Analysis of haunched, continuous bridges, [14] in 1988.
- nonlinear analysis of cable-stayed bridges, [15] in 1988.
- analysis of continuous haunched box girder bridges, [16] in 1989.

Other forms of finite strip method such as the spline finite strip and the compound finite strip, have also been developed. For structures that have internal supports such as bridges supported by multiple piers, the ordinary finite strip method is used in conjunction with the flexibility approach. The compound finite strip method takes care of the need of the flexibility approach. In this method, the stiffness contributions of attached beams and columns are directly added to the plate strip stiffness matrix at the element level. Instead of eigenfunctions, the spline finite strip method uses C_2-continuous B_3-spline functions. The spline finite strip method effectively deals with problems involving abruptly changing longitudinal rigidity and problems that have internal discrete supports.

Recently a comprehensive book [17] was written about the finite strip method by M. S. Cheung, W. Li, and S. E. Chidiac. Two other books which summarize the basic theory of the finite strip method were written by Y. K. Cheung [18] and Y. C. Loo and A. Cusens [19].

1.3 Review of Dynamic Analysis of Bridges

The problem of dynamic amplification was recognized in the middle of the 19th century and its study started with railway bridges. Since then major effort has been directed toward the problem of bridge dynamic analysis using various analysis techniques and different bridge and vehicle models.

Following the collapse of some railway bridges in Great Britain, Wills (1849) conducted laboratory tests in cast iron beam models. Stokes (1867) modeled the bridge as a beam of uniform mass and the vehicle as a moving load. Jeffcot (1929) who was the first to include both the mass of the bridge and the vehicle idealized the bridge as a beam. Inglis (1934) represented the bridge as a beam of uniform mass and the vehicle as a moving mass. He solved the problem by making use of the assumption that the deflection shape of the beam at any time was that of the natural mode of the unloaded beam. Hillerborg (1948) treated the bridge as a beam of uniform mass and the vehicle as a moving load. He made the approximation that the dynamic deflection curve of the beam at any time was proportional to its instantaneous static deflection curve due to the moving load (The deflection curve if the load on the beam at that instant were applied statically). Ayre et al. (1949) studied response analysis of a two-span bridge idealized as a two-span beam of uniform mass under a moving load. The characteristic equation of beam bending problem with general end conditions was used in the analysis. Eichmann (1953) found an exact solution for a bridge modeled as a beam of uniform mass traversed by a massless moving load. Tung et al. (1956) and Biggs et al. (1959) considered the bridge as a beam of uniform mass and the vehicle as a sprung mass connected to an unsprung mass. The deflection shape of the beam at any time was assumed to be proportional to the natural mode of the

unloaded beam. Wen (1960) considered the bridge as a beam of uniform mass and the vehicle as a two-axle load composed of a sprung mass connected to two unsprung masses through linearly elastic springs. He made the approximation that the dynamic deflection curve of the beam at any time was proportional to its instantaneous static deflection curve due to the moving load and the weight of the beam itself. Walker and Velestos (1967) presented the results of an analytical investigation of the response analysis of single-span highway bridges to moving loads. The bridge was idealized as a single span but divided into several damped masses. Sundra and Jagadish (1970) employed orthotropic plate theory to find the responses of a beam and slab bridge idealized as an orthotropic plate under sprung mass vehicle model. Yoshida and Weaver (1971) used finite element to solve an isotropic plate under moving load and mass. Smith (1973) used finite strip method for the response analysis of a highway bridge idealized as an orthtropic plate under the passage of a vehicle represented as a sprung mass connected to an unsprung mass. Chauderi (1975) studied the dynamic response of curved bridges using a two-axle, four-wheel vehicle model and he included the centrifugal forces in the formulation of the problem. Raizadeh and Shore (1975) studied dynamic response of curved box-girder bridges using finite element method. The vehicle was modeled as two sets of concentrated forces having components in the radial direction and transverse direction and moving with constant angular velocity on circumferential paths of the bridge. Toshiro and Noboru (1981) developed analytical methods for determining eigenvalues and eigenvectors of beams with arbitrary boundary conditions and used them for forced vibration analysis of beam bridges. Hugh and Ghali (1981) proposed an analytical procedure for slab-on-girder bridges under the passage of multi-axle trucks. Mirza et al (1985) used SAP IV and carried out an analytical study of the dynamic behavior of box girder bridges. Megnounif (1988) carried out dynamic analysis of box girder

bridges subjected to two sets of concentrated moving forces by using ADINA. Khashaf (1991) presented a detailed study of bridge dynamic analysis by using finite element analysis.

1.4 Objective and Scope

The dynamic character of the response of bridges to moving vehicles is presently well established. However, the existing literature used either the finite element method which is not efficient for bridge analysis or highly simplified methods that can only give approximate solution. The finite strip method is an efficient numerical technique that has been extensively applied to static analysis of bridges. In fact the method can be applied to the dynamic analysis of bridges to a high advantage.

The primary objective of this thesis is to extend the application of the finite strip method to dynamic analysis of bridges. The main topics of the research include the application of the finite strip method to the dynamic analysis of single span slab, slab-on-girder, box girder bridges and multi-span slab bridges and the development of a FORTRAN computer program. I have used this computer program to solve all the numerical examples in this thesis.

1.5 Arrangement of the Thesis

Chapter Two presents an analytical procedure in which the bridge is idealized as a one-dimensional beam. The vibration shape of the beam is represented by a superposition of r harmonic functions. The responses of the beam model under various types of vehicle load, such as a moving load, moving mass, a sprung mass and unsprung mass connected together by an elastic spring and a dash-pot, and a two axle two wheel vehicle, are reviewed. Some examples on beams are carried out to compare them with results reported in the literature, then some real bridges are solved.

Chapter Three is devoted to the dynamic response of a simply supported single-span slab bridge using the finite strip method. Frequency analysis is performed first to obtain the lowest frequencies and mode shapes of all the r harmonic functions considered in the study. Then mode superposition is used to obtain the responses such as deflections, moments, and acceleration induced by the moving vehicle. Besides the vehicle load models used in Chapter Two, a two-axle four-wheel vehicle model is also considered. Plate examples are first carried out to compare them with some existing in the literature, then some real bridges are solved.

Chapter Four presents a study of multi-span bridges. The flexibility method is used in conjunction with the finite strip approach. Several examples on two-span beam bridges and slab bridges are carried out.

Chapter Five covers the dynamic analysis of slab-on-girder and box girder bridges. One numerical example is solved in each case.

Chapter Six contains conclusions of the study and recommendations for future work.

Chapter 2

BEAM MODEL OF BRIDGES

2.1 Introduction

In this chapter the dynamic response of a simply supported bridge, modeled as a one dimensional beam and subjected to a moving vehicle load, is presented. Different vehicle load models which include a moving force, a moving mass, a moving sprung mass connected to an unsprung mass through a dash pot and an elastic spring, and a two-axle two-wheel vehicle are considered. The vibration shape of the beam is represented by a superposition of harmonic functions (Figure 2.1). The problem of the dynamic response is formulated as an equivalent static problem through d'Alemberts's principle. In this way the inertia and damping forces are introduced as externally applied forces which have opposite directions to the directions of the acceleration and velocity of the beam respectively.

The principle of minimum potential energy is used to obtain the equations of motion. The minimization of total potential energy yields a set of uncoupled linear equations for the moving

force case and a set of coupled nonlinear equations for the other three cases. Newmark's numerical integration is used to solve the equations of motion.

2.2 Formulations of The Equations of Motion

2.2.1 Displacement Function

The displacement function, w, at any point along the beam may be expressed as a product of a generalized coordinate, $\{q\}$, which is a function of time, and a vibration mode shape, $[S_y]$, which is a function of only the spatial coordinate y.

$$w(y,t) = [S_y]\{q\} \tag{2.1}$$

where

$$[S_y] = \left[\sin\frac{\pi y}{l} \quad \sin\frac{2\pi y}{l} \quad . \quad . \quad . \quad \sin\frac{r\pi y}{l} \right],$$

r stands for the specified number of harmonics to be used for the solution and l is the length of the beam.

2.2.2 Strain-displacement Relation

The strain is obtained by appropriately differentiating the displacement function with respect to the coordinate y. Consider a beam of uniform thickness and take the xy plane as middle plane of the beam before loading. If the cross sections of the beam remain plane after bending and no normal forces are applied to the end sections of the bar, the neutral surface of the beam coincides with the middle surface of the plate and the longitudinal strain is given by

$$\varepsilon_y = -z\frac{\partial^2 w}{\partial y^2} \tag{2.2}$$

where ε_y is the normal strain and z is the distance from the middle xy plane of the beam section. The positive direction of the z axis is downward

2.2.3 Stress-strain Relation

It follows from Hooke's law that

$$\sigma_y = E\varepsilon_y \tag{2.3}$$

Where σ_y is the normal stress and E is the modulus of elasticity.

2.2.4 Minimization of Total Potential Energy

The strain energy of the beam is given by

$$U = \frac{1}{2}\int_v \varepsilon_y \sigma_y dv \tag{2.4}$$

Substitutions of equations (2.2) and (2.3) into equation (2.4) gives the strain energy as

$$U = \frac{1}{2}\{q\}^T [K_b]\{q\} \tag{2.5}$$

where the stiffness matrix $[K_b]$ is given by

$$[K_b] = EI\int_0^l \left[\dot{S}_y\right]^T \left[\dot{S}_y\right] dy \tag{2.6}$$

with I being the moment of inertia of the beam and $\left[\dot{S}_y\right] = \frac{\partial^2}{\partial y^2}[S_y]$.

Due to orthogonality properties of the sine functions, the elements of the stiffness matrix are:

$$k_{mn} = 0 \qquad m \neq n$$

$$k_{mm} = \frac{m^4 \pi^4 EI}{2l^3}$$

The potential energy due to the external distributed loads p can be written as

$$W_E = -\int_0^l pwdy \tag{2.7}$$

Substituting equation (2.1) into equation (2.7) gives

$$W_E = -\{q\}^T \{F\} \tag{2.8}$$

where $\{F\}$ is the load vector due to the external load and is given by the following integral

$$\{F\} = \int_0^l p[S_y]^T dy \tag{2.9}$$

For a concentrated force f, the above integral becomes the following simple expression.

$$\{F\} = f[S_y(y(t))]^T \tag{2.10}$$

where y represents the position of force which is a function of time for the moving force.

The inertia force per unit length of the beam is obtained from Newton's Second Law as follows:

$$p_I = -\rho A \frac{\partial^2 w}{\partial t^2} \tag{2.11}$$

where ρ is the mass per unit volume and A is the area of the cross-section.

The potential energy due to the inertia force p_I can be written as

$$W_I = -\int_0^l p_I w dy \tag{2.12}$$

After some substitutions, the potential energy due to the inertia force becomes

$$W_I = \{q\}^T [M_b] \{\ddot{q}\} \tag{2.13}$$

where the mass matrix $[M_b]$ is given by

$$[M_b] = \rho A \int_0^l [S_y]^T [S_y] dy \tag{2.14}$$

Again because of the orthogonality of the set of sine functions, the elements of the mass matrix are:

$$m_{mn} = 0 \quad m \neq n$$

$$m_{mm} = \frac{\rho A l}{2}$$

The distributed viscous damping force per unit length of the beam is obtained as follows:

$$p_D = -c\frac{\partial w}{\partial t} \tag{2.15}$$

where c is the distributed viscous damping coefficient.

The potential energy due to the damping force p_D can be written as:

$$W_D = -\int_0^l p_D w dx \tag{2.16}$$

After some substitutions, the potential energy due to the damping force becomes

$$W_D = \{q\}^T [C_b] \{\dot{q}\} \tag{2.17}$$

where the damping matrix $[C_b]$ is given by

$$[C_b] = c\int_0^l [S_y]^T [S_y] dy \tag{2.18}$$

The off-diagonal elements of the damping matrix vanish because of the orthogonality of the set of sine functions, and the diagonal elements become

$$c_{mm} = \frac{cl}{2}$$

The total potential energy of the beam, Π, is the sum of strain energy and potential energy. Thus

$$\Pi = U + W_E + W_I + W_D \tag{2.19}$$

According to the principle of minimum potential energy, the equilibrium configuration is defined by the m algebraic equations.

$$\frac{\partial \Pi}{\partial q_m} = 0 \quad \text{for} \quad m = 1, 2, ..., r \tag{2.20}$$

or in a compact form

$$\left\{ \frac{\partial \Pi}{\partial \{q\}} \right\} = \{0\} \tag{2.21}$$

Substituting equation (2.19) into equation (2.21) and carrying out the partial differentiation produces a set of algebraic equations which can be written in the following matrix form:

$$[M_b]\{\ddot{q}\} + [C_b]\{\dot{q}\} + [K_b]\{q\} = \{F\} \tag{2.22}$$

Newmark's average acceleration method is used to solve equation (2.22)

2.3 Response Under a Moving Force Vehicle Model

If the interaction between the vehicle and the bridge is ignored, the vehicle load can be modeled as a moving force (Figure 2.2). For a vehicle crossing the bridge with a constant acceleration, the *y*-coordinate of its contact point is given by

$$y = -s + vt + \frac{1}{2}at^2 \tag{2.23}$$

where

-s is the position of the vehicle at time $t=0$, v is its velocity and a is its acceleration.

If the vehicle travels with a constant velocity, equation (2.23) reduces to:

$$y = -s + vt \tag{2.24}$$

The concentrated force exerted on the bridge by the moving vehicle is given by

$$f = m_v g \tag{2.25}$$

where

m_v is the mass of the vehicle and g is the acceleration due to gravity.

Substitution of the above equation into equation (2.22) yields:

$$[M_b]\{\ddot{q}\} + [C_b]\{\dot{q}\} + [K_b]\{q\} = m_v g[S]^T \tag{2.26}$$

where, for a vehicle crossing the bridge with a constant acceleration

$$[S]^T = \begin{bmatrix} \sin\frac{\pi}{l}(vt + \frac{1}{2}at^2 - s) \\ \sin\frac{2\pi}{l}(vt + \frac{1}{2}at^2 - s) \\ \vdots \\ \sin\frac{r\pi}{l}(vt + \frac{1}{2}at^2 - s) \end{bmatrix} \tag{2.27}$$

and for a vehicle crossing the bridge with a constant velocity

$$[S]^T = \begin{bmatrix} \sin\frac{\pi}{l}(vt - s) \\ \sin\frac{2\pi}{l}(vt - s) \\ \vdots \\ \sin\frac{r\pi}{l}(vt - s) \end{bmatrix} \tag{2.28}$$

Equation (2.26) is solved for the modal coordinates $\{q\}$, then the deflections and accelerations of the bridge are finally calculated from

$$w = [S_y]\{q\} \tag{2.29}$$

and

$$\ddot{w} = [S_y]\{\ddot{q}\} \tag{2.30}$$

Dynamic bending moment is given by

$$M = EI[\dot{S}_y]\{q\} \tag{2.31}$$

2.4 Response under a Moving Mass Vehicle Model

If the interaction between the bridge and the vehicle is considered, the vehicle load can be modeled as a moving mass (Figure 2.3). Unlike moving loads, a moving mass produces several terms in the formulation of equations of motion. The moving mass is treated as a particle. It is assumed that the moving mass is always in contact with the bridge while it transverses the span. In order to determine the effect of the moving mass i.e., the terms contributed to the equations of motion by the moving mass, the lateral acceleration of the point of contact between the bridge and the moving mass is considered.

The time derivatives of the displacement, w, at the contact point between the vehicle and the bridge are given by

$$\dot{w} = [\dot{S}]\{q\} + [S]\{\dot{q}\} \tag{2.32}$$

$$\ddot{w} = \left[\ddot{S}\right]\{q\} + 2\left[\dot{S}\right]\left\{\dot{q}\right\} + [S]\left\{\ddot{q}\right\} \tag{2.33}$$

The force exerted on the bridge by the moving vehicle is given by

$$f = m_v g - m_v \ddot{w} \tag{2.34}$$

where m_v is the mass of the vehicle.

After some substitutions and rearrangements the equation of motion under a moving mass of the bridge-vehicle system becomes

$$\left([M_b] + [M_I]\right)\left\{\ddot{q}\right\} + \left([C_b] + [C_I]\right)\left\{\dot{q}\right\} + \left([K_b] + [K_I]\right)\{q\} = m_v g[S]^T \tag{2.35}$$

where

$$[M_I] = m_v[S]^T[S]$$

$$[C_I] = 2m_v[S]^T\left[\dot{S}\right]$$

$$[K_I] = m_v[S]^T\left[\ddot{S}\right] \tag{2.36}$$

If the bridge is crossed by multiple moving masses, the equation of dynamic equilibrium of the bridge-vehicle system becomes

$$\left([M_b]+\gamma_i\sum_{i=1}^{NV}[M_I]_i\right)\{\ddot{q}\}+\left([C_b]+\gamma_i\sum_{i=1}^{NV}[C_I]_i\right)\{\dot{q}\}+\left([K_b]+\gamma_i\sum_{i=1}^{NV}[K_I]_i\right)\{q\}=\gamma_i\sum_{i=1}^{NV}m_{vi}g[S]_i^T \tag{2.37}$$

where NV is the number of moving masses; the symbol γ_i is introduced to ensure that any mass outside the bridge will not be included in computing the response of the bridge; γ_i =1 for masses on the bridge and γ_i =0 for masses outside of the bridge.

2.5 Response Under a Moving Sprung Mass Vehicle Model

A vehicle model which comprises a sprung mass m_s which is supported by a spring of stiffness k and a viscous damper of a damping coefficient c, and an unsprung mass m_u that remains in contact with the bridge deck is used here (Figure 2.4). This model simulates a better interaction between the vehicle and the bridge than the previous moving mass model.

The equation of motion of the vehicle can be expressed in the form

$$m_s\ddot{\eta}+c(\dot{\bar{\eta}}-[S]\{\dot{q}\}-[\dot{S}]\{q\})+k(\eta-[S]\{q\})=\{0\} \tag{2.38}$$

where η is the absolute deflection of the sprung mass m_s measured from its rest position under gravity.

The force exerted on the bridge by the moving vehicle is given by

$$f = m_v g - m_u \ddot{w} + c(\dot{\eta} - \dot{w}) + k(\eta - w) \tag{2.39}$$

where m_v is the sum of the sprung mass m_s and the unsprung mass m_u.

After some substitutions and rearrangements the equations of equilibrium of the bridge-vehicle system motion become

$$\begin{bmatrix} ([M_b]+[M_I]) & 0 \\ 0 & [M_v] \end{bmatrix} \begin{Bmatrix} \{\ddot{q}\} \\ \{\ddot{\eta}\} \end{Bmatrix} + \begin{bmatrix} ([C_b]+[C_I]) & [C_{VI}] \\ [C_{HI}] & [C_v] \end{bmatrix} \begin{Bmatrix} \{\dot{q}\} \\ \{\dot{\eta}\} \end{Bmatrix} + \begin{bmatrix} ([K_b]+[K_I]) & [K_{VI}] \\ [K_{HI}] & [K_v] \end{bmatrix} \begin{Bmatrix} \{q\} \\ \{\eta\} \end{Bmatrix} = m_v g \begin{Bmatrix} [S]^T \\ \{0\} \end{Bmatrix} \tag{2.40}$$

where

$$[M_v]_{1x1} = m_s \quad [C_v]_{1x1} = c \quad [K_v]_{1x1} = k$$

$$[C_{HI}] = -c[S] \quad [K_{HI}] = -c\left[\dot{S}\right] - k[S]$$

$$[C_{VI}] = -c[S]^T \quad [K_{VI}] = -k[S]^T$$

$$[K_I] = [S]^T \left(m_u \left[\ddot{S}\right] + c\left[\dot{S}\right] + k[S] \right)$$

$$[C_t]=[S]^T\left(2m_u\left[\dot{S}\right]+c[S]\right)$$

$$[M_t]=m_u[S]^T[S] \tag{2.41}$$

2.6 Response Under a Two Axle Two Wheel Vehicle Model

In this section the vehicle body is considered to be a rigid body with a total sprung mass m_s and mass moment of inertia i_{sl}. The suspension system supporting the front and rear axles are represented by springs of stiffness k_f and k_r and viscous dampers with damping coefficients c_f and c_r respectively (Figure 2.5). The masses of the front and rear chassis and axles are represented by m_f and m_r respectively. This vehicle load model has two degrees of freedom d_1 and d_2 which represent bouncing and pitching motion of the vehicle. Referring to Figure 2.5, the displacements at the front and rear axles, η_f and η_r are respectively related to the two degrees of freedom d_1 and d_2 of the centroid of the vehicle body by the following relationship:

$$\eta_f=\begin{bmatrix}1 & a_f\end{bmatrix}\begin{Bmatrix}d_1\\ sd_2\end{Bmatrix} \tag{2.42a}$$

$$\eta_r=\begin{bmatrix}1 & -a_r\end{bmatrix}\begin{Bmatrix}d_1\\ sd_2\end{Bmatrix} \tag{2.42b}$$

where a_f and a_r are defined in Figure 2.5.

The change of length of the front vehicle spring is given by

$$\Delta_f = \eta_f - w_f \tag{2.43a}$$

where w_f is the vertical displacement at the contact point between the front wheel and the bridge. Similarly the change of length of the rear vehicle spring is given by

$$\Delta_r = \eta_r - w_r \tag{2.43b}$$

where w_r is the vertical displacement at contact point between the rear wheel and the bridge. The vertical displacements at the contact points are given by

$$w_f = \sum_{m=1}^{r} q_m \sin\frac{m\pi}{l}(vt - s_f) \tag{2.44a}$$

$$w_r = \sum_{m=1}^{r} q_m \sin\frac{m\pi}{l}(vt - s_r) \tag{2.44b}$$

In matrix form equations (2.44a) and (2.44b) can be written as follows:

$$w_f = [S]_f \{q\} \tag{2.45a}$$

$$w_r = [S]_r \{q\} \tag{2.45b}$$

Substituting equations (2.42a) and (2.45a) into equation (2.43a) and equations (2.42b) and (2.45b) into equation (2.43b), the following expressions are obtained for the change of length of springs.

$$\Delta_f = [1 \quad a_f]\{d\} - [S]_f \{q\} \tag{2.46a}$$

$$\Delta_r = \begin{bmatrix} 1 & -a_r \end{bmatrix} \{d\} - [S]_r \{q\} \tag{2.46b}$$

where

$$\{d\} = \begin{Bmatrix} d_1 \\ sd_2 \end{Bmatrix} \tag{2.47}$$

The time derivatives of Δ_f and Δ_r are given by

$$\dot{\Delta}_f = \begin{bmatrix} 1 & a_f \end{bmatrix} \left\{\dot{d}\right\} - \left[\dot{S}\right]_f \{q\} - [S]_f \left\{\dot{q}\right\} \tag{2.48a}$$

$$\dot{\Delta}_r = \begin{bmatrix} 1 & -a_r \end{bmatrix} \left\{\dot{d}\right\} - \left[\dot{S}\right]_r \{q\} - [S]_r \left\{\dot{q}\right\} \tag{2.48b}$$

The forces F_f and F_r at the front and rear of the vehicle body respectively due to the springs and dampers are given by

$$F_f = k_f \Delta_f + c_f \dot{\Delta}_f \tag{2.49a}$$

$$F_r = k_r \Delta_r + c_r \dot{\Delta}_r \tag{2.49b}$$

As a result of equations (2.46a), (2.46b), (2.48a) and (2.48b), the forces, F_f and F_r are given by

$$F_f = k_f \left(\begin{bmatrix} 1 & a_f \end{bmatrix} \{d\} - [S]_f \{q\} \right) + c_f \left(\begin{bmatrix} 1 & a_f \end{bmatrix} \left\{\dot{d}\right\} - \left[\dot{S}\right]_f \{q\} - [S]_f \left\{\dot{q}\right\} \right) \tag{2.50a}$$

$$F_r = k_r \left(\begin{bmatrix} 1 & -a_r \end{bmatrix} \{d\} - [S]_r \{q\} \right) + c_r \left(\begin{bmatrix} 1 & a_r \end{bmatrix} \left\{\dot{d}\right\} - \left[\dot{S}\right]_r \{q\} - [S]_r \left\{\dot{q}\right\} \right) \tag{2.50b}$$

The equations of dynamic equilibrium of the vehicle body are obtained by using the principle of virtual displacement. The equilibrium of forces in the vertical direction is obtained by giving a virtual displacement δd_1 to the vehicle body. The equation of virtual work then becomes

$$-F_f \delta\eta_f - F_r \delta\eta_r - m_s \ddot{d}_1 \delta d_1 = 0 \tag{2.51}$$

where the virtual displacements $\delta\eta_f$ and $\delta\eta_r$ due to the virtual displacement δd_1 are given by

$$\delta\eta_f = \delta d_1 \tag{2.52a}$$

$$\delta\eta_r = \delta d_1 \tag{2.52b}$$

Substituting the expressions for the forces F_f and F_r from equations (2.50a) and (2.50b) and also the expressions for the virtual displacements $\delta\eta_f$ and $\delta\eta_r$ from equations (2.52a) and (2.52b) into equation (2.51) gives

$$\begin{aligned}
&-\left(k_f\left(d_1 + a_f s d_2 - [S]_f\{q\}\right) + c_f\left(\dot{d}_1 + a_f s \dot{d}_2 - \left[\dot{S}\right]_f\{q\} - [S]_f\left\{\dot{q}\right\}\right)\right)(\delta d_1) \\
&-\left(k_r\left(d_1 - a_r s d_2 - [S]_r\{q\}\right) + c_r\left(\dot{d}_1 - a_r s \dot{d}_2 - \left[\dot{S}\right]_r\{q\} - [S]_r\left\{\dot{q}\right\}\right)\right)(\delta d_1) \\
&-m_s \ddot{d}_1 \delta d_1 = 0
\end{aligned} \tag{2.53}$$

Factoring out minus δd_1 and rearranging of equation (2.53) produces

$$\begin{aligned}
&\left(\left(k_f + k_r\right)d_1 + \left(a_f k_f - a_r k_r\right)s d_2 + \left(c_f + c_r\right)\dot{d}_1 + \left(a_f c_f - a_r c_r\right)s\dot{d}_2 + m_s \ddot{d}_1\right. \\
&\left.-\left(k_f[S]_f + k_r[S]_r + c_f\left[\dot{S}\right]_f + c_r\left[\dot{S}\right]_r\right)\{q\} - \left(c_f[S]_f + c_r[S]_r\right)\left\{\dot{q}\right\}\right)\left(-\delta d_1\right) = 0
\end{aligned} \tag{2.54}$$

The moment equilibrium of forces about a transverse direction through the centroid of the vehicle is obtained by giving a virtual displacement δd_2 to the vehicle body. The equation of virtual work then becomes

$$-F_f \delta\eta_f + F_r(-\delta\eta_r) - i_{s1}\ddot{d}_2\,\delta d_2 = 0 \tag{2.55}$$

where the virtual displacements $\delta\eta_f$ and $\delta\eta_r$ due to the virtual displacement δd_2 are given by

$$\delta\eta_f = a_f s\delta d_2 \tag{2.56a}$$

$$\delta\eta_r = -a_r s\delta d_2 \tag{2.56b}$$

Substituting the expressions for the forces F_f and F_r from equations (2.50a) and (2.50b) and also the expressions for the virtual displacements $\delta\eta_f$ and $\delta\eta_r$ from equations (2.56a) and (2.56b) into equation (2.55) gives

$$\begin{aligned}
&-\left(k_f\left(d_1 + a_f s d_2 - [S]_f\{q\}\right) + c_f\left(\dot{d}_1 + a_f s\dot{d}_2 - \left[\dot{S}\right]_f\{q\} - [S]_f\left\{\dot{q}\right\}\right)\right)\left(a_f s\delta d_2\right) \\
&+\left(k_r\left(d_1 - a_r s d_2 - [S]_r\{q\}\right) + c_r\left(\dot{d}_1 - a_r s\dot{d}_2 - \left[\dot{S}\right]_r\{q\} - [S]_r\left\{\dot{q}\right\}\right)\right)\left(a_r s\delta d_2\right) \\
&-\frac{i_{s1}}{s^2}s\ddot{d}_2\, s\delta d_2 = 0
\end{aligned} \tag{2.57}$$

Factoring out minus $s\delta d_2$ and rearranging of equation (2.57) produces

$$\{(a_f k_f - a_r k_r)d_1 + (a_f{}^2 k_f + a_r{}^2 k_r)sd_2 + (a_f c_f - a_r c_r)\dot{d}_1 + (a_f{}^2 c_f + a_r{}^2 c_r)s\dot{d}_2$$
$$-\left(a_f k_f [S]_f - a_r k_r [S]_r + a_f c_f \left[\dot{S}\right]_f - a_r c_r \left[\dot{S}\right]_r\right)\{q\} \qquad (2.58)$$
$$-\left(a_f c_f [S]_f - a_r c_r [S]_r\right)\left\{\dot{q}\right\} + \frac{i_{s1}}{s^2} s\ddot{d}_2\}(-s\delta d_2) = 0$$

Since the virtual displacements are arbitrary, the terms δd_1 and δd_2 can take on any value, including zero. This means that the multipliers of δd_1 in equation (2.54) and δd_2 in equation (2.58) must each equal zero.

$$(k_f + k_r)d_1 + (a_f k_f - a_r k_r)sd_2 + (c_f + c_r)\dot{d}_1 + (a_f c_f - a_r c_r)s\dot{d}_2$$
$$+m_s \ddot{d}_1 - \left(k_f [S]_f + k_r [S]_r + c_f \left[\dot{S}\right]_f + c_r \left[\dot{S}\right]_r\right)\{q\} - \left(c_f [S]_f + c_r [S]_r\right)\left\{\dot{q}\right\} = 0 \qquad (2.59)$$

and

$$(a_f k_f - a_r k_r)d_1 + (a_f{}^2 k_f + a_r{}^2 k_r)sd_2 + (a_f c_f - a_r c_r)\dot{d}_1 + (a_f{}^2 c_f + a_r{}^2 c_r)s\dot{d}_2 + \frac{i_{s1}}{s^2} s\ddot{d}_2$$
$$-\left(a_f k_f [S]_f - a_r k_r [S]_r + a_f c_f \left[\dot{S}\right]_f - a_r c_r \left[\dot{S}\right]_r\right)\{q\} - \left(a_f c_f [S]_f - a_r c_r [S]_r\right)\left\{\dot{q}\right\} = 0 \qquad (2.60)$$

Equations (2.59) and (2.60) can be expressed in the following matrix form.

$$[M_v]\left\{\ddot{d}\right\} + [C_v]\left\{\dot{d}\right\} + [K_v]\{d\} + [C_{HI}]\left\{\dot{q}\right\} + [K_{HI}]\{q\} = \{0\} \qquad (2.61)$$

where

$$[M_v]=\begin{bmatrix} m_s & 0 \\ 0 & \frac{i_{s1}}{s^2} \end{bmatrix}$$

$$[K_v]=\begin{bmatrix} k_f+k_r & a_f k_f - a_r k_r \\ a_f k_f - a_r k_r & a_f{}^2 k_f + a_r{}^2 k_r \end{bmatrix}$$

$$[C_v]=\begin{bmatrix} c_f+c_r & a_f c_f - a_r c_r \\ a_f c_f - a_r c_r & a_f{}^2 c_f + a_r{}^2 c_r \end{bmatrix}$$

$$[C_{HI}]=\begin{bmatrix} -c_f \\ -a_f c_f \end{bmatrix}[S]_f+\begin{bmatrix} -c_r \\ a_r c_r \end{bmatrix}[S]_r$$

$$[K_{HI}]=\begin{bmatrix} -k_f \\ -a_f k_f \end{bmatrix}[S]_f+\begin{bmatrix} -c_f \\ -a_f c_f \end{bmatrix}[\dot{S}]_f+\begin{bmatrix} -k_r \\ a_r k_r \end{bmatrix}[S]_r+\begin{bmatrix} -c_r \\ a_r c_r \end{bmatrix}[\dot{S}]_r$$

$[M_v]$, $[C_v]$ and $[K_v]$ are respectively, the mass matrix , damping matrix and stiffness matrix of the vehicle. $[C_{HI}]$ and $[K_{HI}]$ are two matrices that couple the motion of the vehicle with that of the bridge.

The forces exerted on the bridge by the moving vehicle at the contact points are given by

$$\begin{aligned} f_f = &\begin{bmatrix} k_f & a_f k_f \end{bmatrix}\{d\}+\begin{bmatrix} c_f & a_f c_f \end{bmatrix}\{\dot{d}\}-\left(k_f[S]_f+c_f[\dot{S}]_f+m_{uf}[\ddot{S}]_f\right)\{q\} \\ &-\left(c_f[S]_f+2m_{uf}[\dot{S}]_f\right)\{\dot{q}\}-\left(m_{uf}[S]_f\right)\{\ddot{q}\}+\left(m_{uf}+a_r m_s\right)g \end{aligned} \qquad (2.62)$$

and

$$f_r = \begin{bmatrix} k_r & -a_r k_r \end{bmatrix}\{d\} + \begin{bmatrix} c_r & -a_r c_r \end{bmatrix}\left\{\dot{d}\right\} - \left(k_r[S]_r + c_r\left[\dot{S}\right]_r + m_{ur}\left[\ddot{S}\right]_r\right)\{q\}$$
$$-\left(c_r[S]_r + 2m_{ur}\left[\dot{S}\right]_r\right)\left\{\dot{q}\right\} - m_{ur}[S]_r\left\{\ddot{q}\right\} + \left(m_{ur} + a_f m_s\right)g \qquad (2.63)$$

The contact forces f_f and f_r act as external forces on the bridge and the equations of equilibrium of the bridge motion become

$$[M_b]\left\{\ddot{q}\right\} + [C_b]\left\{\dot{q}\right\} + [K_b]\{q\} = [S]_f^T f_f + [S]_r^T f_r \qquad (2.64)$$

where $[M_b]$, $[C_b]$ and $[K_b]$ are respectively, the mass, damping, and stiffness matrices of the bridge.

In order to obtain the response of the bridge under the action of the moving vehicle, equations (2.61) and (2.64) are solved simultaneously.

Substituting for the expressions of the forces f_f and f_r from equations (2.62) and (2.63) into equation (2.64) and combining the result with equation (2.61) produces the following equations of equilibrium of the bridge-vehicle system motion.

$$\begin{bmatrix} \left([M_b]+[M_t]\right) & [0] \\ [0] & [M_v] \end{bmatrix}\begin{Bmatrix} \{\ddot{q}\} \\ \{\ddot{d}\} \end{Bmatrix} + \begin{bmatrix} \left([C_b]+[C_t]\right) & [C_{VI}] \\ [C_{HI}] & [C_v] \end{bmatrix}\begin{Bmatrix} \{\dot{q}\} \\ \{\dot{d}\} \end{Bmatrix}$$
$$+\begin{bmatrix} \left([K_b]+[K_t]\right) & [K_{VI}] \\ [K_{HI}] & [K_v] \end{bmatrix}\begin{Bmatrix} \{q\} \\ \{d\} \end{Bmatrix} = \begin{Bmatrix} \{F\} \\ \{0\} \end{Bmatrix} \qquad (2.65)$$

where

$$[M_t] = m_{uf}[S]_f^T[S]_f + m_{ur}[S]_r^T[S]_r$$

$$[C_t] = [S]_f^T\left(c_f[S]_f + 2m_{uf}\left[\dot{S}\right]_f\right) + [S]_r^T\left(c_r[S]_r + 2m_{ur}\left[\dot{S}\right]_r\right)$$

$$[K_t] = [S]_f^T\left(k_f[S]_f + c_f\left[\dot{S}\right]_f + m_{uf}\left[\ddot{S}\right]_f\right) + [S]_r^T\left(k_r[S]_r + c_r\left[\dot{S}\right]_r + m_{ur}\left[\ddot{S}\right]_r\right)$$

$$[K_{VI}] = [S]_f^T\begin{bmatrix}-k_f & -a_f k_f\end{bmatrix} + [S]_r^T\begin{bmatrix}-k_r & a_r k_r\end{bmatrix}$$

$$[C_{VI}] = [S]_f^T\begin{bmatrix}-c_f & -a_f c_f\end{bmatrix} + [S]_r^T\begin{bmatrix}-c_r & a_r c_r\end{bmatrix}$$

$$\{F\} = [S]_f^T\left(m_{uf} + a_r m_s\right) + [S]_r^T\left(m_{ur} + a_f m_s\right)$$

$[C_{HI}]$ and $[K_{HI}]$ are explained in equation (2.61)

To ensure that any wheel load outside the bridge will not be included in computing the response of the bridge, the terms that are associated with that wheel should not be included in the formation of the matrices $[K^*_{VI}]$, $[C^*_{VI}]$, $[K^*_{HI}]$, $[C^*_{HI}]$, $[K_I]$, $[C_I]$ and $[M_I]$ and the vector $\{F\}$.

2.7 Numerical Examples on Beams

In this section, several illustrative examples are carried out to prove the validity of the equations derived in this chapter and the FORTRAN program I have developed. Examples that exist in the literature are chosen in order to compare their response values with the available results.

2.7.1 Moving Force Problem

Figure 2.6 shows a simply supported beam under a moving force. The magnitude of the moving force is one pound and it travels with a constant velocity equal to 4912 in. /sec. Numerical solutions were obtained from the FORTRAN program I have developed as part of this study. The dynamic response of the center of the beam using one, three, five, ten and fifteen harmonic terms are shown in Table 2.1. The results obtained by Khashaf (1992) and Yoshida (1971) using finite element with consistent mass idealization, Filho (1966) using finite element with lumped mass procedure and by Eichmann (1953) using exact solution are also shown in Table 2.1. Figure 2.7 shows the dynamic response of the center of the beam. The ordinate represents the displacement at the center of the beam divided by maximum static deflection, which is the deflection produced by a one pound force placed at the center of the beam, while the abscissa represents the real time divided by the travel time.

TABLE 2.1

Dynamic Magnification Factors of the Beam

in Figure 2.6 Due to a Moving Load

TERMS	W_{dyn}/W_{stat} (This study)	W_{dyn}/W_{stat} (Khashaf)	W_{dyn}/W_{stat} (Filho)	W_{dyn}/W_{stat} (Yoshida)	W_{dyn}/W_{stat} (Eichman)
1	1.710				
3	1.709				
5	1.708	1.706	1.680	1.700	1.707
10	1.708				
15	1.708				

2.7.2 Moving Mass Problem

The same beam model used for the moving-force problem was analyzed again for the moving mass problem using the same geometric and material constants. A mass ratio of 10.36, i.e., the ratio of the mass of the vehicle to the mass of the beam, which is the mass corresponding to one pound weight is used. The physical constants of the beam are as given before. The dynamic response of the center of the beam using one, three, five, ten and fifteen harmonic terms are shown in Table 2.2. The result obtained by Yoshida (1971) using finite element with consistent mass idealization is also shown in Table 2.2. Figure 2.3 shows plot of the dynamic response of the center of the beam for a velocity of 4912 in. / sec which is the same velocity used for the moving-force problem.

TABLE 2.2

Dynamic Magnification Factors of the Beam

in Figure 2.6 Due to a Moving Mass

TERMS	W_{dyn}/W_{stat} (This Study)	W_{dyn}/W_{stat} (Yoshida)
1	6.233	7.748
3	7.565	
5	7.690	
10	7.730	
15	7.724	

2.8 Examples on Beam Bridges

Analysis of four simply supported concrete beam bridges are carried out. The dimensions and parameters of the bridges are given in Table (2.3).

TABLE 2.3

Geometry and Material Properties of Bridges

Bridge Number	Span (m)	Width (m)	Thickness (m)	Mass density (Kg/m^3)
1	10.0	10.0	0.325	2446.5
2	15.0	10.0	0.400	2446.5
3	20.0	10.0	0.525	2446.5
4	25.0	10.0	0.675	2446.5

Single axle and two-axle vehicle models are used. The first vehicle model consists of a single sprung mass attached to an unsprung mass through a linear spring. The second vehicle model is a set of two moving point loads. The third vehicle model consists of a set of two single sprung masses attached to unsprung masses. The fourth vehicle model is a two-axle two-wheel vehicle model which consists of sprung mass and unsprung masses. All the vehicle models have equal

weights and a constant velocity of 100 km/hr is used in all cases. The sprung vehicle models have equivalent spring stiffnesses, sprung and unsprung masses.

Characteristics of the vehicle models

Vehicle Model I

Sprung mass (m_s) = 30189.0 Kg

Unsprung mass (m_u) = 4209.0 Kg

Spring stiffness (k) = 10726325.54 N/m

Vehicle Model II

Front axle weight = 196134.554 N

Rear axle weight = 140965.846 N

Vehicle Model III

Front sprung mass (m_{sf}) =17207.73 Kg

Rear sprung mass (m_{sr}) = 12981.27 Kg

Front unsprung mass (m_{uf}) 2806 Kg

Rear unsprung mass (m_{ur}) =1403 Kg

Front spring stiffness (k_f) =5363162.77 N/m

Rear spring stiffness (k_r) =5363162.77 N/m

Spacing = 6.19 m

Vehicle Model IV (Two-axle four-wheel model)

Sprung mass (m_s) = 30189.0 Kg

Front unsprung mass (m_{uf}) = 2806.0 Kg

Rear unsprung mass (m_{ur}) = 1403.0 Kg

Front axle stiffness (k_f) = 5363162.77 N/m

Rear axle stiffness (k_r) = 5363162.77 N/m

Axle spacing (s)= 6.19 m

Centroidal distance parameters:

$a_f = 0.43$, $a_r = 0.57$

Mass moments of inertia:

$i_{sl} = 263.052$ tone.m^2

Table (2.4) shows the maximum mid-span static deflections of the four bridges listed in Table (2.3) due to a single point load and a set of two point loads . Tables (2.5), (2.6), (2.7) and (2.8) show the maximum mid-span dynamic deflections and their deflection amplification factors.

TABLE 2.4

Static Deflections at Mid-span of Bridges

Bridge Number	W_{static}**(mm)** **(One point load)**	W_{static}**(mm)** **(Two point loads)**
1	9.26	5.39
2	16.77	13.20
3	17.58	15.39
4	16.16	14.83

TABLE 2.5

Dynamic Deflections and Deflection Magnification Factor at Mid-span of a (10 X 10 m) Bridge

Vehicle Model	$W_{dynamic}$	DAF
I	10.75	1.16
II	7.40	1.37
III	6.76	1.25
IV	6.77	1.26

TABLE 2.6

Dynamic Deflections and Deflection Magnification Factor at Mid-span of a (10 X 15 m)Bridge

Vehicle Model	$W_{dynamic}$	DAF
I	23.44	1.40
II	15.27	1.16
III	15.75	1.19
IV	15.78	1.19

TABLE 2.7

Dynamic Deflections and Deflection Magnification Factor at Mid-span of a (10 X 20 m) Bridge

Vehicle Model	$W_{dynamic}$	DAF
I	26.80	1.52
II	19.36	1.26
III	20.45	1.33
IV	20.42	1.33

TABLE 2.8

Dynamic Deflections and Deflection Magnification Factor at Mid-span of a (10 X 25m) Bridge

Vehicle Model	$W_{dynamic}$	DAF
I	24.73	1.53
II	19.63	1.32
III	20.37	1.37
IV	20.34	1.37

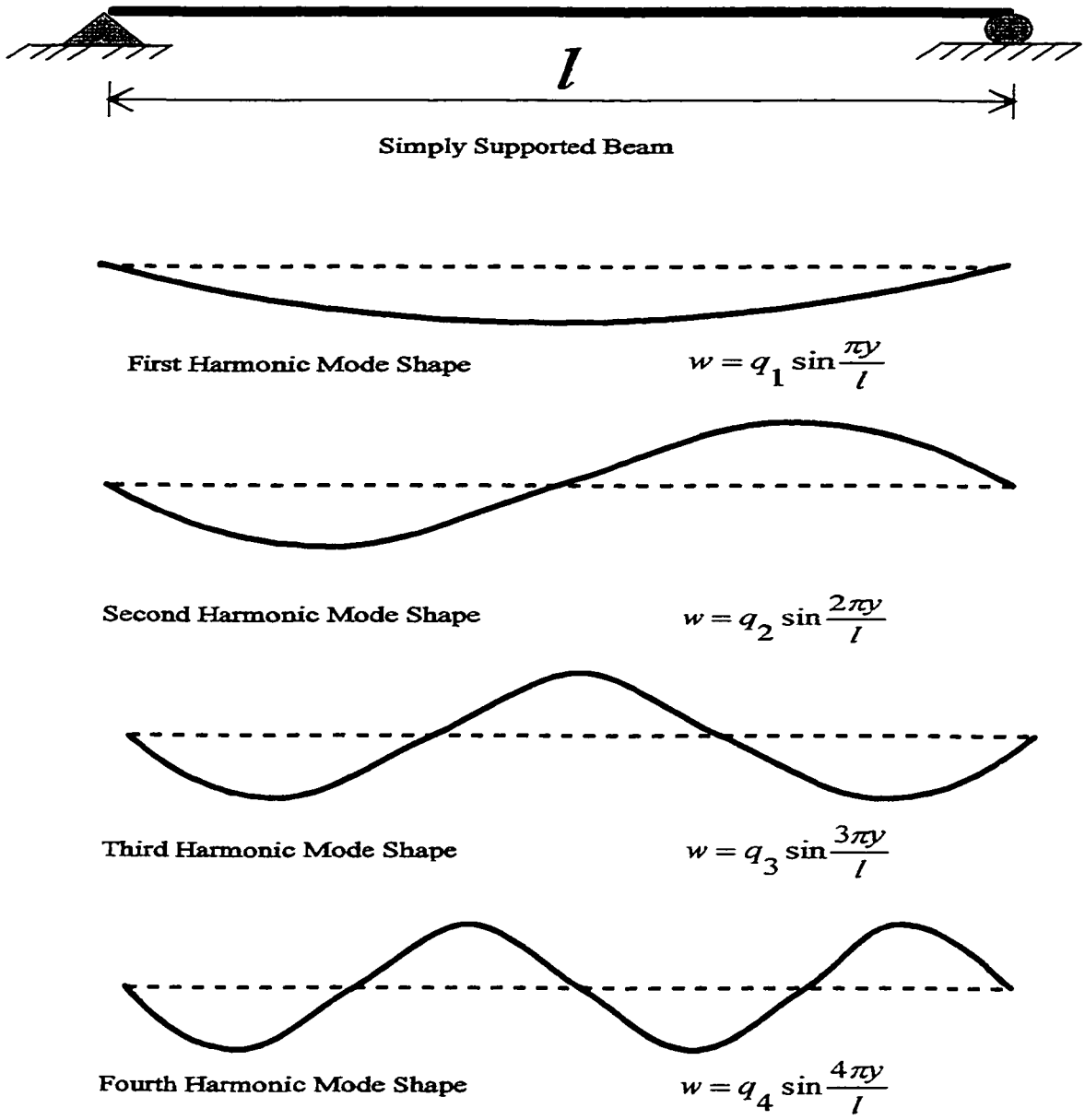

Figure 2.1 A Simply Supported Beam and its Lowest Four Harmonic Mode Shapes

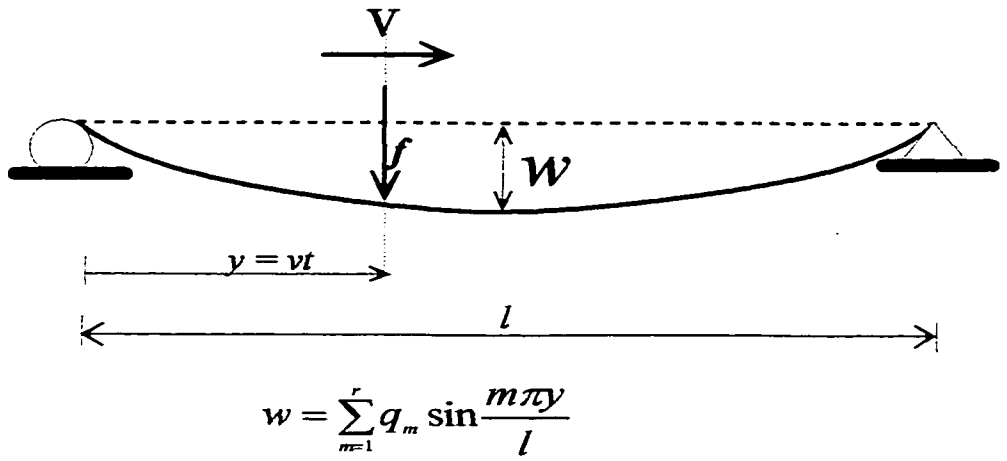

Figure 2.2 Moving Force Vehicle Model

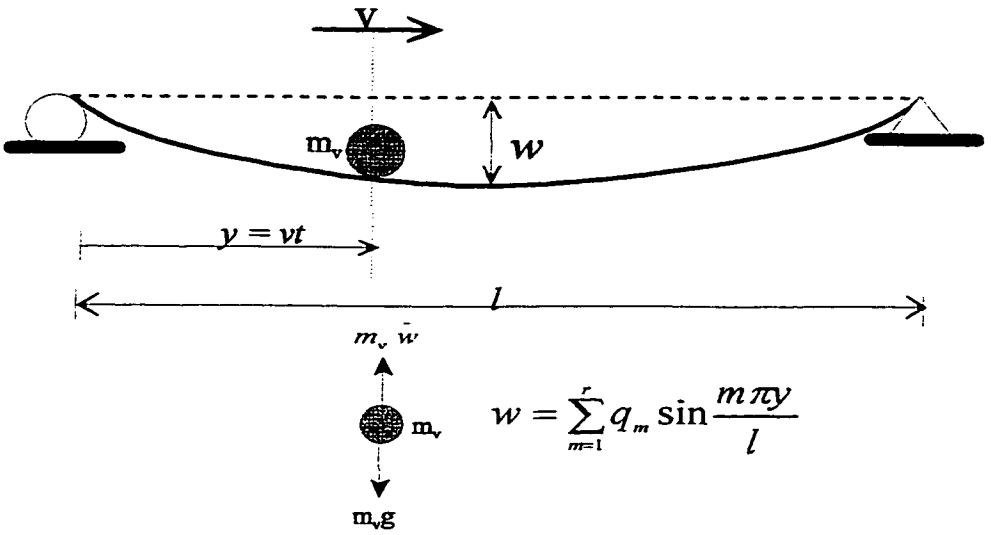

Figure 2.3 Moving Mass Vehicle Model

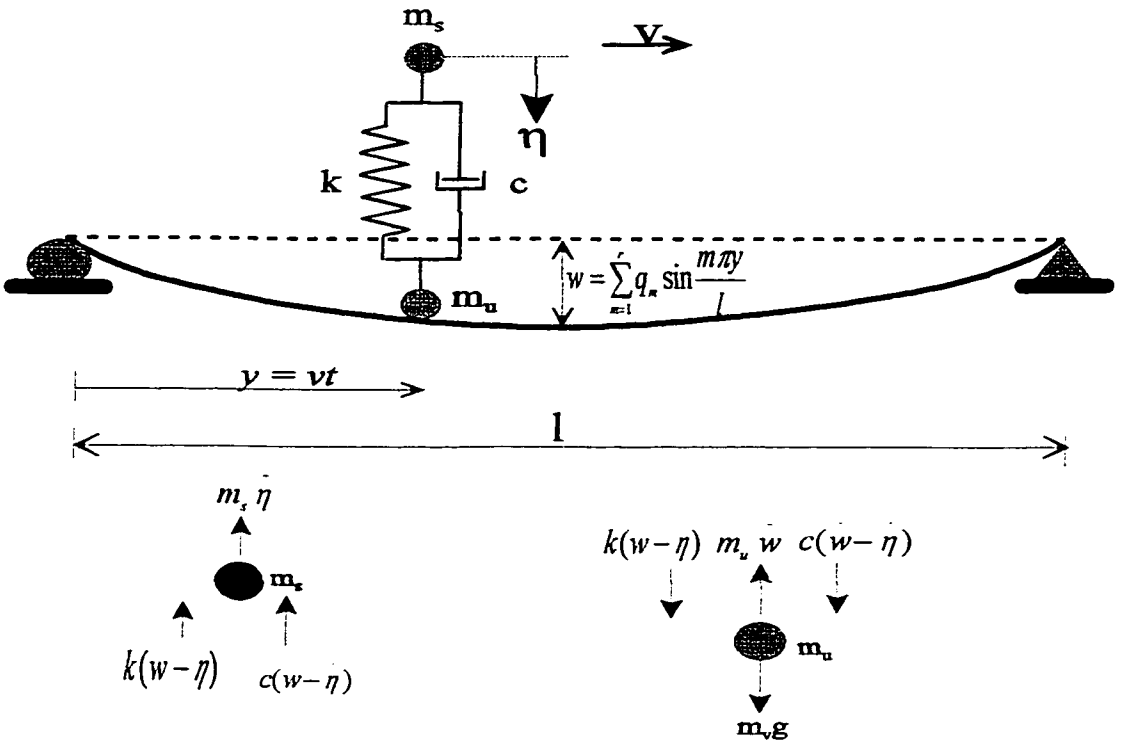

Figure 2.4 Sprung Mass Connected to an Unsprung Mass Vehicle Model

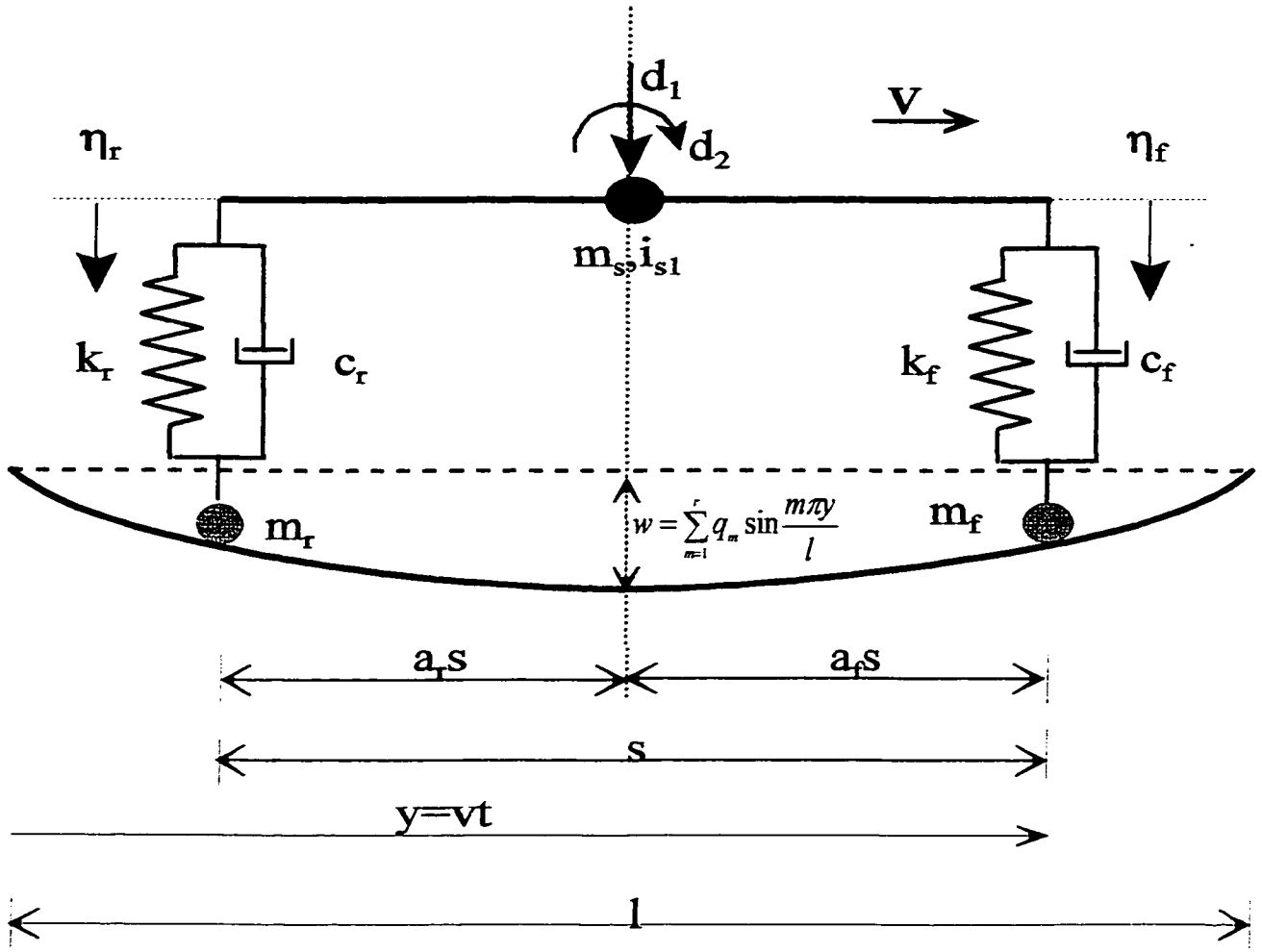

Figure 2.5 Two-axle Two-wheel Vehicle Model

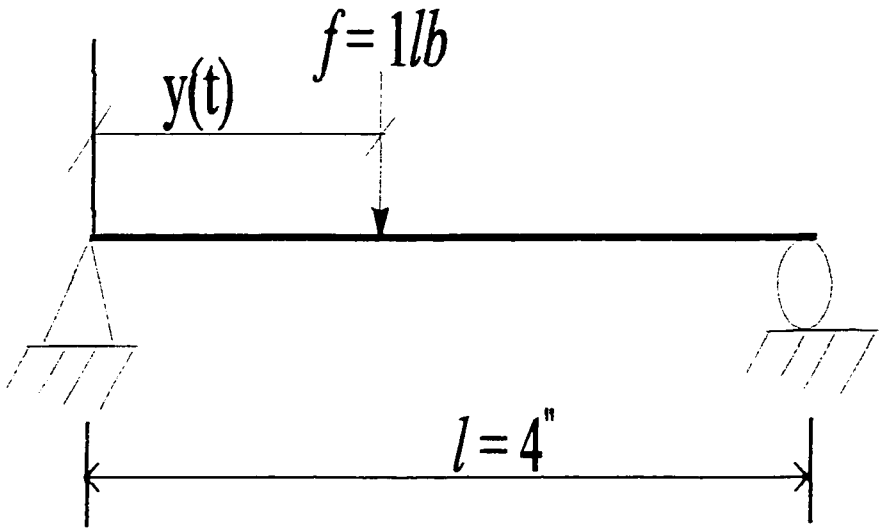

$E = 30 \times 10^6$ psi
$\rho = 0.001$ lb-sec^2/in^4
$A = 0.0625$ in^2
$I = 3.255 \times 10^{-4}$
$l = 4$ in

Figure 2.6 Beam Subjected to a Moving Load

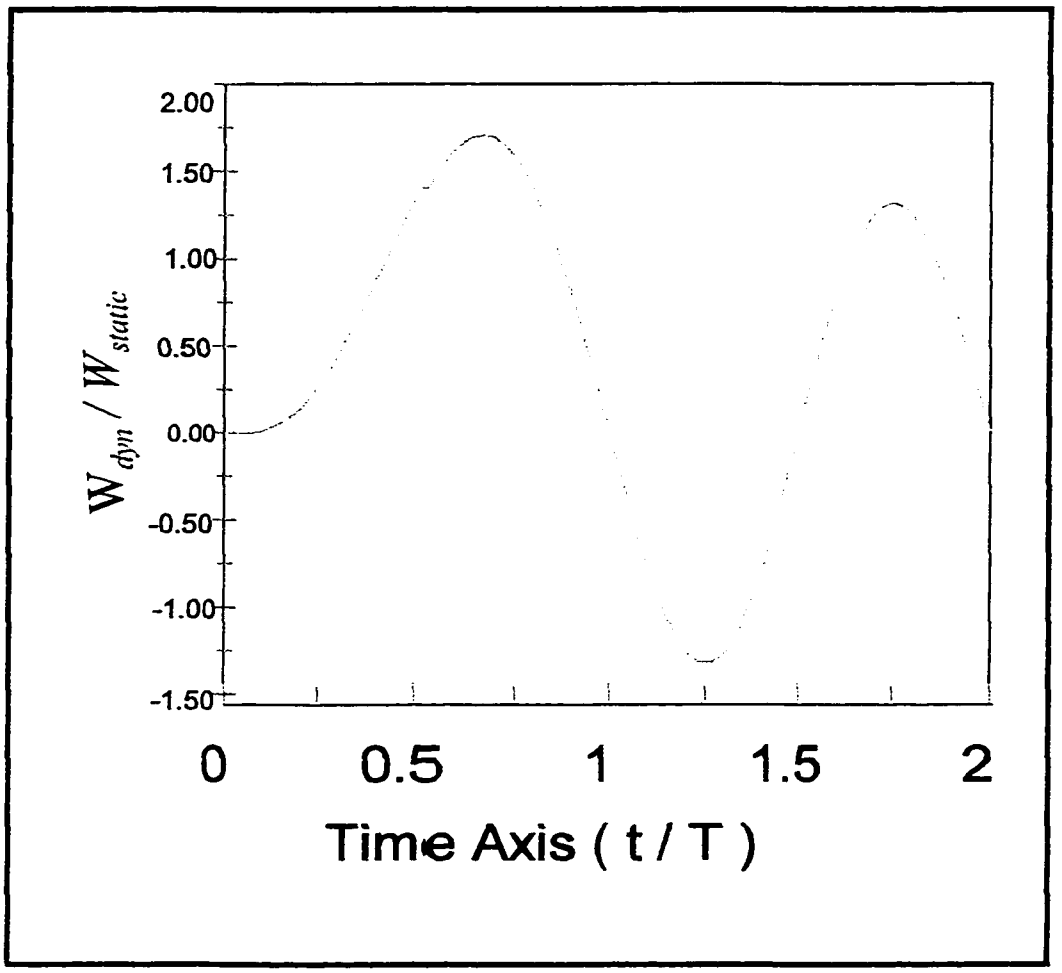

Figure 2.7 Beam Response Under a Moving Load

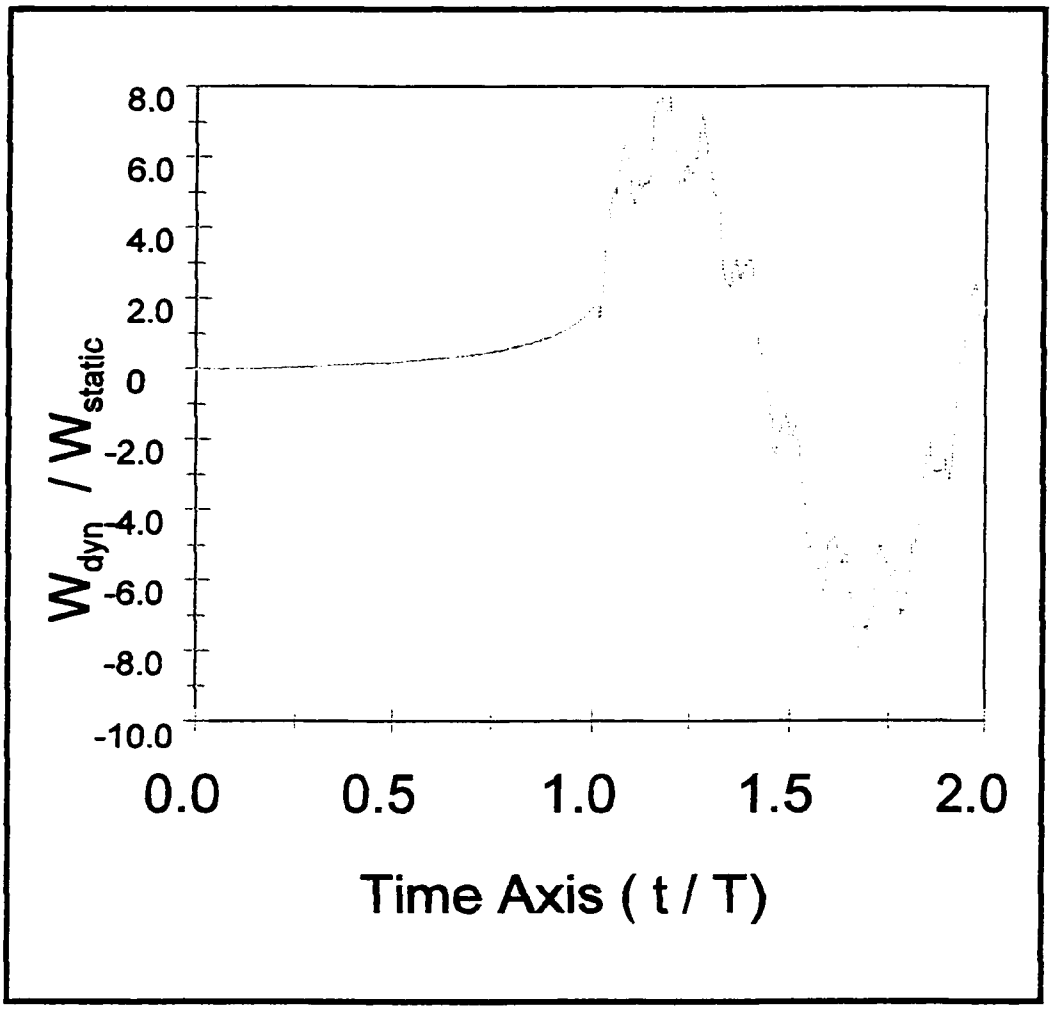

Figure 2.8 Beam Response Under a Moving Mass

Chapter 3

SLAB BRIDGES

3.1 Introduction

In this chapter the finite strip method is applied to dynamic response of simply supported slab bridges, idealized as either isotropic plate or orthotropic plate, under the action of a moving vehicle. The basic concept of the finite strip is reviewed and the governing equations for the dynamic response bridge-vehicle system are formulated. The derived equations are applied to numerical examples on plates and slab bridges.

3.2 Displacement Function

In plate bending strip all the applied loads act normal to the middle surface of the plate . The displacements in the direction normal to the middle surface of the plate is called the deflection

of the plate. If the plate is divided into a number of longitudinal strips, the deflected surface of each strip may be satisfactorily modeled using simple displacement functions The general form of the displacement function is given as a product of polynomials and series. Convergence to the correct results is ensured if the series part of the displacement function satisfies a priori the end conditions of the strip; the polynomial part is able to represent a state of constant strain in the transverse direction and the displacement function satisfies the compatibility of displacements along the boundaries with neighboring strips. Usually the deflection and transverse rotation along the nodal lines *i* and *j* are taken as the degrees of freedom at each nodal line. Thus, the simplest displacement function that satisfies the convergence requirements and the compatibility conditions along the boundary lines *i* and *j* could be represented by an harmonic series along the length of the strip and a complete cubic polynomial along the transverse direction

The nodal line displacement parameters and the nodal line force vector of each plate bending strip corresponding to the *mth* series term are:

$$\{\delta\}_m = \begin{Bmatrix} w_1 \\ \theta_1 \\ w_2 \\ \theta_2 \end{Bmatrix}_m \tag{3.1}$$

$$\{F\}_m = \begin{Bmatrix} W_1 \\ M_1 \\ W_2 \\ M_2 \end{Bmatrix}_m \tag{3.2}$$

For a strip with a constant thickness in the longitudinal direction and simply supported at opposite ends, the displacement components at any point P(x,y) within the strip are expressed in terms of the nodal displacement parameters as follows

$$w(x,y,t) = \sum_{m=1}^{r}(N_1(x)w_{im} + N_2(x)\theta_{im} + N_3(x)w_{jm} + N_4(x)\theta_{jm})\sin\frac{m\pi y}{l} \tag{3.3}$$

where,

$$N_1(x) = (1 - 3X^2 + 2X^3)$$

$$N_2(x) = x(1 - 2X + X^2)$$

$$N_3(x) = (3X^2 - 2X^3)$$

$$N_4(x) = x(X^2 - X)$$

$$X = \frac{x}{b} \tag{3.4}$$

and r is the total number of terms considered in the analysis

or, in a matrix form

$$w(x,y,t) = \sum_{m=1}^{r}\left[N_1, N_2, N_3, N_4\right]\begin{Bmatrix} w_{im} \\ \theta_{im} \\ w_{jm} \\ \theta_{jm} \end{Bmatrix}\sin\frac{m\pi y}{l} \tag{3.5}$$

These expressions can be written in the following more compact form

$$w(x,y,t) = \sum_{m=1}^{r} [N]\{\delta\}_m \sin\frac{m\pi y}{l} \tag{3.6}$$

where $\{\delta\}_m$ contains the displacement parameters and $[N]$ is a matrix of transverse shape functions.

The degree of accuracy in the analysis depends on the number of terms used in the summation and the number of subdivisions.

3.3 Strains

Once the displacement functions are known, the strains are obtained by appropriately differentiating the displacement function with respect to the coordinates x and y in the following manner:

$$\{\kappa\} = \begin{Bmatrix} -\dfrac{\partial^2 w}{\partial x^2} \\ -\dfrac{\partial^2 w}{\partial y^2} \\ 2\dfrac{\partial^2 w}{\partial x \partial y} \end{Bmatrix} = \sum_{m=1}^{r} [B]_m \{\delta\}_m \tag{3.7}$$

where $[B]_m$ is the strain matrix and is explicitly in the form

$$[B]_m = \begin{bmatrix} -N_1^{'} \sin k_m y & -N_2^{'} \sin k_m y & -N_3^{'} \sin k_m y & -N_4^{'} \sin k_m y \\ k_m^2 N_1 \sin k_m y & k_m^2 N_2 \sin k_m y & k_m^2 N_3 \sin k_m y & k_m^2 N_4 \sin k_m y \\ 2k_m N_1^{'} \cos k_m y & 2k_m N_2^{'} \cos k_m y & 2k_m N_3^{'} \cos k_m y & 2k_m N_4^{'} \cos k_m y \end{bmatrix} \tag{3.8}$$

in which $N^{'} = \frac{dN}{dx}$, $N^{''} = \frac{d^2 N}{dx^2}$ and $k_m = \frac{m\pi}{l}$

3.4 Stresses

The stresses at any point in a strip are related to the curvatures as

$$\begin{aligned} M_x &= -(D_x \frac{\partial^2 w}{\partial x^2} + D_1 \frac{\partial^2 w}{\partial y^2}) \\ M_y &= -(D_1 \frac{\partial^2 w}{\partial x^2} + D_y \frac{\partial^2 w}{\partial y^2}) \\ M_{xy} &= 2D_{xy} \frac{\partial^2 w}{\partial x^2} \end{aligned} \tag{3.9}$$

where D_x and D_y are the flexural rigidities and D_{xy} and D_1 are respectively the torsional and coupling rigidity . They are defined as

$$D_x = \frac{E_x h^3}{12(1 - \nu_x \nu_y)}$$

$$D_y = \frac{E_y h^3}{12(1 - \nu_x \nu_y)} \tag{3.10}$$

$$D_{xy} = \frac{E_{xy} h^3}{12}$$

$$D_1 = \nu_x D_x = \nu_y D_y$$

in which ν_x and ν_y are Poisson's ratio in the x and y directions respectively, E_x and E_y are moduli of elasticity in the x and y directions respectively, E_{xy} is the shear rigidity and h is the thickness of the plate strip.

In matrix form, equation (3.9) becomes

$$\{M\} = \begin{Bmatrix} M_x \\ M_y \\ M_{xy} \end{Bmatrix} = \begin{bmatrix} D_x & D_1 & 0 \\ D_1 & D_y & 0 \\ 0 & 0 & D_{xy} \end{bmatrix} \{\kappa\} = [D]\{\kappa\} \tag{3.11}$$

where $[D]$ is referred to as the elasticity matrix containing the terms defined in equation (3.10). For bending of an isotropic plate,

$$[D] = \frac{Eh^3}{12(1-\nu^2)} \begin{bmatrix} 1 & \nu & 0 \\ \nu & 1 & 0 \\ 0 & 0 & \frac{1-\nu}{2} \end{bmatrix} \tag{3.12}$$

where E is the elastic modules and ν is the Poisson's ratio.

Substitution of equation (3.7) into equation (3.11) yields

$$\{M\} = \sum_{m=1}^{\acute{c}} [D][B]_m \{\delta\}_m \tag{3.13}$$

3.5 Minimization of Total Potential Energy

The displacement field of a plate strip subjected to a dynamic loading varies with time and as a result there are two types of distributed body forces which must be taken into account; the inertia forces of the plate strip which arises from its acceleration and the damping forces which originate from the internal friction within the deforming material or from motion through a viscous fluid .

The dynamic analysis can be reduced to static analysis by using D'Alembert's principle by

treating the inertia forces and the damping forces as statically imposed body forces. The inertia force of a body is equal to the product of its mass and acceleration and it acts in the direction of negative acceleration. The damping forces are difficult to identify and usually velocity-dependent damping forces that act in the direction of negative velocity are used. In mode superposition method, mode dependent damping ratios are specified.

The strain energy of a plate strip is given by

$$U = \frac{1}{2}\int_0^L \int_0^b \{M\}^T \{\kappa\} dxdy \tag{3.14}$$

The transpose of {M} is

$$\{M\}^T = \sum_{m=1}^{r} \{\delta\}_m^T [B]_m^T [D] \tag{3.15}$$

Substituting equations (3.7) and (3.15) into equation (3.14) yields

$$U = \frac{1}{2}\sum_{m=1}^{r}\sum_{n=1}^{r} \{\delta\}_m^T \int_0^l \int_0^b [B]_m^T [D]\,[B]_n dxdy \{\delta\}_n \tag{3.16}$$

The product of the three matrices to be integrated in this equation contains products of functions that are orthogonal to each other, and as a result of orthogonality properties of these functions,

the summation in equation (3.16) requires to be carried out once only. Thus equation (3.16) becomes

$$U = \frac{1}{2}\sum_{m=1}^{r}\{\delta\}_m^T \int_0^l \int_0^b [B]_m^T [D]\,[B]_m \, dxdy \{\delta\}_m \tag{3.17}$$

After integration, equation (3.17) is reduced to

$$U = \frac{1}{2}\sum_{m=1}^{r}\{\delta\}_m^T [k]_m \{\delta\}_m \tag{3.18}$$

where $[k]_m$ (a 4 x 4 matrix) is the stiffness matrix and is given by the following integral.

$$[k_m] = \int_0^l \int_0^b [B]_m^T [D][B]_m \, dxdy \tag{3.19}$$

The potential energy due to the distributed external transverse load $q_e(x,y)$ of the plate strip can be written as

$$W_e = -\int_0^l \int_0^b q_e(x,y) w \, dxdy \tag{3.20}$$

By substituting the displacement function in equation (3.6) into equation (3.20), the potential energy of external loading can also be expressed in terms of the displacement parameters:

$$W_e = -\sum_{m=1}^{r}\{\delta\}_m^T \int_0^l \int_0^b [N]^T q_e(x,y) \sin\frac{m\pi y}{l} \, dxdy \tag{3.21}$$

The integration of equation (3.21) produces

$$W_e = -\sum_{m=1}^{r} \{\delta\}_m^T \{p\}_m \tag{3.22}$$

where $\{p\}_m$ (a 4 x 1 vector) is the equivalent nodal force vector of the external load and is given by the following integral:

$$\{p\}_m = \int_0^l \int_0^b [N]^T q_e \sin\frac{m\pi y}{l} dxdy \tag{3.23}$$

For a concentrated load the above integral is reduced to the following simple expression.

$$\{p\}_m = f[N]^T \sin\frac{m\pi y_p}{l} \tag{3.24}$$

where y_p is the position of the load and f is its magnitude.

The inertia force acting on an infinitesimal area dA of mid-plane of a plate strip is

$$q_i = -\rho h \frac{\partial^2 w}{\partial t^2} dA \tag{3.25}$$

where ρ is the mass per unit volume .

Substituting equation (3.6) into equation (3.25) gives

$$q_i = -\rho h \sum_{m=1}^{r} [N] \{\ddot{\delta}\}_m \sin\frac{m\pi y}{l} dxdy \tag{3.26}$$

The potential energy of distributed inertia forces can be calculated as

$$W_i = \sum_{m=1}^{r}\sum_{n}^{r}\{\delta\}_m^T\int_0^l\int_0^b \rho h[N]^T \sin\frac{m\pi y}{l}[N]\sin\frac{n\pi y}{l}dxdy\left\{\ddot{\delta}\right\}_n \tag{3.27}$$

After integration, equation (3.27) is reduced to

$$W_i = \sum_{m=1}^{r}\{\delta\}_m^T[m]\left\{\ddot{\delta}\right\}_m \tag{3.28}$$

where $[m]$ (a 4 x 4 matrix) is the consistent mass matrix and is given by the following integral.

$$[m] = \int_0^l\int_0^b \rho h[N]^T[N]\sin^2\frac{m\pi y}{l}dxdy \tag{3.29}$$

The damping force acting on an infinitesimal area dA of mid-plane of a plate strip is

$$q_d = -c_d\frac{\partial w}{\partial t}dA \tag{3.30}$$

where c_d is the damping coefficient .

Substituting equation (3.6) into equation (3.30) gives

$$q_d = -c_d\sum_{m=1}^{r}[N]\left\{\dot{\delta}\right\}_m \sin\frac{m\pi y}{l}dxdy \tag{3.31}$$

The potential energy of distributed damping forces can be found as

$$W_d = \sum_{m=1}^{r}\sum_{n}^{r} \{\delta\}_m^T \int_0^l \int_0^b c_d [N]^T \sin\frac{m\pi y}{l} [N] \sin\frac{n\pi y}{l} dxdy \left\{\dot{\delta}\right\}_n \tag{3.32}$$

The integration of equation (3.32) yields

$$W_d = \sum_{m=1}^{r} \{\delta\}_m^T [c] \left\{\dot{\delta}\right\}_m \tag{3.33}$$

where $[c]$ (a 4 x 4 matrix) is the consistent damping matrix and is given by the following integral.

$$[c] = \int_0^l \int_0^b c_d [N]^T [N] \sin^2 \frac{m\pi y}{l} dxdy \tag{3.34}$$

The total potential energy of the entire structure, Π, is the sum of U and W contributions from all the strips comprising the slab deck. Thus

$$\Pi = \sum_{s=1}^{NS} (U + W_i + W_d + W_e)_s \tag{3.35}$$

in which *NS* is the total number of strips.

Substituting equations (3.18), (3.22), (3.28) and (3.33) into equation (3.35) produces

$$\begin{aligned} \Pi = \sum_{S=1}^{NS} \Big(\frac{1}{2} \sum_{m=1}^{r} \{\delta\}_m^T [k]_{Sm} \{\delta\}_m + \sum_{m=1}^{r} \{\delta\}_m^T [c]_S \left\{\dot{\delta}\right\}_m \\ + \sum_{m=1}^{r} \{\delta\}_m^T [m]_S \left\{\ddot{\delta}\right\}_m - \sum_{m=1}^{r} \{\delta\}_m^T \{p\}_{Sm} \Big) \end{aligned} \tag{3.36}$$

The equations of dynamic equilibrium is obtained by minimizing the total potential energy Π with respect to each of the displacement parameters $\{\delta\}_{tm}$ of the whole bridge, as follows:

$$\left\{\frac{\partial \Pi}{\partial \{\delta\}_{tm}}\right\} = \{0\} \tag{3.37}$$

where *tm* is equal the number of harmonic terms *r* times the total number of degrees of freedom of the structure *N*.

Substituting equation (3.36) into equation (3.37) and performing the partial differentiation produces a system of algebraic equations for each harmonic term which can be written in the following matrix form:

$$[M_b]\{\ddot{\delta}\}_m + [C_b]\{\dot{\delta}\}_m + [K_b]_m\{\delta\}_m = \{F\}_m \tag{3.38}$$

in which $[K_b]_m$, $[M_b]$, $[C_b]$, $\{F\}_m$,$\{\delta\}_m$,$\{\dot{\delta}\}_m$ and$\{\ddot{\delta}\}_m$ are the stiffness matrix, the mass matrix, the damping matrix, the nodal force vector, the nodal displacement vector, the nodal velocity vector, and the nodal acceleration vector of the whole structure respectively.

Because of the orthogonal property of the harmonic functions, structures that have simple supports at both ends produce equations of equilibrium whose system matrices have narrow half-bandwidth, i.e., $[K]_{mn} = [M]_{mn} = [C]_{mn} = 0$ for $m \neq n$. Thus, the computer storage and time consumption are reduced significantly.

3.6 Free Vibration Analysis

A special case of the dynamic problem is the undamped free vibration system. Analysis of undamped free vibration response provides the natural frequencies of vibration and the corresponding mode shapes . The knowledge of the frequencies and mode shapes allow us to:

- obtain a solution for the forced vibration analysis.
- obtain the displacements and stresses in such a system when it is subjected to disturbances in the form of initial displacements, or initial velocities, or both, along one or more of its degree of freedom.
- understand the behavior of the bridge under moving loads and to compare them with the frequencies of the excitation forces.
- to use the highest frequency as a basis for choosing a suitable time step for the numerical integration of the equation of motion.
- to use the lowest frequency to obtain the frequency ratio for the parametric study of the bridge-vehicle system. The dynamic equilibrium equation of undamped free vibration is of the following form:

$$[M_b]\{\ddot{\delta}\}_m + [K_b]_m \{\delta\}_m = \{0\} \tag{3.39}$$

The solution of equation (3.39) is of the form:

$$\{\delta\}_m = \{\phi\}_m \sin(\omega_m t - \theta_m) \tag{3.40}$$

where $\{\phi\}_m$ is an arbitrary vector, ω_m is referred to as the frequency of vibration, and θ_m is a phase angle.

Substituting equation (3.40) into equation (3.39), the following generalized eigenproblem is obtained.

$$([K_b]_m - \omega_m^2[M_b])\{\phi\}_m \sin(\omega_m t - \theta_m) = \{0\} \tag{3.41}$$

Equation (3.41) is true for all values of t and therefore can be written as

$$([K_b]_m - \omega_m^2[M_b])\{\phi\}_m = \{0\} \tag{3.42}$$

Many numerical procedures (Bathe, 1996 and Humar, 1990) exist for the determination of the eigenvalues and eigenvectors. In this study inverse vector iteration with shift in conjunction with Gram-Schmidt orthogonalization is used .

The eigenproblem in equation (3.42) is solved for $m = 1, 2, 3,...r$ until the required number of modes in the analysis which have the lowest eigenvalues are obtained. The eigenvalues are arranged in an ascending order of their magnitude in a single matrix $[\Lambda_b]$ and their corresponding eigenvectors are also arranged side by side in a single matrix $[\Phi_b]$ called modal matrix. A record of the appropriate harmonic term for each mode is also kept. If n mode shapes (eigenvectors) are required in the analysis, then $(\omega^2_1, \{\phi_1\}, m_1)$, $(\omega^2_2, \{\phi_2\}, m_2),...,(\omega^2_j, \{\phi_j\}, m_j),...,(\omega^2_n \{\phi_n\}, m_n)$ are obtained. With m_j being the m^{th} harmonic term that produces j^{th} eigenvalue and eigenvector. When eigenvectors are mass-orthonormalized, they satisfy the following properties.

$$\{\phi_i\}^T[M_b]\{\phi_j\} = \begin{cases} 1 & i = j \\ 0 & i \neq j \end{cases} \tag{3.43}$$

$$\{\phi_i\}^T[K_b]_m\{\phi_j\} = \begin{cases} \omega_i^2 & i = j \\ 0 & i \neq j \end{cases} \tag{3.44}$$

where $\{\phi_i\}$, and $\{\phi_j\}$ are the i^{th} and j^{th} eigenvectors (mode shapes) and ω^2_i is the

eigenvalue(square of the frequency) of the i^{th} eigenvector. Each harmonic term has its unique mode shapes.

The frequencies satisfy $\omega_{1m} \le \omega_{2m} \le \omega_{3m} \cdots$ and $\omega_{1m} \le \omega_{1(m+1)} \le \omega_{1(m+2)} \le \omega_{1(m+3)} \cdots$

3.7 Forced Vibration Analysis

In this study mode superposition method combined with constant-average acceleration method is adopted for the solution of equilibrium equations of motion. Free vibration analysis of the bridge is performed first to obtain the mode shapes (eigenvectors) and frequencies (square root of eigenvalues) of the bridge then the equations of motion of the bridge are formulated in normal coordinates and are combined with the equilibrium equations of the vehicle.

The nodal displacements of the bridge are expressed in terms of modal coordinates by means of transformation.

$$\{\delta\}_{N\times 1} = [\Phi_b]_{N\times NM} \{z_b\}_{NM\times 1} \tag{3.45}$$

where [Φ_b] is the matrix of undamped mode shapes and $\{z_b\}$ is a vector of the modal coordinates or normal coordinates of the bridge and N and NM are respectively the number of degrees of freedom of the bridge and number of modes used in the analysis.

The displacement at a point $P(x,y)$ in a strip bounded by the i^{th} and j^{th} nodal line are given by

$$w = [N] \sin\frac{m_j \pi y}{l} [G] \{z_b\} \tag{3.46}$$

where $[G]$ is a sub-matrix of $[\Phi_b]$ whose elements correspond to the *i-j* strip that contains the point *P(x,y)*.

In modal coordinates the equations of the damped forced vibration can be written as follows:

$$\left[M_b^*\right]\left\{\ddot{z}_b\right\}+\left[C_b^*\right]\left\{\dot{z}_b\right\}+\left[K_b^*\right]\left\{z_b\right\}=\left\{F^*\right\} \tag{3.47}$$

where

$$\begin{aligned}\left[M_b^*\right]&=\left[\Phi_b\right]^T\left[M_b\right]\left[\Phi_b\right]\\ \left\{C_b^*\right\}&=\left[\Phi_b\right]^T\left[C_b\right]\left[\Phi_b\right]\\ \left\{\Lambda_b\right\}&=\left[\Phi_b\right]^T\left[K_b\right]\left[\Phi_b\right]\\ \left\{F^*\right\}&=\left[\Phi_b\right]^T\left[F\right]\end{aligned} \tag{3.48}$$

Because of the orthogonal properties of the mode shapes, both the modal mass matrix $[M_b^*]$ and the modal stiffness matrix $[\Lambda_b]$ are diagonal. Moreover, if the mode shapes are mass-orthonormal, the modal mass matrix is an identity matrix. The modal stiffness matrix $[\Lambda_b]$ which is also called the spectral matrix is a diagonal matrix which contains the square of the frequencies ω. If the damping matrix $[C_b]$ is assumed to be proportional to $[M_b]$ or $[K_b]$ or a linear combination of both, the modal damping matrix $[C_b^*]$ is also diagonal and its i^{th} diagonal element contains $2\omega_i\xi_i$ with ξ_i being the damping ratio.

3.7.1 Response Under a Moving Force Vehicle Model

If the interaction between the vehicle and the bridge is ignored, the vehicle can be modeled as a moving load (Fig. 3.1). The y-coordinate of the contact point between the bridge and a vehicle crossing the bridge with a constant acceleration is given by

$$y = -s + vt + \frac{1}{2}at^2 \tag{3.49}$$

where

$-s$ is the position of the vehicle at time $t = 0$, v is its velocity and a is its acceleration.

The concentrated force exerted on the bridge by the moving vehicle is given by

$$f = m_v g \tag{3.50}$$

where

m_v is the mass of the vehicle and g is the acceleration due to gravity.

Substitution of equation (3.50) into equation (3.24) and the result into equation (3.48) yields:

$$[M_b^*]\{\ddot{z}_b\} + [C_b^*]\{\dot{z}_b\} + [\Lambda_b]\{z_b\} = m_v g[G]^T[S_{mj}]^T \tag{3.51}$$

where

$$[S_{mj}]^T = [N]^T \sin\frac{m_j \pi}{l}(vt + \frac{1}{2}at^2 - s) \tag{3.52}$$

Equation (3.51) is solved for the modal coordinates $\{z_b\}$, then the deflections and accelerations of the bridge are finally calculated from

$$w = [S_{mj}][G]\{z_b\} \tag{3.53}$$

and

$$\ddot{w} = [S_{mj}][G]\{\ddot{z}_b\} \tag{3.54}$$

Dynamic bending moments are given by

$$\{M\} = [D][B]_{mj}[G]\{z_b\} \tag{3.55}$$

3.7.2 Response Under a Moving Mass Vehicle Model

If the interaction between the bridge and the vehicle is considered, the vehicle can be modeled as a moving mass (Fig. 3.2). Unlike moving loads, a moving mass produces several terms in the formulation of equations of motion. The moving mass is treated as a particle. It is assumed that the moving mass is always in contact with the bridge while it transverses the span. In order to determine the effect of the moving mass i.e., the terms contributed to the equations of motion by the moving mass, the lateral acceleration of the point of contact between the bridge and the moving mass is considered.

Since the vehicle is moving parallel to nodal lines, y is a function of time while x is not. Then the time derivatives of the displacement w at the contact point between the vehicle and the bridge are given by

$$\dot{w}(y,t) = \frac{\partial w}{\partial t}\dot{y} + \frac{\partial w}{\partial t} \tag{3.56}$$

$$\ddot{w}(y,t) = \frac{\partial^2 w}{\partial y^2}\ddot{y}^2 + 2\frac{\partial^2 w}{\partial y \partial t}\dot{y} + \frac{\partial w}{\partial y}\ddot{y} + \frac{\partial^2 w}{\partial y^2} \tag{3.57}$$

The position along the longitudinal direction of the contact point between the vehicle and the bridge is given in equation (3.49) and the horizontal velocity and acceleration of the vehicle are obtained from there as follows:

$$\dot{y}(t) = v + at \tag{3.58}$$

$$\ddot{y} = a \tag{3.59}$$

The vertical displacement at the contact point between the bridge and the vehicle is given in terms of the generalized coordinate by:

$$w = [N][G]\{z_b\}\sin\frac{m_j\pi}{l}(-s + vt + \frac{1}{2}at^2) \tag{3.60}$$

The time derivatives of w are given by

$$\begin{aligned}\dot{w} = {} & [N][G]\{\dot{z}_b\}\sin\frac{m_j\pi}{l}(-s + vt + \frac{1}{2}at^2) \\ & + \frac{m_j\pi}{l}(v + at)[N][G]\{z_b\}\cos\frac{m_j\pi}{l}(-s + vt + \frac{1}{2}at^2)\end{aligned} \tag{3.61}$$

$$\begin{aligned}\ddot{w} = &-(\frac{m_j\pi}{l})^2(v+at)^2[N][G]\{z_b\}\sin\frac{m_j\pi}{l}(-s+vt+\frac{1}{2}at^2)\\ &+2\frac{m_j\pi}{l}(v+at)[N][G]\{\dot{z}_b\}\cos\frac{m_j\pi}{l}(-s+vt+\frac{1}{2}at^2)\\ &+\frac{m_j\pi}{l}a[N][G]\{z_b\}\cos\frac{m_j\pi}{l}(-s+vt+\frac{1}{2}at^2)\\ &+[N][G]\{\ddot{z}_b\}\sin\frac{m_j\pi}{l}(-s+vt+\frac{1}{2}at^2)\end{aligned} \tag{3.62}$$

If the vehicle travels with a constant velocity, the vertical displacement at the point of contact between the vehicle and the bridge reduces to

$$w = [S_{mj}][G]\{z_b\} \tag{3.63}$$

while the velocity reduces to

$$\dot{w} = [S_{mj}][G]\{\dot{z}_b\} + [\dot{S}_{mj}][G]\{z_b\} \tag{3.64}$$

and the acceleration becomes

$$\ddot{w} = [\ddot{S}_{mj}][G]\{z_b\} + 2[\dot{S}_{mj}][G]\{\dot{z}_b\} + [S_{mj}][G]\{\ddot{z}_b\} \tag{3.65}$$

where

$$[S_{mj}] = [N]\sin\frac{m_j\pi}{l}(vt - s) \tag{3.66}$$

$$\left[\dot{S}_{mj}\right] = [N]\frac{m_j \pi v}{l}\cos\frac{m_j \pi}{l}(vt - s) \tag{3.67}$$

$$\left[\ddot{S}_{mj}\right] = -[N](\frac{m_j \pi v}{l})^2 \sin\frac{m_j \pi}{l}(vt - s) \tag{3.68}$$

The force exerted on the bridge by the moving vehicle is given by

$$f = m_v g - m_v \ddot{w} \tag{3.69}$$

After some substitutions and rearrangements the equation of motion under a moving mass m_v becomes

$$\left(\left[M_b^*\right] + \left[M_I\right]\right)\left\{\ddot{z}_b\right\} + \left(\left[C_b^*\right] + \left[C_I\right]\right)\left\{\dot{z}_b\right\} + \left(\left[\Lambda_b\right] + \left[K_I\right]\right)\left\{z_b\right\} = m_v g\left[G\right]^T\left[S_{mj}\right]^T \tag{3.70}$$

where

$$\left[M_I\right] = m_v\left[G\right]^T\left[S_{mj}\right]^T\left[S_{mj}\right]\left[G\right] \tag{3.71}$$

$$\left[C_I\right] = 2m_v\left[G\right]^T\left[S_{mj}\right]^T\left[\dot{S}_{mj}\right]\left[G\right] \tag{3.72}$$

$$\left[K_I\right] = m_v\left[G\right]^T\left[S_{mj}\right]^T\left[\ddot{S}_{mj}\right]\left[G\right] \tag{3.73}$$

For multiple moving masses, the equation of dynamic equilibrium becomes

$$\left(\left[M_b^*\right]+\sum_{i=1}^{NV}\left[M_I\right]_i\right)\left\{\ddot{z}_b\right\}+\left(\left[C_b^*\right]+\sum_{i=1}^{NV}\left[C_I\right]_i\right)\left\{\dot{z}_b\right\}+\left(\left[\Lambda_b\right]+\sum_{i=1}^{NV}\left[K_I\right]_i\right)\left\{z_b\right\}= \sum_{i=1}^{NV} m_{vi} g\left[G\right]_i^T\left[S_{mj}\right]^T \tag{3.74}$$

where NV is the number of vehicles crossing the bridge and

$$\left[M_I\right]_i = m_{vi}\left[G\right]_i^T\left[S_{mj}\right]_i^T\left[S_{mj}\right]_i\left[G\right]_i \tag{3.75}$$

$$\left[C_I\right]_i = 2m_{vi}\left[G\right]_i^T\left[S_{mj}\right]_i^T\left[\dot{S}_{mj}\right]_i\left[G\right]_i \tag{3.76}$$

$$\left[K_I\right]_i = m_{vi}\left[G\right]_i^T\left[S_{mj}\right]_i^T\left[\ddot{S}_{mj}\right]_i\left[G\right]_i \tag{3.77}$$

3.7.3 Response Under a Moving Sprung Mass Vehicle Model

A vehicle model which comprises of a sprung mass m_s connected to an unsprung mass m_u through a spring of stiffness k and a viscous damper of a damping coefficient c is used here (Fig. 3.3). The unsprung mass m_u remains in contact with the bridge deck. This model stimulates a better interaction between the vehicle and the bridge than the previous moving mass model.

The equation of motion of the vehicle can be expressed in the form

$$m_s\ddot{\eta}+c(\dot{\eta}-\left[S_{mj}\right]\left[G\right]\left\{\dot{z}_b\right\}-\left[\dot{S}_{mj}\right]\left[G\right]\left\{z_b\right\})+k(\eta-\left[S_{mj}\right]\left[G\right]\left\{z_b\right\})=\{0\} \tag{3.78}$$

where η is the vertical displacement of the sprung mass m_s.

The force exerted on the bridge by the moving vehicle is given by

$$f = m_v g - m_u \ddot{w} + c(\dot{\eta} - \dot{w}) + k(\eta - w) \tag{3.79}$$

where m_v is the sum of the sprung mass m_s and the unsprung mass m_u.

After some substitutions and rearrangements the equation of motion becomes

$$\begin{bmatrix} ([M_b^*]+[M_I]) & 0 \\ 0 & [M_v] \end{bmatrix} \begin{Bmatrix} \{\ddot{z}_b\} \\ \{\ddot{\eta}\} \end{Bmatrix} + \begin{bmatrix} ([C_b^*]+[C_I]) & [C_{VI}] \\ [C_{HI}] & [C_v] \end{bmatrix} \begin{Bmatrix} \{\dot{z}_b\} \\ \{\dot{\eta}\} \end{Bmatrix} + \begin{bmatrix} ([\Lambda_b]+[K_I]) & [K_{VI}] \\ [K_{HI}] & [K_v] \end{bmatrix} \begin{Bmatrix} \{z_b\} \\ \{\eta\} \end{Bmatrix} = \begin{Bmatrix} \{m_v g[G]^T[S_{mj}]^T\} \\ 0 \end{Bmatrix} \tag{3.80}$$

where

$$[M_v]_{1x1} = m_s \quad [C_v]_{1x1} = c \quad [K_v]_{1x1} = k$$

$$[K_{VI}] = -k[G]^T[S_{mj}]^T \quad [C_{VI}] = -c[G]^T[S_{mj}]^T$$

$$[K_{HI}] = \left(-k[S_{mj}] - c[\dot{S}_{mj}]\right)[G] \quad [C_{HI}] = -c[S_{mj}][G]$$

$$[K_I] = [G]^T[S_{mj}]^T\left(m_u[\ddot{S}_{mj}] + c[\dot{S}_{mj}] + k[S_{mj}]\right)[G]$$

$$[C_I] = [G]^T[S_{mj}]^T\left(2m_u[\dot{S}_{mj}] + c[S_{mj}]\right)[G]$$

$$[M_t] = m_u[G]^T[S_{mj}]^T[S_{mj}][G] \tag{3.81}$$

3.7.4 Response Under a Two Axle Two Wheel Vehicle Model

This vehicle model is shown in Figure 3.4 and is already described in section 2.6. Referring to figure (3.4), the displacements at the front and rear axles η_f and η_r are related to the two degrees of freedom d_1 and d_2 of the vehicle body by the following relationship:

$$\eta_f = d_1 + a_f s d_2 \tag{3.82a}$$

$$\eta_r = d_1 - a_r s d_2 \tag{3.82b}$$

In matrix form, equations (3.82a) and (3.82b) can be written as follows

$$\eta_f = \begin{bmatrix} 1 & a_f \end{bmatrix}\{d\} \tag{3.83a}$$

$$\eta_r = \begin{bmatrix} 1 & -a_r \end{bmatrix}\{d\} \tag{3.83b}$$

where

$$\{d\} = \begin{Bmatrix} d_1 \\ s d_2 \end{Bmatrix} \tag{3.84}$$

The change of length of the front vehicle spring is given by

$$\Delta_f = \eta_f - w_f \tag{3.85a}$$

where w_f is the vertical displacement at the contact point between the front wheel and the bridge. Similarly the change of length of the rear vehicle spring is given by

$$\Delta_r = \eta_r - w_r \tag{3.85b}$$

where w_r is the vertical displacement at contact point between the rear wheel and the bridge. The vertical displacements at the contact points are given by

$$w_f = [N][G]\{z_b\} \sin\frac{m_j \pi}{l}(vt - s_f) \tag{3.86a}$$

$$w_r = [N][G]\{z_b\} \sin\frac{m_j \pi}{l}(vt - s_r) \tag{3.86b}$$

Substituting equations (3.83a) and (3.86a) into equation (3.85a) and equations (3.83b) and (3.86b) into equation (3.85b), the following expressions are obtained for the spring distortions.

$$\Delta_f = \begin{bmatrix} 1 & a_f \end{bmatrix}\{d\} - [S_{mj}]_f [G]\{z_b\} \tag{3.87a}$$

$$\Delta_r = \begin{bmatrix} 1 & -a_r \end{bmatrix}\{d\} - [S_{mj}]_r [G]\{z_b\} \tag{3.87b}$$

The time derivatives Δ_f and Δ_r are given by

$$\dot{\Delta}_f = \begin{bmatrix} 1 & a_f \end{bmatrix}\{\dot{d}\} - [S_{mj}]_f [G]\{\dot{z}_b\} - [\dot{S}_{mj}]_f [G]\{z_b\} \tag{3.88a}$$

$$\dot{\Delta}_r = \begin{bmatrix} 1 & -a_r \end{bmatrix}\{\dot{d}\} - [S_{mj}]_r [G]\{\dot{z}_b\} - [\dot{S}_{mj}]_r [G]\{z_b\} \tag{3.88b}$$

The forces F_f and F_r at the front and rear of the vehicle body respectively due to the springs and

dampers are given by

$$F_f = k_f \Delta_f + c_f \dot{\Delta}_f \tag{3.89a}$$

$$F_r = k_r \Delta_r + c_r \dot{\Delta}_r \tag{3.89b}$$

After some substitutions, the forces F_f and F_r are given by

$$\begin{aligned} F_f = k_f & \left(\begin{bmatrix} 1 & a_f \end{bmatrix} \{d\} - \left[S_{mj} \right]_f [G] \{z_b\} \right) \\ + c_f & \left(\begin{bmatrix} 1 & a_f \end{bmatrix} \{\dot{d}\} - \left[\dot{S}_{mj} \right]_f [G] \{z_b\} - \left[S_{mj} \right]_f [G] \{\dot{z}_b\} \right) \end{aligned} \tag{3.90a}$$

$$\begin{aligned} F_r = k_r & \left(\begin{bmatrix} 1 & -a_r \end{bmatrix} \{d\} - \left[S_{mj} \right]_r [G] \{z_b\} \right) \\ + c_r & \left(\begin{bmatrix} 1 & -a_r \end{bmatrix} \{\dot{d}\} - \left[\dot{S}_{mj} \right]_r [G] \{z_b\} - \left[S_{mj} \right]_r [G] \{\dot{z}_b\} \right) \end{aligned} \tag{3.90b}$$

The equations of dynamic equilibrium of the vehicle body is obtained by using the principle of virtual displacement. The equilibrium of forces in the vertical direction is obtained by giving a virtual displacement δd_1 to the vehicle body. The equation of virtual work then becomes

$$-F_f \delta \eta_f - F_r \delta \eta_r - m_s \ddot{d}_1 \delta d_1 = 0 \tag{3.91}$$

where the virtual displacements $\delta \eta_f$ and $\delta \eta_r$ due to the virtual displacement δd_1 are given by

$$\delta \eta_f = \delta d_1 \tag{3.92a}$$

$$\delta \eta_r = \delta d_1 \tag{3.92b}$$

Substituting the expressions for the forces F_f and F_r from equations (3.90a) and (3.90b) and also the expressions for the virtual displacements $\delta\eta_f$ and $\delta\eta_r$ from equations (3.92a) and (3.92b) into equation (3.91) gives

$$
\begin{aligned}
&-\left(k_f\left(\begin{bmatrix}1 & a_f\end{bmatrix}\{d\}-\left[S_{mj}\right]_f[G]\{z_b\}\right)+c_f\left(\begin{bmatrix}1 & a_f\end{bmatrix}\{\dot{d}\}-\left[\dot{S}_{mj}\right]_f[G]\{z_b\}-\left[S_{mj}\right]_f[G]\{\dot{z}_b\}\right)\right)(\delta d_1)\\
&-\left(k_r\left(\begin{bmatrix}1 & -a_r\end{bmatrix}\{d\}-\left[S_{mj}\right]_r[G]\{z_b\}\right)+c_r\left(\begin{bmatrix}1 & -a_r\end{bmatrix}\{\dot{d}\}-\left[\dot{S}_{mj}\right]_r\{z_b\}-\left[S_{mj}\right]_r[G]\{\dot{z}_b\}\right)\right)(\delta d_1)\\
&-m_s\ddot{d}_1\,\delta d_1=0
\end{aligned}
\tag{3.93}
$$

Factoring out minus δd_1 and rearranging of equation (3.93) produces

$$
\begin{aligned}
&\left(\left(k_f+k_r\right)d_1+\left(a_fk_f-a_rk_r\right)sd_2+\left(c_f+c_r\right)\dot{d}_1+\left(a_fc_f-a_rc_r\right)s\dot{d}_2+m_s\ddot{d}_1\right.\\
&-\left(k_f\left[S_{mj}\right]_f+k_r\left[S_{mj}\right]_r+c_f\left[\dot{S}_{mj}\right]_f+c_r\left[\dot{S}_{mj}\right]_r\right)[G]\{z_b\}\\
&\left.-\left(c_f\left[S_{mj}\right]_f+c_r\left[S_{mj}\right]_r\right)[G]\{\dot{z}_b\}\right)(-\delta d_1)=0
\end{aligned}
\tag{3.94}
$$

The moment equilibrium of forces about the transverse direction is obtained by giving a virtual displacement δd_2 to the vehicle body. The equation of virtual work then becomes

$$
-F_f\delta\eta_f+F_r\left(-\delta\eta_r\right)-i_{s2}\ddot{d}_2\,\delta d_2=0 \tag{3.95}
$$

where the virtual displacements $\delta\eta_f$ and $\delta\eta_r$ due to the virtual displacement δd_2 are given by

$$\delta\eta_f = a_f s\delta d_2 \tag{3.96a}$$

$$\delta\eta_r = -a_r s\delta d_2 \tag{3.96b}$$

Substituting the expressions for the forces F_f and F_r from equations (3.90a) and (3.90b) and also the expressions for the virtual displacements $\delta\eta_f$ and $\delta\eta_r$ from equations (3.96a) and (3.96b) into equation (3.95) gives

$$\begin{aligned}
&-\left(k_f\left(\begin{bmatrix}1 & a_f\end{bmatrix}\{d\} - \left[S_{mj}\right]_f[G]\{z_b\}\right) + c_f\left(\begin{bmatrix}1 & a_f\end{bmatrix}\{\dot{d}\} - \left[\dot{S}_{mj}\right]_f[G]\{z_b\} - \left[S_{mj}\right]_f[G]\{\dot{z}_b\}\right)\right)\left(a_f s\delta d_2\right)\\
&+\left(k_r\left(\begin{bmatrix}1 & -a_r\end{bmatrix}\{d\} - \left[S_{mj}\right]_r[G]\{z_b\}\right) + c_r\left(\begin{bmatrix}1 & -a_r\end{bmatrix}\{\dot{d}\} - \left[\dot{S}_{mj}\right]_r[G]\{z_b\} - \left[S_{mj}\right]_r[G]\{\dot{z}_b\}\right)\right)\left(a_r s\delta d_2\right)\\
&-\frac{i_{s2}}{s^2}\ddot{sd}_2\, s\delta d_2 = 0
\end{aligned} \tag{3.97}$$

Factoring out minus $s\delta d_2$ and rearranging of equation (3.97) produces

$$\begin{aligned}
&\left(\left(a_f k_f - a_r k_r\right)d_1 + \left(a_f^2 k_f + a_r^2 k_r\right)sd_2 + \left(a_f c_f - a_r c_r\right)\dot{d}_1 + \left(a_f^2 c_f + a_r^2 c_r\right)s\dot{d}_2\right.\\
&+\frac{i_{s2}}{s^2}s\ddot{d}_2 - \left(a_f k_f\left[S_{mj}\right]_f - a_r k_r\left[S_{mj}\right]_r + a_f c_f\left[\dot{S}_{mj}\right]_f - a_r c_r\left[\dot{S}_{mj}\right]_r\right)[G]\{z_b\}\\
&\left.-\left(a_f c_f\left[S_{mj}\right]_f - a_r c_r\left[S_{mj}\right]_r\right)[G]\{\dot{z}_b\}\right)\left(-s\delta d_2\right) = 0
\end{aligned} \tag{3.98}$$

Since the virtual displacements are arbitrary, the terms δd_1 and δd_2 can take on any value, including zero. This means that the multipliers of δd_1 and δd_2 in equations (3.94) and (3.98) respectively must each equal zero.

$$\begin{aligned}&\left(k_f + k_r\right)d_1 + \left(a_f k_f - a_r k_r\right)s d_2 + \left(c_f + c_r\right)\dot{d}_1 + \left(a_f c_f - a_r c_r\right)s\dot{d}_2 \\ &+ m_s \ddot{d}_1 - \left(k_f\left[S_{mj}\right]_f + k_r\left[S_{mj}\right]_r + c_f\left[\dot{S}_{mj}\right]_f + c_r\left[\dot{S}_{mj}\right]_r\right)[G]\{z_b\} \\ &-\left(c_f\left[S_{mj}\right]_f + c_r\left[S_{mj}\right]_r\right)\{\dot{z}_b\} = 0\end{aligned} \tag{3.99}$$

and

$$\begin{aligned}&\left(a_f k_f - a_r k_r\right)d_1 + \left(a_f^2 k_f + a_r^2 k_r\right)s d_2 + \left(a_f c_f - a_r c_r\right)\dot{d}_1 + \left(a_f^2 c_f + a_r^2 c_r\right)s\dot{d}_2 + \frac{i_{s2}}{s^2}s\ddot{d}_2 \\ &-\left(a_f k_f\left[S_{mj}\right]_f - a_r k_r\left[S_{mj}\right]_r + a_f c_f\left[\dot{S}_{mj}\right]_f - a_r c_r\left[\dot{S}_{mj}\right]_r\right)[G]\{z_b\} \\ &-\left(a_f c_f\left[S_{mj}\right]_f - a_r c_r\left[S_{mj}\right]_r\right)[G]\{\dot{z}_b\} = 0\end{aligned} \tag{3.100}$$

Equations (3.99) and (3.100) can be expressed in the following matrix form.

$$\left[M_v\right]\{\ddot{d}\} + \left[C_v\right]\{\dot{d}\} + \left[K_v\right]\{d\} + \left[C_{HI}\right]\{\dot{z}_b\} + \left[K_{HI}\right]\{z_b\} = \{0\} \tag{3.101}$$

where

$$\left[M_v\right] = \begin{bmatrix} m_s & 0 \\ 0 & \frac{i_{s2}}{s^2} \end{bmatrix}$$

$$[K_v]=\begin{bmatrix} k_f+k_r & a_f k_f - a_r k_r \\ a_f k_f - a_r k_r & a_f^2 k_f + a_r^2 k_r \end{bmatrix}$$

$$[C_v]=\begin{bmatrix} c_f+c_r & a_f c_f - a_r c_r \\ a_f c_f - a_r c_r & a_f^2 c_f + a_r^2 c_r \end{bmatrix}$$

$$[C_{HI}]=\begin{bmatrix} -c_f \\ -a_f c_f \end{bmatrix}[S_{mj}]_f[G]+\begin{bmatrix} -c_r \\ a_r c_r \end{bmatrix}[S_{mj}]_r[G]$$

$$[K_{HI}]=\left(\begin{bmatrix} -k_f \\ -a_f k_f \end{bmatrix}[S_{mj}]_f[G]+\begin{bmatrix} -c_f \\ -a_f c_f \end{bmatrix}[\dot{S}_{mj}[G]]_f\right)+\left(\begin{bmatrix} -k_r \\ a_r k_r \end{bmatrix}[S_{mj}]_r[G]+\begin{bmatrix} -c_r \\ a_r c_r \end{bmatrix}[\dot{S}_{mj}[G]]_r\right)$$

$[M_v]$, $[C_v]$ and $[K_v]$ are respectively, the mass, damping, and stiffness matrices of the vehicle. $[C_{HI}]$ and $[K_{HI}]$ are two matrices that couple the motion of the vehicle with that of the bridge.

The vehicle displacements can be expressed in terms of modal coordinates by means of a transformation.

$$\{d\}=[\Phi_v]\{z_v\} \tag{3.102}$$

where $\{z_v\}$ is a vector of transformed coordinate called modal coordinates and $[\Phi_v]$ is a (2 x 2) matrix formed by arranging side by side the two mode shapes of the vehicle. This matrix is referred to as the modal matrix of the vehicle.

Substituting equation (3.102) into equation (3.101) and pre-multiplying both sides of it by $[\Phi_v]^T$ the equation of motion of the vehicle can be obtained in the following form.

$$[M_v^*]\{\ddot{z}_v\} + [C_v^*]\{\dot{z}_v\} + [\Lambda_v]\{z_v\} + [C_{HI}^*]\{\dot{z}_b\} + [K_{HI}^*]\{z_b\} = \{0\} \qquad (3.103)$$

where

$$[\Lambda_v] = [\Phi_v]^T[K_v][\Phi_v] \qquad [C_v^*] = [\Phi_v]^T[C_v][\Phi_v]$$

$$[C^*_{HI}] = [\Phi_v]^T\begin{bmatrix} -c_f \\ -a_f c_f \end{bmatrix}[S_{mj}]_f[G] + [\Phi_v]^T\begin{bmatrix} -c_r \\ a_r c_r \end{bmatrix}[S_{mj}]_r[G]$$

$$[K^*_{HI}] = [\Phi_v]^T\left(\begin{bmatrix} -k_f \\ -a_f k_f \end{bmatrix}[S_{mj}]_f[G] + \begin{bmatrix} -c_f \\ -a_f c_f \end{bmatrix}[\dot{S}_{mj}]_f[G]\right)$$
$$+[\Phi_v]^T\left(\begin{bmatrix} -k_r \\ a_r k_r \end{bmatrix}[S_{mj}]_r[G] + \begin{bmatrix} -c_r \\ a_r c_r \end{bmatrix}[\dot{S}_{mj}]_r[G]\right)$$

$[\Lambda_v]$, $[M^*_v]$ and $[C^*_v]$ are respectively the spectral matrix, the modal mass matrix and the modal damping matrix of the vehicle.

The forces exerted on the bridge by the moving vehicle at the contact points are given by

$$
\begin{aligned}
f_f = {} & k_f\begin{bmatrix}1 & a_f\end{bmatrix}\{d\} + c_f\begin{bmatrix}1 & a_f\end{bmatrix}\left\{\dot{d}\right\} \\
& -\left(k_f\left[S_{mj}\right]_f + c_f\left[\dot{S}_{mj}\right]_f + m_{uf}\left[\ddot{S}_{mj}\right]_f\right)[G]\{z_b\} \\
& -\left(c_f\left[S_{mj}\right]_f + 2m_{uf}\left[\dot{S}_{mj}\right]_f\right)[G]\left\{\dot{z}_b\right\} \\
& -\left(m_{uf}\left[S_{mj}\right]_f\right)[G]\left\{\ddot{z}_b\right\} \\
& +\left(m_{uf} + a_r m_s\right)g
\end{aligned}
\tag{3.104a}
$$

and

$$
\begin{aligned}
f_r = {} & \begin{bmatrix}k_r & -a_r k_r\end{bmatrix}\begin{Bmatrix}d_1 \\ sd_2\end{Bmatrix} + \begin{bmatrix}c_r & -a_r c_r\end{bmatrix}\begin{Bmatrix}\dot{d}_1 \\ s\dot{d}_2\end{Bmatrix} \\
& -\left(k_r\left[S_{mj}\right]_r + c_r\left[\dot{S}_{mj}\right]_r + m_{ur}\left[\ddot{S}_{mj}\right]_r\right)[G]\{z_b\} \\
& -\left(c_r\left[S_{mj}\right]_r + 2m_{ur}\left[\dot{S}_{mj}\right]_r\right)[G]\left\{\dot{z}_b\right\} - m_{ur}\left[S_{mj}\right]_r[G]\left\{\ddot{z}_b\right\} \\
& +\left(m_{ur} + a_f m_s\right)g
\end{aligned}
\tag{3.104b}
$$

The contact forces f_f and f_r act as external forces on the bridge and the equations of equilibrium of bridge motion become

$$[M_b^*]\{\ddot{z}_b\} + [C_b^*]\{\dot{z}_b\} + [\Lambda_b]\{z_b\} = [G]^T\left([S_{mj}]_f^T f_f + [S_{mj}]_r^T f_r\right) \quad (3.105a)$$

where $[\Lambda_b]$, $[C^*_b]$ and $[M^*_b]$ are as defined in equation (3.48).

In order to obtain the response of the bridge under the action of the moving vehicle, equations (3.103) and (3.105a) are solved simultaneously.

Substituting the expressions for the forces f_f and f_r from equations (3.104a) and (3.104b) into equation (3.105a) and combining the result with equation (3.103) produces the following equations of motion of the bridge-vehicle system.

$$\begin{bmatrix} ([M_b^*]+[M_I]) & [0] \\ [0] & [M_v^*] \end{bmatrix} \begin{Bmatrix} \{\ddot{z}_b\} \\ \{\ddot{z}_v\} \end{Bmatrix} + \begin{bmatrix} ([C^*_b]+[C_I]) & [C^*_{VI}] \\ [C^*_{HI}] & [C^*_v] \end{bmatrix} \begin{Bmatrix} \{\dot{z}_b\} \\ \{\dot{z}_v\} \end{Bmatrix} + \begin{bmatrix} ([\Lambda_b]+[K_I]) & [K^*_{VI}] \\ [K^*_{HI}] & [\Lambda_v] \end{bmatrix} \begin{Bmatrix} \{z_b\} \\ \{z_v\} \end{Bmatrix} = \begin{Bmatrix} \{F^*\} \\ \{0\} \end{Bmatrix} \quad (3.105b)$$

where

$$[M_I]_{NM\times NM} = m_{uf}[G]^T[S_{mj}]_f^T[S_{mj}]_f[G] + m_{ur}[G]^T[S_{mj}]_r^T[S_{mj}]_r[G]$$

$$[C_I]_{NM\times NM} = [G]^T[S_{mj}]_f^T\left(c_f[S_{mj}]_f + 2m_{uf}[\dot{S}_{mj}]_f\right)[G] + [G]^T[S_{mj}]_r^T\left(c_r[S_{mj}]_r + 2m_{ur}[\dot{S}_{mj}]_r\right)[G]$$

$$[K_I]_{NMxNM} = [G]^T[S_{mj}]_f^T\left(k_f[S_{mj}]_f + c_f[\dot{S}_{mj}]_f + m_{uf}[\ddot{S}_{mj}]_f\right)[G]$$
$$+[G]^T[S_{mj}]_r^T\left(k_r[S_{mj}]_r + c_r[\dot{S}_{mj}]_r + m_{ur}[\ddot{S}_{mj}]_r\right)[G]$$

$$[K_{VI}]_{NMx2} = -[G]^T[S_{mj}]_f^T[k_f \quad a_f k_f][\Phi_v] - [G]^T[S_{mj}]_r^T[k_r \quad -a_r k_r][\Phi_v]$$

$$[C_{VI}]_{NMx2} = -[G]^T[S_{mj}]_f^T[c_f \quad a_f c_f][\Phi_v] - [G]^T[S_{mj}]_r^T[c_r \quad -a_r c_r][\Phi_v]$$

$$\{F^*\}_{NMx1} = [G]^T[S_{mj}]_f^T\left(m_{uf} + a_r m_s\right) + [G]^T[S_{mj}]_r^T\left(m_{ur} + a_f m_s\right)$$

$[K^*_{HI}]$ and $[C^*_{HI}]$ are defined in equation (3.103)

The motion of the bridge is coupled with that of the vehicle through the matrices $[K^*_{VI}]$ and $[C^*_{VI}]$. To ensure that any wheel load outside the bridge will not be included in computing the response of the bridge, the terms that are associated with that wheel should not be included in the formation of the matrices $[K^*_{VI}]$, $[C^*_{VI}]$, $[K^*_{HI}]$, $[C^*_{HI}]$, $[K_I]$, $[C_I]$, and $[M_I]$ and the load vector $\{F^*\}$.

3.7.5 Response Under a Two-axle Four-wheel Vehicle Model

In this section the dynamic behavior of the moving vehicle is represented by a sprung mass, m_s, with mass moments of inertia i_{s1} and i_{s2} for pitching and rolling motions, and unsprung masses, m_{uf} and m_{ur} (Figure 3.5). The sprung mass is supported by a system of springs and dash-pots on two axle, four wheels which are assumed to be always in contact with the bridge surface. The dash-pots provide viscous damping in the system. The mass of the suspension system, axles, drive shafts, brakes and wheels represent the unsprung masses in the system. The sprung mass of the vehicle body has three independent degrees of freedom d_{s3}, d_{s4} and d_{s5} which are the bouncing effect, the lateral rolling effect and the pitching effect in the vehicle respectively. The yawning motion is neglected as it contributes little to the response of the bridge-vehicle system. Translations along the transverse and longitudinal directions don not contribute to the response of the bridge-vehicle system as they are assumed to be rigid motions. The unsprung masses are assumed to be concentrated at the centers of the front and rear axles. The displacements of the unsprung masses d_{uf3}, d_{ur3}, d_{uf5} and d_{ur5} are not independent but are related to the vertical displacements of the contact points between the wheels and the bridge surface. The vehicle thus contributes three degrees of freedom to the overall degrees of freedom of the vehicle-bridge system. Hence the degrees of freedom of the bridge-vehicle system becomes $(N+3)$.

3.7.5.1 Equations of Motion of the Sprung Mass

The displacements at the front-left, front-right, rear-left and rear-right axles η_{fl}, η_{fr}, η_{rl}, and η_{rr} are related to the three degrees of freedom d_{s3}, d_{s4} and d_{s5} of the vehicle body by the following relationship:

$$\eta_{fl} = \begin{bmatrix} 1 & a_f & a_t \end{bmatrix} \begin{Bmatrix} d_{s3} \\ sd_{s4} \\ bd_{s5} \end{Bmatrix} \tag{3.106a}$$

$$\eta_{fr} = \begin{bmatrix} 1 & a_f & -a_t \end{bmatrix} \begin{Bmatrix} d_{s3} \\ sd_{s4} \\ bd_{s5} \end{Bmatrix} \tag{3.106b}$$

$$\eta_{rl} = \begin{bmatrix} 1 & -a_r & a_t \end{bmatrix} \begin{Bmatrix} d_{s3} \\ sd_{s4} \\ bd_{s5} \end{Bmatrix} \tag{3.106c}$$

$$\eta_{rr} = \begin{bmatrix} 1 & -a_r & -a_t \end{bmatrix} \begin{Bmatrix} d_{s3} \\ sd_{s4} \\ bd_{s5} \end{Bmatrix} \tag{3.106d}$$

where a_f, a_r and a_t are defined in Figure 3.5.

The change of length of the front-right and front-left vehicle springs are respectively given by

$$\Delta_{fl} = \eta_{fl} - \left(\frac{1}{2} + a_t\right) w_{fl} - \left(\frac{1}{2} - a_t\right) w_{fr} \tag{3.107a}$$

and

$$\Delta_{fl} = \eta_{fl} - \left(\frac{1}{2} + a_t\right) w_{fl} - \left(\frac{1}{2} - a_t\right) w_{fl} \tag{3.107b}$$

where w_{fl} and w_{fl} are the vertical displacements at the contact points between the bridge and the front-left and front-right wheel of the vehicle respectively.

Similarly the change of length of the rear-left and the rear-right vehicle springs are respectively given by

$$\Delta_{rl} = \eta_{rl} - \left(\frac{1}{2} + a_t\right) w_{rl} - \left(\frac{1}{2} - a_t\right) w_{rl} \tag{3.107c}$$

and

$$\Delta_{rl} = \eta_{rl} - \left(\frac{1}{2} + a_t\right) w_{rl} - \left(\frac{1}{2} - a_t\right) w_{rl} \tag{3.107d}$$

where w_{rl} and w_{rl} are the vertical displacements at the contact points between the bridge and the rear-left and rear-right wheel of the vehicle.

The vertical displacements at the contact points are given by

$$w_{fl} = [N][G]_j \{z_b\} \sin\frac{m_j \pi}{l}(vt - s_f) \tag{3.108a}$$

$$w_{fl} = [N][G]_i \{z_b\} \sin\frac{m_j \pi}{l}(vt - s_f) \tag{3.108b}$$

$$w_{rl} = [N][G]_j \{z_b\} \sin\frac{m_j \pi}{l}(vt - s_r) \tag{3.108c}$$

$$w_{ri} = [N][G]_i \{z_b\} \sin \frac{m_j \pi}{l}(vt - s_r) \tag{3.108d}$$

Substituting equations (3.106a-b) and (3.108a-b) into equations (3.107a-b) and equations (3.106c-d) and (3.108c-d) into equations (3.107c-d), the following expressions are obtained for the spring distortions.

$$\Delta_{fij} = \begin{bmatrix} 1 \\ a_f \\ a_t \end{bmatrix}^T \{d\} - \left(\frac{1}{2} + a_t\right)[S_{mj}]_f [G]_j \{z_b\} - \left(\frac{1}{2} - a_t\right)[S_{mj}]_f [G]_i \{z_b\} \tag{3.109a}$$

$$\Delta_{fri} = \begin{bmatrix} 1 \\ a_f \\ -a_t \end{bmatrix}^T \{d\} - \left(\frac{1}{2} + a_t\right)[S_{mj}]_f [G]_i \{z_b\} - \left(\frac{1}{2} - a_t\right)[S_{mj}]_f [G]_j \{z_b\} \tag{3.109b}$$

$$\Delta_{rij} = \begin{bmatrix} 1 \\ -a_r \\ a_t \end{bmatrix}^T \{d\} - \left(\frac{1}{2} + a_t\right)[S_{mj}]_r [G]_j \{z_b\} - \left(\frac{1}{2} - a_t\right)[S_{mj}]_r [G]_i \{z_b\} \tag{3.109c}$$

$$\Delta_{rri} = \begin{bmatrix} 1 \\ -a_r \\ -a_t \end{bmatrix}^T \{d\} - \left(\frac{1}{2} + a_t\right)[S_{mj}]_r [G]_i \{z_b\} - \left(\frac{1}{2} - a_t\right)[S_{mj}]_r [G]_j \{z_b\} \tag{3.109d}$$

where

$$\{d\} = \begin{Bmatrix} d_1 \\ sd_2 \\ bd_3 \end{Bmatrix}$$

The time derivatives *of* Δ_{fi}, Δ_{fj}, Δ_{ri} and Δ_{rj} are given by

$$\dot{\Delta}_{fj} = \begin{bmatrix} 1 \\ a_f \\ a_t \end{bmatrix}^T \{\dot{d}\} - \left(\frac{1}{2} + a_t\right)[S_{mj}]_f [G]_j \{\dot{z}_b\} \\ -\left(\frac{1}{2} + a_t\right)[\dot{S}_{mj}]_f [G]_j \{z_b\} - \left(\frac{1}{2} - a_t\right)[S_{mj}]_f [G]_i \{\dot{z}_b\} - \left(\frac{1}{2} - a_t\right)[\dot{S}_{mj}]_f [G]_i \{z_b\} \tag{3.110a}$$

$$\dot{\Delta}_{fi} = \begin{bmatrix} 1 \\ a_f \\ -a_t \end{bmatrix}^T \{\dot{d}\} - \left(\frac{1}{2} + a_t\right)[\dot{S}_{mj}]_f [G]_i \{z_b\} - \left(\frac{1}{2} + a_t\right)[S_{mj}]_f [G]_i \{\dot{z}_b\} \\ -\left(\frac{1}{2} - a_t\right)[\dot{S}_{mj}]_f [G]_j \{z_b\} - \left(\frac{1}{2} - a_t\right)[S_{mj}]_f [G]_j \{\dot{z}_b\} \tag{3.110b}$$

$$\dot{\Delta}_{rj} = \begin{bmatrix} 1 \\ -a_r \\ a_t \end{bmatrix}^T \{\dot{d}\} - \left(\frac{1}{2} + a_t\right)[S_{mj}]_r [G]_j \{\dot{z}_b\} - \left(\frac{1}{2} + a_t\right)[\dot{S}_{mj}]_r [G]_j \{z_b\} - \left(\frac{1}{2} - a_t\right)[\dot{S}_{mj}]_r [G]_i \{z_b\} - \left(\frac{1}{2} - a_t\right)[S_{mj}]_r [G]_i \{\dot{z}_b\} \quad (3.110c)$$

$$\dot{\Delta}_{ri} = \begin{bmatrix} 1 \\ -a_r \\ -a_t \end{bmatrix}^T \{\dot{d}\} - \left(\frac{1}{2} + a_t\right)[\dot{S}_{mj}]_r [G]_i \{z_b\} - \left(\frac{1}{2} + a_t\right)[S_{mj}]_r [G]_i \{\dot{z}_b\} - \left(\frac{1}{2} - a_t\right)[\dot{S}_{mj}]_r [G]_j \{z_b\} - \left(\frac{1}{2} - a_t\right)[S_{mj}]_r [G]_j \{\dot{z}_b\} \quad (3.110d)$$

The forces at the front-left, front-right, rear-left and rear-right of the vehicle body due to the springs and dampers which are denoted by F_{fl}, F_{fr}, F_{rl} and F_{rr} respectively are given by

$$F_{fl} = k_f \Delta_{fl} + c_f \dot{\Delta}_{fl} \quad (3.111a)$$

$$F_{fr} = k_f \Delta_{fr} + c_f \dot{\Delta}_{fr} \quad (3.111b)$$

$$F_{rl} = k_r \Delta_{rl} + c_r \dot{\Delta}_{rl} \quad (3.111c)$$

$$F_{rr} = k_r \Delta_{rr} + c_r \dot{\Delta}_{rr} \quad (3.111d)$$

Substituting equations (3.109a-b) and equations (3.110a-b) into equations (3.111a-b) and equations (3.109c-d) and equations (3.110c-d) into equations (3.111c-d), the following equations

are obtained for the forces F_{fi}, F_{fj}, F_{ri} and F_{rj}.

$$F_{fi} = k_f \begin{bmatrix} 1 \\ a_f \\ a_t \end{bmatrix}^T \{d\} + c_f \begin{bmatrix} 1 \\ a_f \\ a_t \end{bmatrix}^T \{\dot{d}\}$$
$$-\left(\left(\frac{1}{2}+a_t\right) c_f \left[S_{mj}\right]_f [G]_j + \left(\frac{1}{2}-a_t\right) c_f \left[S_{mj}\right]_f [G]_i\right) \{\dot{z}_b\} \qquad (3.112a)$$
$$-\left(\left(\frac{1}{2}+a_t\right)\left(k_f \left[S_{mj}\right]_f + c_f \left[\dot{S}_{mj}\right]_f\right)[G]_j + \left(\frac{1}{2}-a_t\right)\left(k_f \left[S_{mj}\right]_f + c_f \left[\dot{S}_{mj}\right]_f\right)[G]_i\right) \{z_b\}$$

$$F_{fi} = k_f \begin{bmatrix} 1 \\ a_f \\ -a_t \end{bmatrix}^T \{d\} + c_f \begin{bmatrix} 1 \\ a_f \\ -a_t \end{bmatrix}^T \{\dot{d}\}$$
$$-\left(\left(\frac{1}{2}+a_t\right) c_f \left[S_{mj}\right]_f [G]_i + \left(\frac{1}{2}-a_t\right) c_f \left[S_{mj}\right]_f [G]_j\right) \{\dot{z}_b\} \qquad (3.112b)$$
$$-\left(\left(\frac{1}{2}+a_t\right)\left(k_f \left[S_{mj}\right]_f + c_f \left[\dot{S}_{mj}\right]_f\right)[G]_i + \left(\frac{1}{2}-a_t\right)\left(k_f \left[S_{mj}\right]_f + c_f \left[\dot{S}_{mj}\right]_f\right)[G]_j\right) \{z_b\}$$

$$
\begin{aligned}
F_{rj} &= k_r \begin{bmatrix} 1 \\ -a_r \\ a_t \end{bmatrix}^T \{d\} + c_r \begin{bmatrix} 1 \\ -a_r \\ a_t \end{bmatrix}^T \{\dot{d}\} \\
&-\left(\left(\frac{1}{2}+a_t\right) c_r \left[S_{mj}\right]_r [G]_j + \left(\frac{1}{2}-a_t\right) c_r \left[S_{mj}\right]_r [G]_i\right)\{\dot{z}_b\} \\
&-\left(\left(\frac{1}{2}+a_t\right)\left(k_r \left[S_{mj}\right]_r + c_r \left[\dot{S}_{mj}\right]_r\right)[G]_j + \left(\frac{1}{2}-a_t\right)\left(k_r \left[S_{mj}\right]_r + c_r \left[\dot{S}_{mj}\right]_r\right)[G]_i\right)\{z_b\}
\end{aligned}
\tag{3.112c}
$$

$$
\begin{aligned}
F_{rl} &= k_r \begin{bmatrix} 1 \\ -a_r \\ -a_t \end{bmatrix}^T \{d\} + c_r \begin{bmatrix} 1 \\ -a_r \\ -a_t \end{bmatrix}^T \{\dot{d}\} \\
&-\left(\left(\frac{1}{2}+a_t\right) c_r \left[S_{mj}\right]_r [G]_i + \left(\frac{1}{2}-a_t\right) c_r \left[S_{mj}\right]_r [G]_j\right)\{\dot{z}_b\} \\
&-\left(\left(\frac{1}{2}+a_t\right)\left(k_r \left[S_{mj}\right]_r + c_r \left[\dot{S}_{mj}\right]_r\right)[G]_i + \left(\frac{1}{2}-a_t\right)\left(k_r \left[S_{mj}\right]_r + c_r \left[\dot{S}_{mj}\right]_r\right)[G]_j\right)\{z_b\}
\end{aligned}
\tag{3.112d}
$$

The equations of motion of the vehicle body are obtained by using the principle of virtual displacement. Three independent virtual displacements are given to the vehicle body to obtain the three equations of equilibrium.

The first equilibrium equation, equilibrium of forces in the vertical direction, e_3, is obtained by giving a virtual displacements δd_{s3} to the vehicle body. The equation of virtual work then becomes

$$-F_{fj}\delta\eta_{fj} - F_{fi}\delta\eta_{fi} - \delta\eta_{rj}F_{rj} - \delta\eta_{ri}F_{ri} - m_s\ddot{d}_{s3}\,\delta d_{s3} = 0 \tag{3.113}$$

where the virtual displacements $\delta\eta_{fi}$, $\delta\eta_{fj}$, $\delta\eta_{ri}$ and $\delta\eta_{rj}$ due to the virtual displacement δd_{s3} are given by

$$\delta\eta_{fi} = \delta\eta_{fj} = \delta\eta_{ri} = \delta\eta_{rj} = \delta d_{s3} \tag{3.114}$$

Substituting the expressions for the virtual displacements $\delta\eta_{fi}$, $\delta\eta_{fj}$, $\delta\eta_{ri}$ and $\delta\eta_{rj}$ due to the virtual displacement δd_{s3} from equation (3.114) into equation (3.113) gives

$$-\left(F_{fi} + F_{fj} + F_{ri} + F_{rj} + m_s\ddot{d}_{s3}\right)\delta d_{s3} = 0 \tag{3.115}$$

Since the virtual displacements are arbitrary, the terms δd_{s3} can take on any value, including zero. This means that the multiplier of δd_{s3} in equation (3.115) must equal zero.

$$F_{fi} + F_{fj} + F_{ri} + F_{rj} + m_s\ddot{d}_{s3} = 0 \tag{3.116}$$

Substituting the expressions for the forces F_{fi}, F_{fj}, F_{ri} and F_{rj} from equations (3.112a-d) into equation (3.116) gives

$$\begin{aligned}
&\begin{bmatrix} 2(k_f + k_r) & 2(a_f k_f - a_r k_r) & 0 \end{bmatrix}\{d\} \\
&+\begin{bmatrix} 2(c_f + c_r) & 2(a_f c_f - a_r c_r) & 0 \end{bmatrix}\{\dot{d}\} + \begin{bmatrix} m_s & 0 & 0 \end{bmatrix}\{\ddot{d}\} \\
&-\Big(\left(k_f[S_{mj}]_f + c_f[\dot{S}_{mj}]_f\right)[G]_j + \left(k_f[S_{mj}]_f + c_f[\dot{S}_{mj}]_f\right)[G]_i \\
&+\left(k_r[S_{mj}]_r + c_r[\dot{S}_{mj}]_r\right)[G]_j + \left(k_r[S_{mj}]_r + c_r[\dot{S}_{mj}]_r\right)[G]_i\Big)\{z_b\} \\
&-\left(c_f[S_{mj}]_f[G]_j + c_f[S_{mj}]_f[G]_i + c_r[S_{mj}]_r[G]_j + c_r[S_{mj}]_r[G]_i\right)\{\dot{z}_b\} = 0
\end{aligned} \tag{3.117}$$

The second equilibrium equation, moment equilibrium of forces about the transverse direction, e_1, is obtained by giving a virtual displacements δds_4 to the vehicle body. The equation of virtual work then becomes

$$-F_{fl}\delta\eta_{fl} - F_{fr}\delta\eta_{fr} + F_{rl}\left(-\delta\eta_{rl}\right) + F_{rr}\left(-\delta\eta_{rr}\right) - i_{s1}\ddot{d}_{s4}\delta d_{s4} = 0 \tag{3.118}$$

where the virtual displacements $\delta\eta_{fl}$, $\delta\eta_{fr}$, $\delta\eta_{rl}$ and $\delta\eta_{rr}$ due to the virtual displacement δd_{s4} are given by

$$\delta\eta_{fl} = \delta\eta_{fr} = a_f s\delta d_{s4} \qquad \& \qquad \delta\eta_{rl} = \delta\eta_{rr} = -a_r s\delta d_{s4} \tag{3.119}$$

Substituting the expressions for the virtual displacements $\delta\eta_{fl}$, $\delta\eta_{fr}$, $\delta\eta_{rl}$ and $\delta\eta_{rr}$ due to the virtual displacement δd_{s4} from the above expressions into equation (3.118) gives

$$-\left(a_f F_{fl} + a_f F_{fr} - a_r F_{rl} - a_r F_{rr} + \frac{i_{s1}}{s^2}s\ddot{d}_{s4}\right)s\delta d_{s4} = 0 \tag{3.120}$$

The multiplier of the virtual displacement δd_{s4} in the above equation must be zero, since the virtual displacement δd_{s4} is arbitrarily chosen and can take on any value, including zero.

$$a_f F_{fl} + a_f F_{fr} - a_r F_{rl} - a_r F_{rr} + \frac{i_{s1}}{s^2}s\ddot{d}_{s4} = 0 \tag{3.121}$$

Substituting the expressions for the forces F_{fl}, F_{fr}, F_{rl} and F_{rr} from equations (3.112a-d) into equation (3.121) gives

$$
\begin{aligned}
&\left[2\left(a_f k_f - a_r k_r\right) \quad 2\left(a_f^{\,2} k_f + a_r^{\,2} k_r\right) \quad 0\right]\{d\} \\
&+\left[2\left(a_f c_f - a_r c_r\right) \quad 2\left(a_f^{\,2} c_f + a_r^{\,2} c_r\right) \quad 0\right]\left\{\dot{d}\right\} + \left[0 \quad \frac{i_{s1}}{s^2} \quad 0\right]\left\{\ddot{d}\right\} \\
&-\Big(a_f\Big(k_f\left[S_{mj}\right]_f + c_f\left[\dot{S}_{mj}\right]_f\Big)[G]_j + a_f\Big(k_f\left[S_{mj}\right]_f + c_f\left[\dot{S}_{mj}\right]_f\Big)[G]_i \\
&-a_r\Big(k_r\left[S_{mj}\right]_r + c_r\left[\dot{S}_{mj}\right]_r\Big)[G]_j + a_r\Big(k_r\left[S_{mj}\right]_r + c_r\left[\dot{S}_{mj}\right]_r\Big)[G]_i\Big)\left\{z_b\right\} \\
&-\Big(a_f\Big(c_f\left[S_{mj}\right]_f[G]_j + c_f\left[S_{mj}\right]_f[G]_i\Big) - a_r\Big(c_r\left[S_{mj}\right]_r[G]_j + c_r\left[S_{mj}\right]_r[G]_i\Big)\Big)\left\{\dot{z}_b\right\} = 0
\end{aligned}
\tag{3.122}
$$

The third equilibrium equation, moment equilibrium about the longitudinal axis, e_3, is obtained by giving a virtual displacements δd_{s5} to the vehicle body. The equation of virtual work then becomes

$$
-F_{fj}\delta\eta_{fj} + F_{fi}\left(-\delta\eta_{fi}\right) - F_{rj}\delta\eta_{rj} + F_{ri}\left(-\delta\eta_{ri}\right) - i_{s2}\,\ddot{d}_{s5}\,\delta d_{s5} = 0 \tag{3.123}
$$

where the virtual displacements $\delta\eta_{fi}$, $\delta\eta_{fj}$, $\delta\eta_{ri}$ and $\delta\eta_{rj}$ due to the virtual displacement δd_{s5} are given by

$$
\delta\eta_{fj} = \delta\eta_{rj} = a_t b\,\delta d_{s5} \qquad \& \qquad \delta\eta_{fi} = \delta\eta_{ri} = -a_t b\,\delta d_{s5} \tag{3.124}
$$

If the above expressions for the virtual displacements $\delta\eta_{fi}$, $\delta\eta_{fj}$, $\delta\eta_{ri}$ and $\delta\eta_{rj}$ due to the virtual displacement δd_{s5} are substituted into equation (3.123), the following equilibrium equation is obtained

$$-\left(a_t F_{fi} - a_t F_{fi} + a_t F_{ri} - a_t F_{ri} + \frac{i_{s2}}{b^2} b \ddot{d}_{s5}\right) b \delta d_{s5} = 0 \tag{3.125}$$

The multiplier of the virtual displacement δd_{s5} (the term within the braces) in the above equation must be zero, since the virtual displacement δd_{s5} is arbitrary and can take on any value, including zero.

$$a_t F_{fi} - a_t F_{fi} + a_t F_{ri} - a_t F_{ri} + \frac{i_{s2}}{b^2} b \ddot{d}_{s5} = 0 \tag{3.126}$$

Substituting the expressions for the forces F_{fi}, F_{fj}, F_{ri} and F_{rj} from equations (3.112a-d) into equation (3.126) yields

$$\begin{aligned}
&\left[0 \quad 0 \quad 2a_t^2\left(k_f + k_r\right)\right]\{d\} + \left[0 \quad 0 \quad 2a_t^2\left(c_f + c_r\right)\right]\left\{\dot{d}\right\} + \left[0 \quad 0 \quad \frac{i_{s2}}{b^2}\right]\left\{\ddot{d}\right\} \\
&-2a_t^2\left(\left(k_f\left[S_{mj}\right]_f + c_f\left[\dot{S}_{mi}\right]_f\right)[G]_j - \left(k_f\left[S_{mj}\right]_f + c_f\left[\dot{S}_{mi}\right]_f\right)[G]_i\right. \\
&\left.+\left(k_r\left[S_{mj}\right]_r + c_r\left[\dot{S}_{mj}\right]_r\right)[G]_j - \left(k_r\left[S_{mj}\right]_r + c_r\left[\dot{S}_{mj}\right]_r\right)[G]_i\right)\left\{z_b\right\} \\
&-2a_t^2\left(c_f\left[S_{mj}\right]_f[G]_j - c_f\left[S_{mj}\right]_f[G]_i + c_r\left[S_{mj}\right]_r[G]_j - c_r\left[S_{mj}\right]_r[G]_i\right)\left\{\dot{z}_b\right\} = 0
\end{aligned} \tag{3.127}$$

Equations (3.117), (3.122), and (3.127) can be expressed in the following matrix form.

$$[M_v]\{\ddot{d}\} + [C_v]\{\dot{d}\} + [K_v]\{d\} + [C_{HI}]\{\dot{z}_b\} + [K_{HI}]\{z_b\} = 0 \qquad (3.128)$$

where

$$[M_v] = \begin{bmatrix} m_s & 0 & 0 \\ 0 & \frac{i_{s1}}{s^2} & 0 \\ 0 & 0 & \frac{i_{s2}}{b^2} \end{bmatrix}$$

$$[K_v] = \begin{bmatrix} 2(k_f + k_r) & 2(a_f k_f - a_r k_r) & 0 \\ 2(a_f k_f - a_r k_r) & 2(a_f{}^2 k_f + a_r{}^2 k_r) & 0 \\ 0 & 0 & 2a_t{}^2(k_f + k_r) \end{bmatrix}$$

$$[C_v] = \begin{bmatrix} 2(c_f + c_r) & 2(a_f c_f - a_r c_r) & 0 \\ 2(a_f c_f - a_r c_r) & 2(a_f{}^2 c_f + a_r{}^2 c_r) & 0 \\ 0 & 0 & 2a_t{}^2(c_f + c_r) \end{bmatrix}$$

$$[C_{HI}] = \begin{bmatrix} -c_f \\ -a_f c_f \\ -2a_t^2 c_f \end{bmatrix} [S_{mj}]_f [G]_j + \begin{bmatrix} -c_f \\ -a_f c_f \\ 2a_t^2 c_f \end{bmatrix} [S_{mj}]_f [G]_i$$
$$+ \begin{bmatrix} -c_r \\ a_r c_r \\ -2a_t^2 c_r \end{bmatrix} [S_{mj}]_r [G]_j + \begin{bmatrix} -c_r \\ a_r c_r \\ 2a_t^2 c_r \end{bmatrix} [S_{mj}]_r [G]_i$$

$$[K_{HI}] = \begin{bmatrix} -k_f \\ -a_f k_f \\ -2a_t^2 k_f \end{bmatrix} [S_{mj}]_f [G]_j + \begin{bmatrix} -k_f \\ -a_f k_f \\ 2a_t^2 k_f \end{bmatrix} [S_{mj}]_f [G]_i + \begin{bmatrix} -c_f \\ -a_f c_f \\ -2a_t^2 c_f \end{bmatrix} [\dot{S}_{mj}]_f [G]_j + \begin{bmatrix} -c_f \\ -a_f c_f \\ 2a_t^2 c_f \end{bmatrix} [\dot{S}_{mj}]_f [G]_j$$
$$+ \begin{bmatrix} -k_r \\ a_r k_r \\ -2a_t^2 k_r \end{bmatrix} [S_{mj}]_r [G]_j + \begin{bmatrix} -k_r \\ a_r k_r \\ 2a_t^2 k_r \end{bmatrix} [S_{mj}]_r [G]_i + \begin{bmatrix} -c_r \\ a_r c_r \\ -2a_t^2 c_r \end{bmatrix} [\dot{S}_{mj}]_r [G]_j + \begin{bmatrix} -c_r \\ a_r c_r \\ 2a_t^2 c_r \end{bmatrix} [\dot{S}_{mj}]_r [G]_j$$

$[M_v]$, $[C_v]$ and $[K_v]$ are respectively, the mass, damping, and stiffness matrices of the vehicle. $[C_{HI}]$ and $[K_{HI}]$ are two matrices that couple the motion of the vehicle with that of the bridge.

The vehicle displacements can be expressed in terms of modal coordinates by means of a transformation.

$$\{d\} = [\Phi_v]\{z_v\} \tag{3.129}$$

where $\{z_v\}$ is a vector of transformed coordinate called modal coordinates of the vehicle and $[\Phi_v]$ is a (3 x3) matrix formed by arranging side by side the three mode shapes of the vehicle.

Substituting equation (3.129) into equation (3.128) and pre-multiplying both sides of it by $[\Phi_v]^T$ the equation of motion of the vehicle can be obtained in the following form.

$$[M_v^*]\{\ddot{z}_v\} + [C_v^*]\{\dot{z}_v\} + [\Lambda_v]\{z_v\} + [C_{HI}^*]\{\dot{z}_b\} + [K_{HI}^*]\{z_b\} = \{0\} \tag{3.130}$$

where

$$[\Lambda_v] = [\Phi_v]^T [K_v][\Phi_v]$$

$$[M_v^*] = [\Phi_v]^T [M_v][\Phi_v]$$

$$[C^*_v] = [\Phi_v]^T [C_v][\Phi_v]$$

$$[C^*_{HI}] = [\Phi_v]^T [C_{HI}]$$

$$[K^*_{HI}] = [\Phi_v]^T [K_{HI}]$$

3.7.5.2 Contact Forces

The forces exerted on the bridge by the moving vehicle at the contact points can be obtained as follows:

The contact force at point P_{fj} can be obtained by taking moments of forces at point P_{fi} in Fig. 3.6,

$$f_{fj}(b)-\left(F_{fj}+\frac{a_r m_s g}{2}\right)\left(\frac{1}{2}+a_t\right)b-\left(F_{fi}+\frac{a_r m_s g}{2}\right)\left(\frac{1}{2}-a_t\right)b$$
$$+m_{uf}\left(\ddot{d}_{uf3}-g\right)\frac{b}{2}+i_{uf2}\ddot{d}_{uf5}=0 \tag{3.131}$$

Since the vehicle is always in contact with the bridge surface, the displacements and rotations of the unsprung masses are dependent on the bridge displacements . The relations between the unsprung mass degrees of freedom and the bridge degrees of freedom are given by

$$\ddot{d}_{uf3}=\frac{\ddot{w}_{fi}+\ddot{w}_{fj}}{2} \tag{3.132a}$$

$$\ddot{d}_{uf5}=\frac{\ddot{w}_{fj}-\ddot{w}_{fi}}{b} \tag{3.132b}$$

Substituting for $\ddot{d}_{uf3}$ and $\ddot{d}_{uf5}$ from equations (3.132a-b) and the expressions for the forces F_{fi} and F_{fj} from equations (3.112a-b) into equation (3.131) and re-arranging it yields

$$
\begin{aligned}
f_{fi} = {} & 2k_f\left[\frac{1}{2} \quad \frac{a_f}{2} \quad a_t^2\right]\{d\} + 2c_f\left[\frac{1}{2} \quad \frac{a_f}{2} \quad a_t^2\right]\{\dot{d}\} \\
& -\left[\left(\frac{1}{2}+2a_t^2\right)\left(k_f\left[S_{mj}\right]_f + c_f\left[\dot{S}_{mj}\right]_f\right)[G]_j + \left(\frac{1}{2}-2a_t^2\right)\left(k_f\left[S_{mj}\right]_f + c_f\left[\dot{S}_{mj}\right]_f\right)[G]_i\right. \\
& \left.+\left(\frac{m_{uf}}{4}+\frac{i_{uf2}}{b^2}\right)\left[\ddot{S}_{mj}\right]_f[G]_j + \left(\frac{m_{uf}}{4}-\frac{i_{uf2}}{b^2}\right)\left[\ddot{S}_{mj}\right]_f[G]_i\right]\{z_b\} \\
& -\left[\left(\frac{1}{2}+2a_t^2\right)c_f\left[S_{mj}\right]_f[G]_j + \left(\frac{1}{2}-2a_t^2\right)c_f\left[S_{mj}\right]_f[G]_i\right. \\
& \left.+2\left(\frac{m_{uf}}{4}+\frac{i_{uf2}}{b^2}\right)\left[\dot{S}_{mj}\right]_f[G]_j + 2\left(\frac{m_{uf}}{4}-\frac{i_{uf2}}{b^2}\right)\left[\dot{S}_{mj}\right]_f[G]_i\right]\{\dot{z}_b\} \\
& -\left[\left(\frac{m_{uf}}{4}+\frac{i_{uf2}}{b^2}\right)\left[S_{mj}\right]_f[G]_j + \left(\frac{m_{uf}}{4}-\frac{i_{uf2}}{b^2}\right)\left[S_{mj}\right]_f[G]_i\right]\{\ddot{z}_b\} \\
& \frac{a_r m_s g}{2} + \frac{m_{uf} g}{2}
\end{aligned}
\tag{3.133}
$$

The contact force at point P_{fi} can be obtained by taking moments of forces at point P_{fj} (Fig. 3.6).

$$
\begin{aligned}
f_{fi}(b) - \left(F_{fj} + \frac{a_r m_s g}{2}\right)\left(\frac{1}{2}-a_t\right)b - \left(F_{fi} + \frac{a_r m_s g}{2}\right)\left(\frac{1}{2}+a_t\right)b & \\
+ m_{uf}\left(\ddot{d}_{uf3} - g\right)\frac{b}{2} - i_{uf2}\ddot{d}_{uf5} = 0 &
\end{aligned}
\tag{3.134}
$$

Substituting for $\ddot{d}_{uf3}$ and $\ddot{d}_{uf5}$ from equations (3.132a-b) and the expressions for the forces F_{fi} and F_{fj} from equations (3.112a-b) into equation (3.134) and re-arranging it yields

$$
\begin{aligned}
f_{fi} = {} & 2k_f\left[\frac{1}{2} \quad \frac{a_f}{2} \quad -a_t^2\right]\{d\} + 2c_f\left[\frac{1}{2} \quad \frac{a_f}{2} \quad -a_t^2\right]\{\dot{d}\} \\
& -\left[\left(\frac{1}{2}-2a_t^2\right)\left(k_f[S_{mj}]_f + c_f\left[\dot{S}_{mj}\right]_f\right)[G]_j + \left(\frac{1}{2}+2a_t^2\right)\left(k_f[S_{mj}]_f + c_f\left[\dot{S}_{mj}\right]_f\right)[G]_i\right. \\
& \left.\left(\frac{m_{uf}}{4}-\frac{i_{uf2}}{b^2}\right)\left[\ddot{S}_{mj}\right]_f[G]_j + \left(\frac{m_{uf}}{4}+\frac{i_{uf2}}{b^2}\right)\left[\ddot{S}_{mj}\right]_f[G]_i\right]\{z_b\} \\
& -\left[\left(\frac{1}{2}-2a_t^2\right)c_f[S_{mj}]_f[G]_j + \left(\frac{1}{2}+2a_t^2\right)c_f[S_{mj}]_f[G]_i\right. \\
& \left.2\left(\frac{m_{uf}}{4}-\frac{i_{uf2}}{b^2}\right)\left[\dot{S}_{mj}\right]_f[G]_j + 2\left(\frac{m_{uf}}{4}+\frac{i_{uf2}}{b^2}\right)\left[\dot{S}_{mj}\right]_f[G]_i\right]\{\dot{z}_b\} \\
& -\left[\left(\frac{m_{uf}}{4}-\frac{i_{uf2}}{b^2}\right)[S_{mj}]_f[G]_j + \left(\frac{m_{uf}}{4}+\frac{i_{uf2}}{b^2}\right)[S_{mj}]_f[G]_i\right]\{\ddot{z}_b\} \\
& \frac{a_r m_s g}{2} + \frac{m_{uf} g}{2}
\end{aligned}
\tag{3.135}
$$

The contact force at point P_{rj} can be obtained by taking moments of forces at point P_{ri} (Fig. 3.7).

$$
\begin{aligned}
f_{rj}(b) - \left(F_{rj} + \frac{a_f m_s g}{2}\right)\left(\frac{1}{2}+a_t\right)b - \left(F_{ri} + \frac{a_r m_s g}{2}\right)\left(\frac{1}{2}-a_t\right)b & \\
+ m_{ur}\left(\ddot{d}_{ur3} - g\right)\frac{b}{2} + i_{ur2}\ddot{d}_{ur5} = 0 &
\end{aligned}
\tag{3.136}
$$

The relations between the rear unsprung mass degrees of freedom and the bridge degrees of freedom are given by

$$\ddot{d}_{ur3} = \frac{\ddot{w}_{rl} + \ddot{w}_{rj}}{2} \tag{3.137a}$$

$$\ddot{d}_{ur5} = \frac{\ddot{w}_{rj} - \ddot{w}_{rl}}{b} \tag{3.137b}$$

Substituting for $\ddot{d}_{ur3}$ and $\ddot{d}_{ur5}$ from equations (3.137a-b) and the expressions for the forces F_{rl} and F_{rj} from equations (3.112c-d) into equation (3.136) and re-arranging it yields

$$\begin{aligned}
f_{rj} = {} & 2k_r\left[\frac{1}{2} \quad -\frac{a_r}{2} \quad a_t^2\right]\{d\} + 2c_r\left[\frac{1}{2} \quad \frac{a_r}{2} \quad a_t^2\right]\{\dot{d}\} \\
& -\left[\left(\frac{1}{2}+2a_t^2\right)\left(k_r[S_{mj}]_r + c_r\left[\dot{S}_{mj}\right]_r\right)[G]_j + \left(\frac{1}{2}-2a_t^2\right)\left(k_r[S_{mj}]_r + c_r\left[\dot{S}_{mj}\right]_r\right)[G]_i\right. \\
& \left.+\left(\frac{m_{ur}}{4}+\frac{i_{ur2}}{b^2}\right)\left[\ddot{S}_{mj}\right]_r[G]_j + \left(\frac{m_{ur}}{4}-\frac{i_{ur2}}{b^2}\right)\left[\ddot{S}_{mj}\right]_r[G]_i\right]\{z_b\} \\
& -\left[\left(\frac{1}{2}+2a_t^2\right)c_r[S_{mj}]_r[G]_j + \left(\frac{1}{2}-2a_t^2\right)c_r[S_{mj}]_r[G]_i\right. \\
& \left.+2\left(\frac{m_{ur}}{4}+\frac{i_{ur2}}{b^2}\right)\left[\dot{S}_{mj}\right]_r[G]_j + 2\left(\frac{m_{ur}}{4}-\frac{i_{ur2}}{b^2}\right)\left[\dot{S}_{mj}\right]_r[G]_i\right]\{\dot{z}_b\} \\
& -\left[\left(\frac{m_{ur}}{4}+\frac{i_{ur2}}{b^2}\right)[S_{mj}]_r[G]_j + \left(\frac{m_{ur}}{4}-\frac{i_{ur2}}{b^2}\right)[S_{mj}]_r[G]_i\right]\{\ddot{z}_b\} \\
& \frac{a_f m_s g}{2} + \frac{m_{ur} g}{2}
\end{aligned} \tag{3.138}$$

The contact force at point P_{ri} can be obtained by taking moments of forces at point P_{rj} (Fig. 3.7).

$$f_{ri}(b)-\left(F_{rj}+\frac{a_f m_s g}{2}\right)\left(\frac{1}{2}-a_t\right)b-\left(F_{ri}+\frac{a_f m_s g}{2}\right)\left(\frac{1}{2}+a_t\right)b + m_{ur}\left(\ddot{d}_{ur3}-g\right)\frac{b}{2}-i_{ru2}\ddot{d}_{ur5}=0 \tag{3.139}$$

Substituting for $\ddot{d}_{ur3}$ and $\ddot{d}_{ur5}$ from equations (3.137a-b) and the expressions for the forces F_{ri} and F_{rj} from equations (3.112c-d) into equation (3.139) and re-arranging yields

$$\begin{aligned}
f_{ri} &= 2k_r\left[\frac{1}{2}\quad -\frac{a_r}{2}\quad -a_t^{\,2}\right]\{d\}+2c_r\left[\frac{1}{2}\quad \frac{a_f}{2}\quad -a_t^{\,2}\right]\{\dot{d}\}\\
&-\left[\left(\frac{1}{2}-2a_t^{\,2}\right)\left(k_r[S_{mj}]_r+c_r\left[\dot{S}_{mj}\right]_r\right)[G]_j+\left(\frac{1}{2}+2a_t^{\,2}\right)\left(k_r[S_{mj}]_r+c_r\left[\dot{S}_{mj}\right]_r\right)[G]_i\right.\\
&\left.+\left(\frac{m_{ur}}{4}-\frac{i_{ur2}}{b^2}\right)\left[\ddot{S}_{mj}\right]_r[G]_j+\left(\frac{m_{ur}}{4}+\frac{i_{ur2}}{b^2}\right)\left[\ddot{S}_{mj}\right]_r[G]_i\right]\{z_b\}\\
&-\left[\left(\frac{1}{2}-2a_t^{\,2}\right)c_r[S_{mj}]_r[G]_j+\left(\frac{1}{2}+2a_t^{\,2}\right)c_r[S_{mj}]_r[G]_i\right.\\
&\left.+2\left(\frac{m_{ur}}{4}-\frac{i_{ur2}}{b^2}\right)\left[\dot{S}_{mj}\right]_r[G]_j+2\left(\frac{m_{ur}}{4}+\frac{i_{ur2}}{b^2}\right)\left[\dot{S}_{mj}\right]_r[G]_i\right]\{\dot{z}_b\}\\
&-\left[\left(\frac{m_{ur}}{4}-\frac{i_{ur2}}{b^2}\right)[S_{mj}]_r[G]_j+\left(\frac{m_{ur}}{4}+\frac{i_{ur2}}{b^2}\right)[S_{mj}]_r[G]_i\right]\{\ddot{z}_b\}\\
&\frac{a_f m_s g}{2}+\frac{m_{ur}g}{2}
\end{aligned} \tag{3.140}$$

3.7.5.3 Equations of Motion of the Bridge

The contact forces f_{fi}, f_{fj}, f_{ri} and f_{rj} act as external forces on the bridge and the equations of equilibrium of the bridge become

$$\begin{aligned}&\left[M_b^*\right]\left\{\ddot{z}_b\right\}+\left[C_b^*\right]\left\{\dot{z}_b\right\}+\left[\Lambda_b\right]\left\{z_b\right\}=\\&[G]_i^T\left[S_{mj}\right]_f^T f_{fi}+[G]_j^T\left[S_{mj}\right]_f^T f_{fj}+[G]_i^T\left[S_{mj}\right]_r^T f_{ri}+[G]_j^T\left[S_{mj}\right]_r^T f_{rj}\end{aligned} \tag{3.141}$$

3.7.5.4 Equations of Motion of Bridge-vehicle System

In order to obtain the response of the bridge-vehicle system under the action of the moving vehicle, equations (3.130) and (3.141) are solved simultaneously.

Substituting the expressions for the forces f_{fi}, f_{fj}, f_{ri} and f_{rj} from equations (3.133), (3.135), (3.138) and (3.140) into equation (3.141) and combining the result with equation (3.130) yield the following equations of motion of the bridge-vehicle system.

$$\begin{bmatrix} \left(\left[M_b^*\right]+\left[M_I\right]\right) & [0] \\ [0] & \left[M_v^*\right] \end{bmatrix} \begin{Bmatrix} \{\ddot{z}_b\} \\ \{\ddot{z}_v\} \end{Bmatrix} + \begin{bmatrix} \left(\left[C_b^*\right]+\left[C_I\right]\right) & \left[C_{VI}^*\right] \\ \left[C_{HI}^*\right] & \left[C_v^*\right] \end{bmatrix} \begin{Bmatrix} \{\dot{z}_b\} \\ \{\dot{z}_v\} \end{Bmatrix} + \begin{bmatrix} \left(\left[\Lambda_b\right]+\left[K_I\right]\right) & \left[K_{VI}^*\right] \\ \left[K_{HI}^*\right] & \left[\Lambda_v\right] \end{bmatrix} \begin{Bmatrix} \{z_b\} \\ \{z_v\} \end{Bmatrix} = \begin{Bmatrix} \{F^*\} \\ \{0\} \end{Bmatrix} \tag{3.142}$$

where

$$\begin{aligned} \left[M_I\right] = {} & [G]_j^T \left[S_{mj}\right]_f^T \left(\left(\frac{m_{uf}}{4} + \frac{i_{uf2}}{b^2} \right) \left[S_{mj}\right]_f [G]_j + \left(\frac{m_{uf}}{4} - \frac{i_{uf2}}{b^2} \right) \left[S_{mj}\right]_f [G]_i \right) \\ & + [G]_i^T \left[S_{mj}\right]_f^T \left(\left(\frac{m_{uf}}{4} - \frac{i_{uf2}}{b^2} \right) \left[S_{mj}\right]_f [G]_j + \left(\frac{m_{uf}}{4} + \frac{i_{uf2}}{b^2} \right) \left[S_{mj}\right]_f [G]_i \right) \\ & + [G]_j^T \left[S_{mj}\right]_r^T \left(\left(\frac{m_{ur}}{4} + \frac{i_{ur2}}{b^2} \right) \left[S_{mj}\right]_r [G]_j + \left(\frac{m_{ur}}{4} - \frac{i_{ur2}}{b^2} \right) \left[S_{mj}\right]_r [G]_i \right) \\ & + [G]_i^T \left[S_{mj}\right]_r^T \left(\left(\frac{m_{ur}}{4} - \frac{i_{ur2}}{b^2} \right) \left[S_{mj}\right]_r [G]_j + \left(\frac{m_{ur}}{4} + \frac{i_{ur2}}{b^2} \right) \left[S_{mj}\right]_r [G]_i \right) \end{aligned}$$

$$[K_{VT}^{*}] = [G]_j^T [S_{mj}]_f^T \begin{bmatrix} -k_f & -a_f k_f & -2a_t^2 k_f \end{bmatrix} [\Phi_v] + [G]_i^T [S_{mj}]_f^T \begin{bmatrix} -k_f & -a_f k_f & 2a_t^2 k_f \end{bmatrix} [\Phi_v]$$
$$+ [G]_j^T [S_{mj}]_r^T \begin{bmatrix} -k_r & a_r k_r & -2a_t^2 k_r \end{bmatrix} [\Phi_v] + [G]_i^T [S_{mj}]_r^T \begin{bmatrix} -k_r & a_r k_r & 2a_t^2 k_r \end{bmatrix} [\Phi_v]$$

$$[C_t] = [G]_j^T [S_{mj}]_f^T \left(\left(\left(\frac{1}{2} + 2a_t^2 \right) c_f [S_{mj}]_f + 2 \left(\frac{m_{uf}}{4} + \frac{i_{uf2}}{b^2} \right) [\dot{S}_{mj}]_f \right) [G]_j \right.$$
$$\left. + \left(\left(\frac{1}{2} - 2a_t^2 \right) c_f [S_{mj}]_f + 2 \left(\frac{m_{uf}}{4} - \frac{i_{uf2}}{b^2} \right) [\dot{S}_{mj}]_f \right) [G]_i \right)$$
$$+ [G]_i^T [S_{mj}]_f^T \left(\left(\left(\frac{1}{2} - 2a_t^2 \right) c_f [S_{mj}]_f + 2 \left(\frac{m_{uf}}{4} - \frac{i_{uf2}}{b^2} \right) [\dot{S}_{mj}]_f \right) [G]_j \right.$$
$$\left. + \left(\left(\frac{1}{2} + 2a_t^2 \right) c_f [S_{mj}]_f + 2 \left(\frac{m_{uf}}{4} + \frac{i_{uf2}}{b^2} \right) [\dot{S}_{mj}]_f \right) [G]_i \right)$$
$$+ [G]_j^T [S_{mj}]_r^T \left(\left(\left(\frac{1}{2} + 2a_t^2 \right) c_r [S_{mj}]_r + 2 \left(\frac{m_{ur}}{4} + \frac{i_{ur2}}{b^2} \right) [\dot{S}_{mj}]_r \right) [G]_j \right.$$
$$\left. + \left(\left(\frac{1}{2} - 2a_t^2 \right) c_r [S_{mj}]_r + 2 \left(\frac{m_{ur}}{4} - \frac{i_{ur2}}{b^2} \right) [\dot{S}_{mj}]_r \right) [G]_i \right)$$
$$+ [G]_i^T [S_{mj}]_r^T \left(\left(\left(\frac{1}{2} - 2a_t^2 \right) c_r [S_{mj}]_r + 2 \left(\frac{m_{ur}}{4} - \frac{i_{ur2}}{b^2} \right) [\dot{S}_{mj}]_r \right) [G]_j \right.$$
$$\left. + \left(\left(\frac{1}{2} + 2a_t^2 \right) c_r [S_{mj}]_r + 2 \left(\frac{m_{ur}}{4} + \frac{i_{ur2}}{b^2} \right) [\dot{S}_{mj}]_r \right) [G]_i \right)$$

$$[C_{vt}] = [G]_j^T [S_{mj}]_f^T \begin{bmatrix} -c_f & -a_f c_f & -2a_t^2 c_f \end{bmatrix} [\Phi_v] + [G]_i^T [S_{mj}]_f^T \begin{bmatrix} -c_f & -a_f c_f & 2a_t^2 c_f \end{bmatrix} [\Phi_v]$$
$$+ [G]_j^T [S_{mj}]_r^T \begin{bmatrix} -c_r & a_r c_r & -2a_t^2 c_r \end{bmatrix} [\Phi_v] + [G]_i^T [S_{mj}]_r^T \begin{bmatrix} -c_r & a_r c_r & 2a_t^2 c_r \end{bmatrix} [\Phi_v]$$

$$[K_t] = [G]_j^T [S_{mj}]_f^T \left(\left(\left(\frac{1}{2} + 2a_t^2 \right) \left(k_f [S_{mj}]_f + c_f [\dot{S}_{mj}]_f \right) + 2 \left(\frac{m_{uf}}{4} + \frac{i_{uf2}}{b^2} \right) [\ddot{S}_{mj}]_f \right) [G]_j \right.$$
$$\left. + \left(\left(\frac{1}{2} - 2a_t^2 \right) \left(k_f [S_{mj}]_f + c_f [\dot{S}_{mj}]_f \right) + 2 \left(\frac{m_{uf}}{4} - \frac{i_{uf2}}{b^2} \right) [\ddot{S}_{mj}]_f \right) [G]_i \right)$$
$$+ [G]_i^T [S_{mj}]_f^T \left(\left(\left(\frac{1}{2} - 2a_t^2 \right) \left(k_f [S_{mj}]_f + c_f [\dot{S}_{mj}]_f \right) + 2 \left(\frac{m_{uf}}{4} - \frac{i_{uf2}}{b^2} \right) [\ddot{S}_{mj}]_f \right) [G]_j \right.$$
$$\left. + \left(\left(\frac{1}{2} + 2a_t^2 \right) \left(k_f [S_{mj}]_f + c_f [\dot{S}_{mj}]_f \right) + 2 \left(\frac{m_{uf}}{4} + \frac{i_{uf2}}{b^2} \right) [\ddot{S}_{mj}]_f \right) [G]_i \right)$$
$$+ [G]_j^T [S_{mj}]_r^T \left(\left(\left(\frac{1}{2} + 2a_t^2 \right) \left(\left(k_r [S_{mj}]_r + c_r [\dot{S}_{mj}]_r \right) + 2 \left(\frac{m_{ur}}{4} + \frac{i_{ur2}}{b^2} \right) [\ddot{S}_{mj}]_r \right) [G]_j \right. \right.$$
$$\left. \left. + \left(\left(\frac{1}{2} - 2a_t^2 \right) \left(k_r [S_{mj}]_r + c_f [\dot{S}_{mj}]_r \right) + 2 \left(\frac{m_{ur}}{4} - \frac{i_{ur2}}{b^2} \right) [\ddot{S}_{mj}]_r \right) [G]_i \right) \right.$$
$$+ [G]_i^T [S_{mj}]_r^T \left(\left(\left(\frac{1}{2} - 2a_t^2 \right) \left(k_r [S_{mj}]_r + c_f [\dot{S}_{mj}]_r \right) + 2 \left(\frac{m_{ur}}{4} - \frac{i_{ur2}}{b^2} \right) [\ddot{S}_{mj}]_r \right) [G]_j \right.$$
$$\left. \left. + \left(\left(\frac{1}{2} + 2a_t^2 \right) \left(k_r [S_{mj}]_r + c_f [\dot{S}_{mj}]_r \right) + 2 \left(\frac{m_{ur}}{4} + \frac{i_{ur2}}{b^2} \right) [\ddot{S}_{mj}]_r \right) [G]_i \right) \right.$$

$$\{F\} = \left(\frac{a_f m_s g}{2} + \frac{m_{wf} g}{2}\right)[G]_j^T \{S_{mj}\}_f^T + \left(\frac{a_r m_s g}{2} + \frac{m_{wf} g}{2}\right)[G]_i^T \{S_{mj}\}_f^T$$
$$+\left(\frac{a_f m_s g}{2} + \frac{m_{wr} g}{2}\right)[G]_j^T \{S_{mj}\}_r^T + \left(\frac{a_f m_s g}{2} + \frac{m_{wr} g}{2}\right)[G]_i^T \{S_{mj}\}_r^T$$

To ensure that any wheel load outside the bridge will not be included in computing the response of the bridge, the terms that are associated with that wheel should not be included in the formation of the matrices $[K^*_{VI}]$, $[C^*_{VI}]$, $[K^*_{HI}]$, $[C^*_{HI}]$, $[K_I]$, $[C_I]$, and $[M_I]$ and the vector $\{F^*\}$.

3.8 Examples on Plates

As in Chapter Two, several illustrative examples that exist in the literature are carried out to prove the validity of the equations derived in this chapter and the FORTRAN program I have developed as part of the study. The examples do not represent real bridges but their available results are useful for comparison.

3.8.1 Moving Load Problem

The response analysis of a square plate simply supported on all sides was carried out to demonstrate the accuracy of the theory and the methods of solution presented in this chapter and the computer program I have developed as part of this study. The solution methods have shown

to be numerically stable and accurate. Figure (3.9) shows the characteristics of the plate and its finite strip discretization. The dynamic response was first obtained for a force of two pounds traveling at the center line with a velocity of 1029 in./sec. A free vibration analysis is performed first to obtain the frequencies and mode shapes of the plate. Table (3.1) shows the lowest eleven frequencies of the plate. The dynamic magnification factor for deflection which is defined as the ratio of dynamic to maximum static deflection at the center of the plate are compared to those obtained by Yoshida (1971) using finite element method with consistent mass procedure, by Wilson and Tsirk (1967) and Kashif (1992) using finite element method with lumped mass procedure. The results are listed in Table 3.2. Figure (3.10) shows the dynamic response due to a moving load along the center of the plate. The vertical axis represents magnification factor for deflection at the center of plate, while the horizontal axis represents real time divided by travel time, the time it takes the vehicle to transverse the bridge

3.8.2 Moving Mass Problem

The same plate was used again to obtain the dynamic response under a moving mass. Different mass ratios were used. The mass ratio is the ratio between the mass of the moving mass and the mass of the plate. The mass ratios used were 0.1,1.0, 3.0 and 10.0. The results were compared again to those obtained by Yoshida and Khashaf. Table 3.3 shows the results. The dynamic magnification factor for deflection for these mass ratios are plotted in Figure (3.11).The results obtained from the above problems show the reliability of the procedure used in this study.

TABLE 3.1

Lowest Eleven Frequencies of the Simply supported plate in Figure 3.9

Frequency Number	Frequency (cycles/sec) (This study)	Frequency (cycles/sec) (Khashaf)	Frequency (cycles/sec) (Exact)
1	0.1029E+04	0.1047E+04	0.1029E+04
2	0.2573E+04	0.2659E+04	0.2573E+04
3	0.5146E+04	0.5174E+04	0.5146E+04
4	0.5146E+04	0.5174E+04	0.5146E+04
5	0.6690E+04	0.6276E+04	0.6690E+04
6	0.8748E+04	0.7408E+04	0.8748E+04
7	0.9263E+04	0.2368E+05	0.9263E+04
8	0.1286E+05	0.3159E+05	0.1287E+05
9	0.1338E+05	0.3161E+05	0.1338E+05
10	0.1339E+05	0.3510E+05	0.1338E+05
11	0.1493E+05	0.3565E+05	0.1493E+05

TABLE 3.2

Dynamic Magnification Factor for Deflection at the Center of the Plate in Figure 3.9 Due to a Moving Load.

Number of Modes	$\frac{W_{dyn}}{W_{stat}}$ (This study)	$\frac{W_{dyn}}{W_{stat}}$ (Khashaf)	$\frac{W_{dyn}}{W_{stat}}$ (Yoshida)
1	1.557	1.513	1.568
3	1.558		
5	1.558		
10	1.558		
15	1.558		

TABLE 3.3

Dynamic Magnification Factor for Deflection at the Center of the Plate in Figure 3.9 Due to Moving Masses.

Mass Ratio (m_v/m_b)	Modes	W_{dyn}/W_{stat} (This study)	W_{dyn}/W_{stat} (Khashaf)	W_{dyn}/W_{stat} (Yoshida)
0.1	1	1.021	-	1.125
	5	1.084		
	10	1.113		
	15	1.119		
0.3	1	1.034	1.077	-
	5	1.060		
	10	1.095		
	15	1.101		
1.0	1	1.042	0.946	1.111
	5	1.106		
	10	1.098		
	15	1.100		
3.0	1	1.442	1.492	1.505
	5	1.509		
	10	1.517		
	15	1.525		
10.0	1	2.830	2.871	"Extremely large"
	5	2.816		
	10	3.047		
	15	3.166		

3.9 Free Vibration Analysis of Slab bridges

Analysis of four simply supported concrete slab bridges has been carried out. The dimensions and parameters of the bridges are given in Table (3.4).

TABLE 3.4

Geometry and Material Properties

Bridge Number	Span (m)	Width (m)	Thickness (m)	ν	E (N/m^2)	ρ (Kg/m^3)
1	10.0	10.0	0.325	0.15	2.65×10^{10}	2446.5
2	15.0	10.0	0.400	0.15	2.65×10^{10}	2446.5
3	20.0	10.0	0.525	0.15	2.65×10^{10}	2446.5
3	20.0	10.0	0.675	0.15	2.65×10^{10}	2446.5

The natural frequencies and modal shapes were calculated and arranged in order of increasing magnitude. A record is also kept of the series terms corresponding to the mode shapes and frequencies. The results of this part of analysis are shown in Tables (3.5), (3.6), (3.7) and (3.8). It may be seen that among the first ten mode shapes only the first three harmonic terms are represented for the ten- meter long bridge and only the first four harmonic terms for the fifteen-meter, twenty- meter and twenty five-meter long bridges. For the ten-meter long bridge, of these ten modes, four modes correspond to each of the first and second harmonic terms and two modes correspond to the third harmonic term. For the fifteen-meter long bridge, four modes

correspond to the first harmonic, three modes correspond to the second harmonic, two modes correspond to the third harmonic and one mode correspond to the fourth. For the twenty-meter long bridge, of these ten modes, three modes correspond to each of the first and second harmonic terms and two modes correspond to each of the third and fourth harmonic terms and for the twenty five-meter long bridge of these ten modes, three modes correspond to each of the first and second harmonic terms and two modes correspond to each of the third and fourth harmonic terms.

In general, bridges that have large ratios of longitudinal to transverse bending rigidities require more vibration mode shapes to represent higher harmonic terms.

TABLE 3.5

Free Vibration Characteristics

10 X 10 m Simple Slab Bridge

Mode number (j)	Natural frequency (Hz)	Series term (m_j)
1	4.88	1
2	8.51	1
3	8.91	1
4	9.57	2
5	3.92	2
6	6.29	2
7	8.00	1
8	4.07	3
9	8.60	3
10	6.55	2

TABLE 3.6

Free Vibration Characteristics

10 X 15 m Simple Slab Bridge

Mode number (j)	**Natural frequency (Hz)**	**Series term (m_j)**
1	2.66	1
2	6.34	1
3	10.69	2
4	15.61	2
5	18.36	1
6	24.08	3
7	29.33	2
8	29.44	3
9	41.90	1
10	42.84	4

TABLE 3.7

Free Vibration Characteristics

10 X 20 m Simple Slab Bridge

Mode number (j)	**Natural frequency (Hz)**	**Series term (m_j)**
1	1.96	1
2	6.00	1
3	7.88	2
4	13.74	2
5	17.62	3
6	21.58	1
7	24.42	3
8	30.54	2
9	31.61	4
10	38.64	4

TABLE 3.8

Free Vibration Characteristics

10 X 25 m Simple Slab Bridge

Mode number (j)	Natural frequency (Hz)	Series term (m_j)
1	1.62	1
2	6.06	1
3	6.48	2
4	13.31	2
5	14.60	3
6	22.65	3
7	25.99	4
8	26.14	1
9	34.04	2
10	34.68	4

3.10 Forced Vibration Analysis of Slab Bridges

The dynamic response analysis of the four bridges whose dimensions and parameters are reported in Table 3.4 are carried out. Four different vehicle models that have equal weights are used. The first vehicle model consists of a single sprung mass attached to an unsprung mass through a linear spring. The second vehicle model consists of a set of two point forces. The third vehicle model consists of two sprung masses traveling in sequence and abreast with two other sprung masses. The fourth vehicle model is a two-axle four-wheel vehicle model consisting of

sprung mass and unsprung masses. The sprung models have equivalent spring stiffnesses and equal sprung and unsprung masses. A constant velocity of 100 km/hr is used in all cases. All the vehicles travel symmetrically along the center of the bridges.

Characteristics of the vehicle models

Vehicle Model I

Sprung mass (m_s) = 30189.0 Kg

Unsprung mass (m_u) = 4209.0 Kg

Spring stiffness (k) =10726325.54 N/m

Vehicle Model II

Front axle weight 2x(P_f)=196134.554 N

Rear axle weight 2x(P_r)=140965.846 N

Vehicle Model III

Front sprung mass 2x (m_{sf}) =2x(8603.865) g

Rear sprung mass 2x (m_{sr}) =2x(6490.635) Kg

Front unsprung mass 2x(m_{uf}) =2x(1403.0) Kg

Rear Unsprung mass 2x(m_{ur}) =2x(701.50) Kg

Spring Stiffness 4x(k) = 10726325.54 N/m

Spacing (transverse) = 1.83 m

Spacing (longitudinal) = 6.19 m

Vehicle Model IV (Two-axle four-wheel model)

Sprung mass (m_s) = 30189.0 Kg

Front unsprung mass (m_{uf}) = 2806.0 Kg

Rear unsprung mass (m_{ur}) = 1403.0 Kg

Front axle stiffness 2x(k_f) = 5363162.77 N/m

Rear axle Stiffness 2x(k_r) = 5363162.77 N/m

Width of the vehicle (b) = 1.83 m

Wheel base of the vehicle (s) = 6.19 m

Centroidal distance parameters:

$a_f = 0.43$, $a_r = 0.57$

Mass moments of inertia:

$i_{s1} = 263.052$ tone.m^2

$i_{s2} = 23.448$ tone.m^2

$_{uf2} = 4.982$ tone.m^2

$i_{ur2} = 0.879$ tone.m^2

Table (3.9) shows the maximum static deflection at center of mid-span of the bridges under one point load and a set of two point loads. Tables (3.10), (3.11), (3.12) and (3.13) show the maximum dynamic deflections at center of mid-span and deflection magnification factor of the bridges under the four vehicle models.

TABLE 3.9

Static Deflections at Center of Mid-span of Bridges

Bridge Number	$W_{static}(mm)$ (One point load)	$W_{static}(mm)$ (Two point loads)
1	10.13	5.72
2	16.96	13.08
3	17.48	15.17
4	16.02	14.64

TABLE 3.10

Dynamic Deflections and Deflection Magnification Factor

at Center of a 10x10 m Mid-span of Bridge

Vehicle Model	$W_{dynamic}$	DAF
I	11.33	1.12
II	7.57	1.32
III	6.96	1.22
IV	6.64	1.16

TABLE 3.11

Dynamic Deflections and Deflection Magnification Factor

at Center of Mid-span of a 10x15 m Bridge

Vehicle Model	$W_{dynamic}$	DAF
I	23.49	1.39
II	15.08	1.15
III	15.50	1.19
IV	15.50	1.19

TABLE 3.12

Dynamic Deflections and Deflection Magnification Factor

at Center of Mid-span of a 10x20 m Bridge

Vehicle Model	$W_{dynamic}$	DAF
I	26.41	1.51
II	19.01	1.25
III	20.06	1.32
IV	19.95	1.32

TABLE 3.13

Dynamic Deflections and Deflection Magnification Factor

at Center of Mid-span of a 10x25 m Bridge

Vehicle Model	$W_{dynamic}$	DAF
I	24.63	1.54
II	19.37	1.32
III	20.06	1.37
IV	22.47	1.37

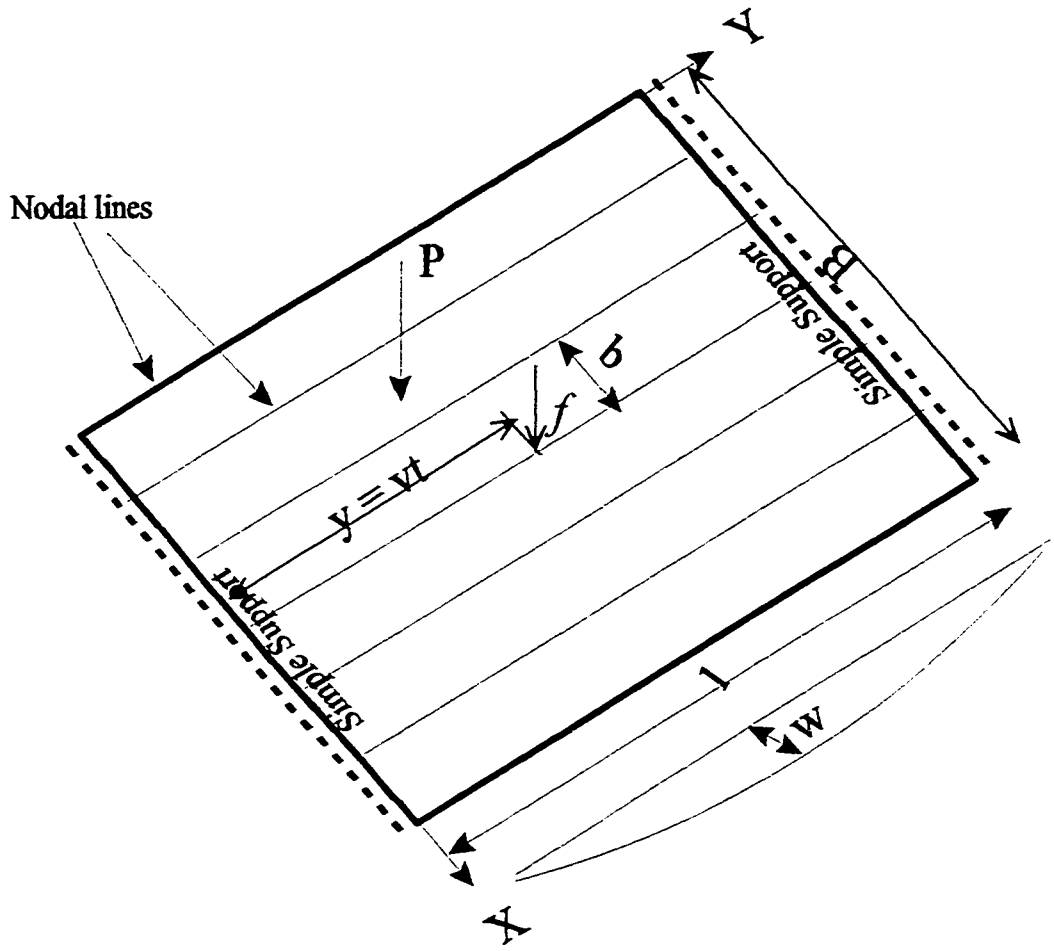

Figure 3.1 Simply Supported Slab Bridge under a Moving force

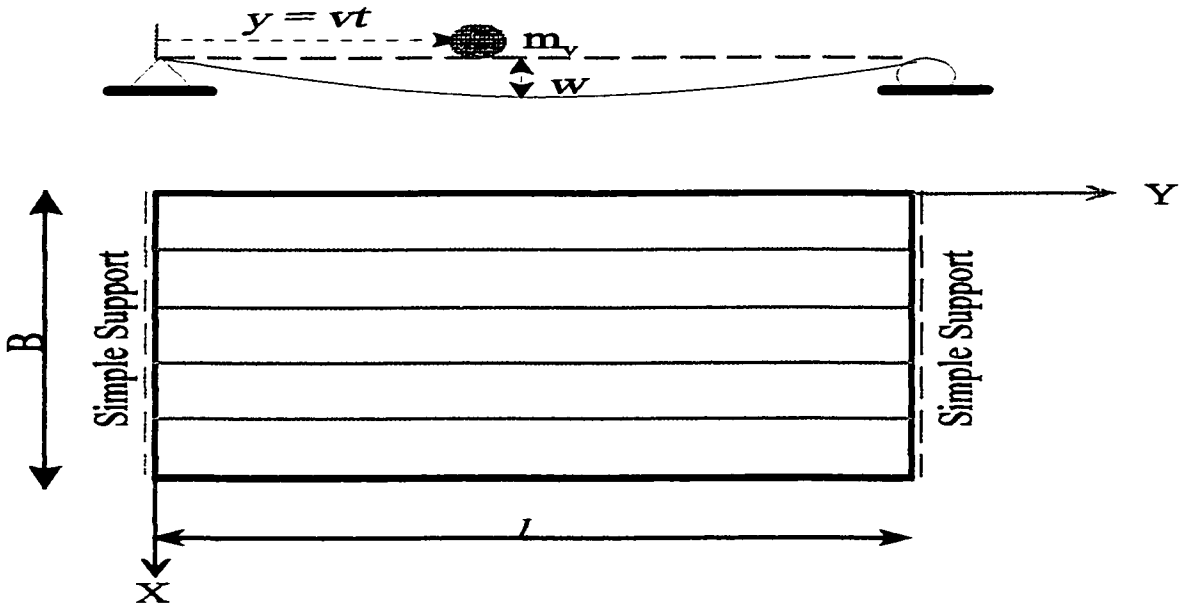

Figure 3.2 Simply Supported Slab Bridge Under a Moving Mass

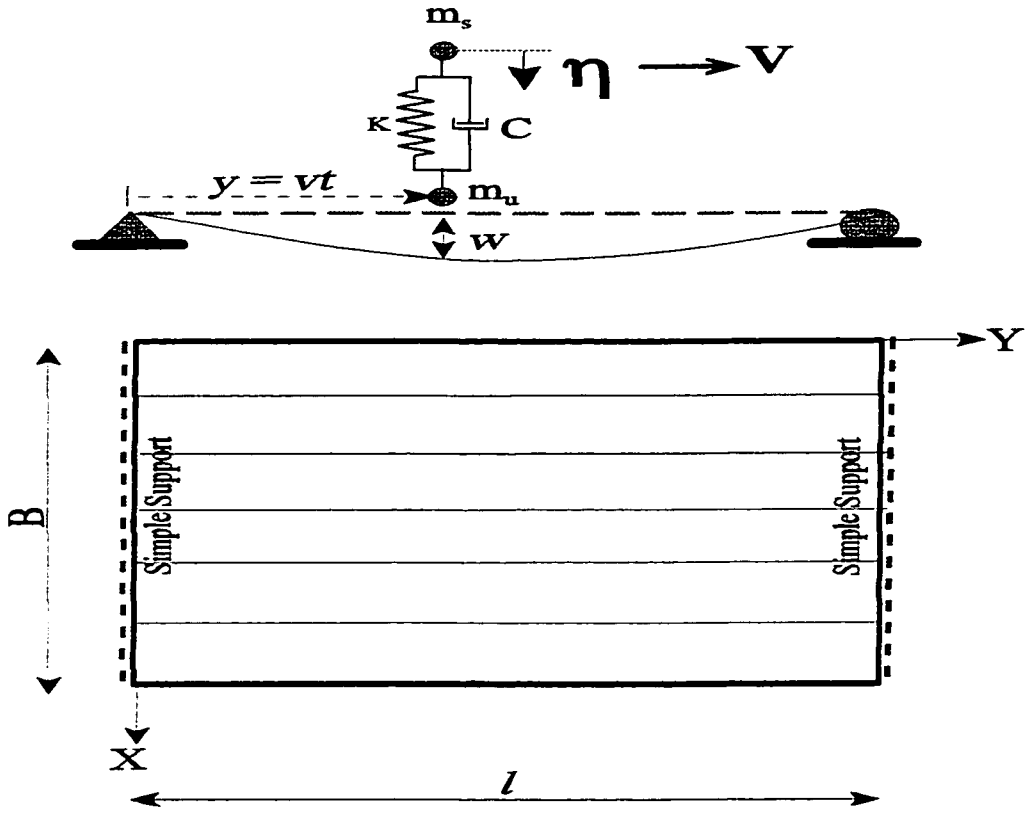

Figure 3.3 Simply Supported Slab Bridge Under a Sprung Mass

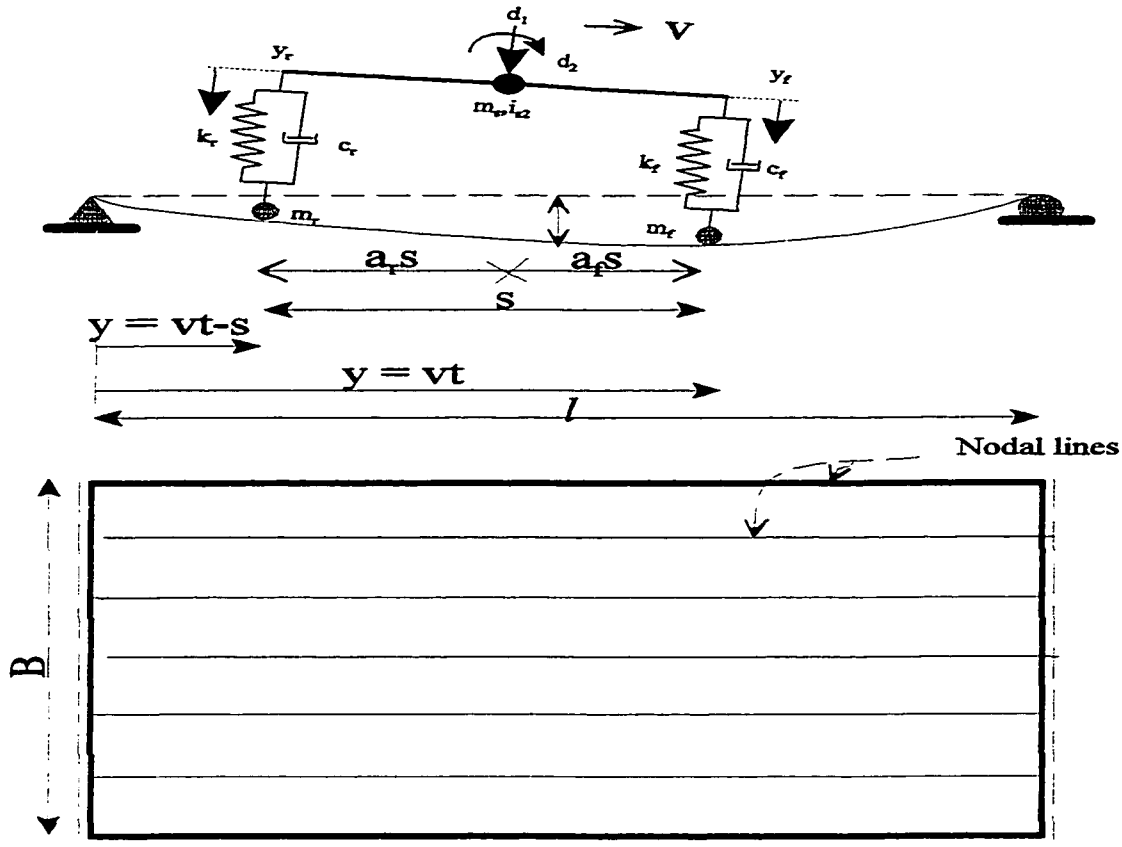

Figure 3.4 Simply Supported Slab Bridge Under a Two-axle Two-wheel Vehicle Load

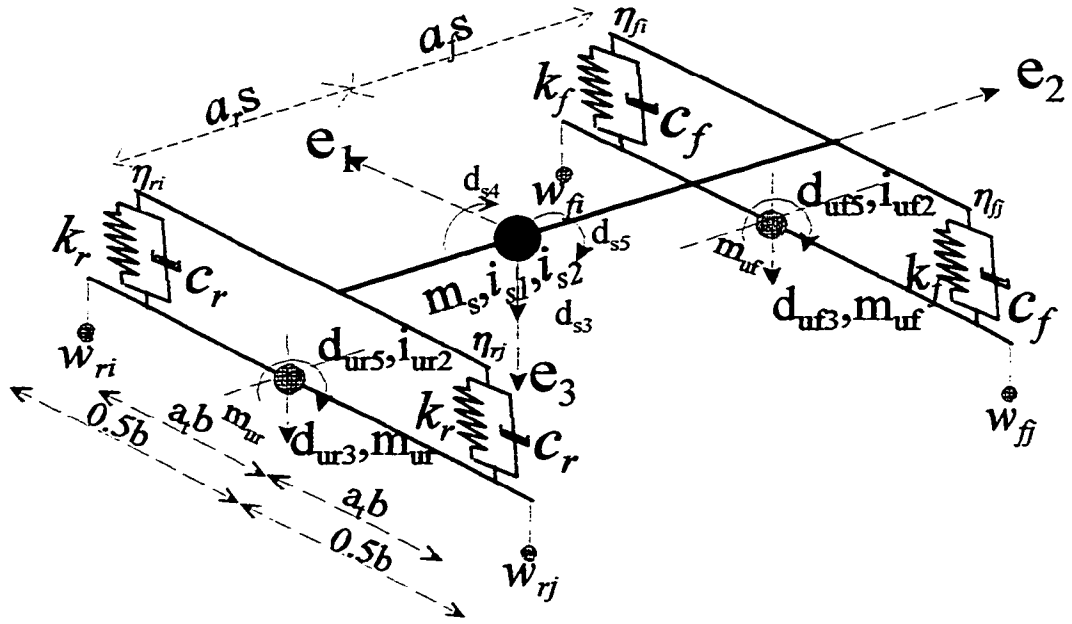

Figure 3.5 Two-axle Four-wheel Vehicle Model

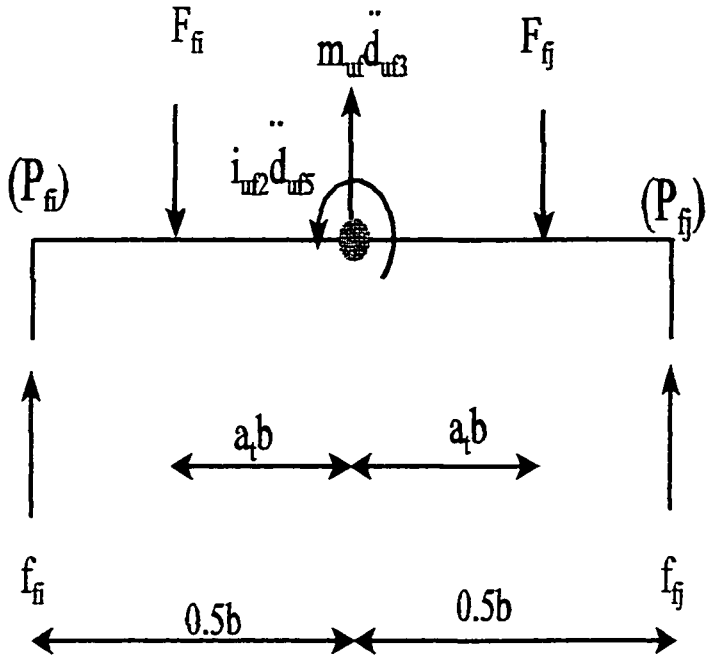

Figure 3.6 Free Body diagram of the front axle

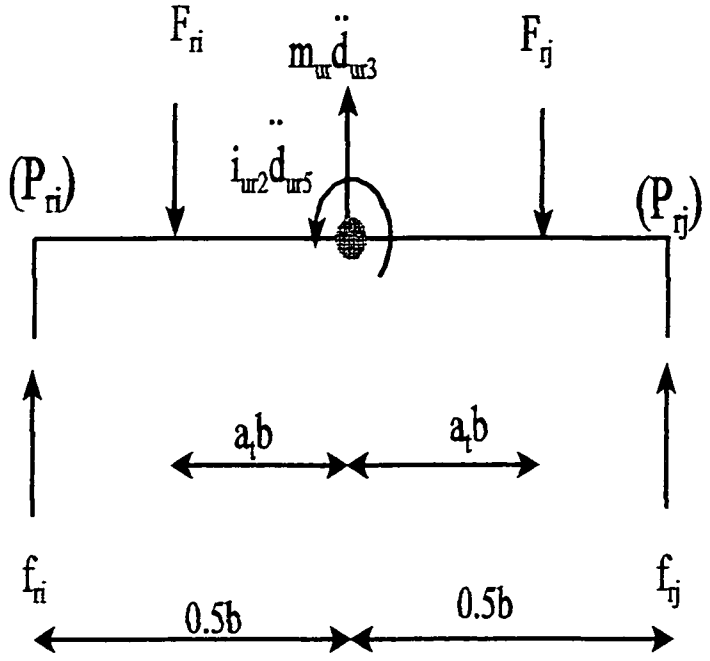

Figure 3.7 Free Body diagram of the rear axle

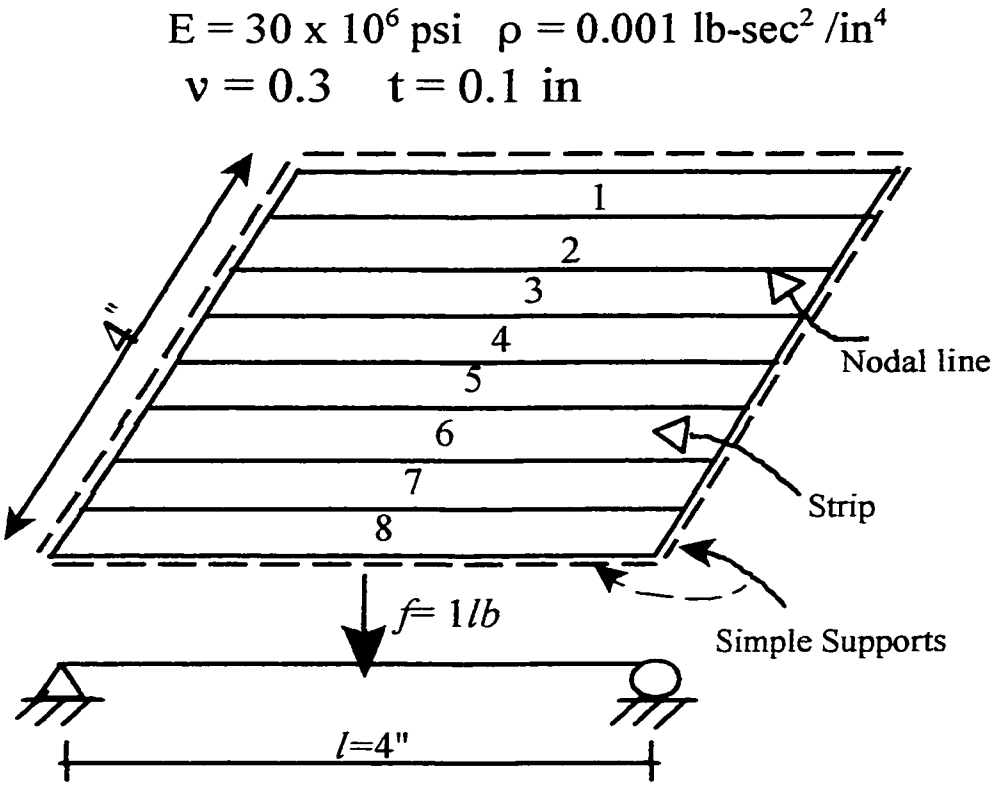

Figure 3.8 plate and its Finite Strip Idealization

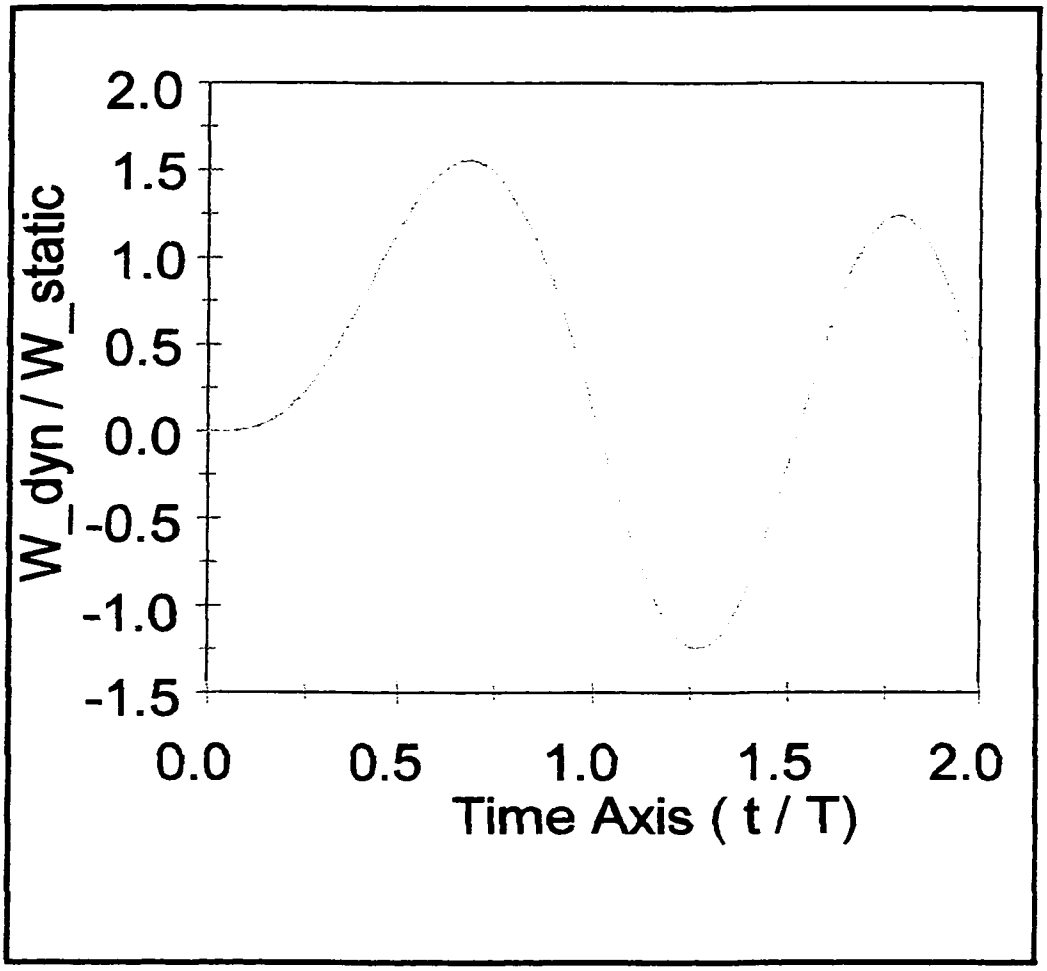

Figure 3.9 Plate Response due to a Moving Load

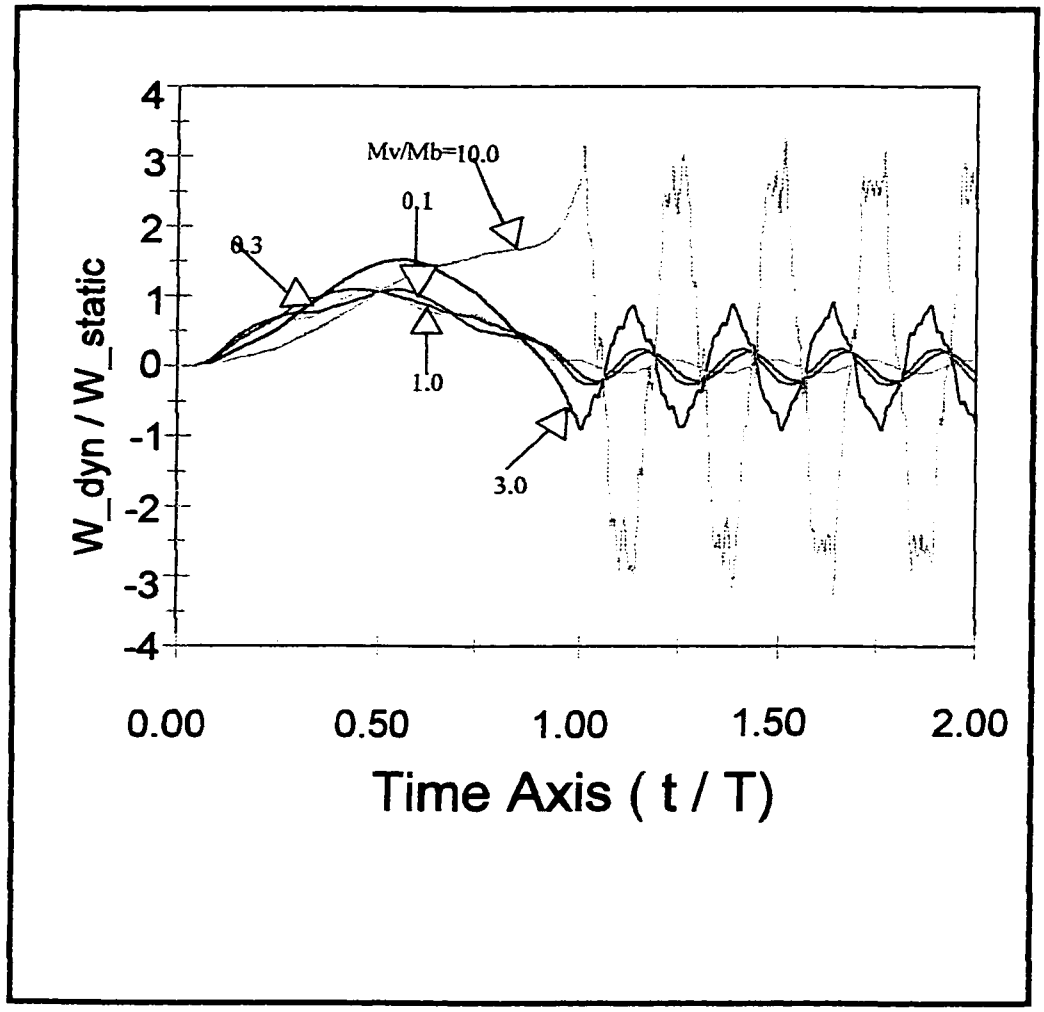

Figure 3.10 Plate Response due to a Moving Mass

Chapter 4

MULTI-SPAN BEAM AND SLAB BRIDGES

4.1 Introduction

This chapter deals with dynamic analysis of beam bridges and slab bridges with right simply supported ends resting on arbitrarily placed discrete intermediate columns or over a continued line support. The finite strip in conjunction with flexibility method is used.

4.2 Free Vibration Analysis

The application of finite strip method in conjunction with flexibility method to the free vibration analysis of continuous bridges can be summarized in the following steps.

1. Treat the bridge as simply supported at its ends by releasing its deck from all the internal

restraints.

2. Assume a frequency ω^k and a vibration mode shape $\{D\}^k$ and start iteration ($k = 1,2,...$).

3. Calculate the inertia force due to the vibration mode shape.

4. Calculate the displacements {a} at the points where the internal restraints have been removed and also the nodal line or generalized displacement parameters $\{\delta_i\}^k$ of the released bridge due to inertia forces .

5. Calculate the displacements at the same points in the released bridge due to the internal restraints and the nodal line or generalized displacement parameters $\{\delta\}_j^k$ due to each internal restraint j. In this step, the flexibility [F] matrix is formed.

6. The compatibility requirement of displacements at each point where an internal restraint has been removed yields a set of equations from which the reactions of the internal restraints $\{R\}^k$ can be evaluated

$$[F]_{(NR\times NR)}\{R\}^k_{(NR)} + \{a\}^k_{(NR)} = 0 \tag{4.1}$$

where NR is the number of internal restraints. For simplicity, all the internal restraints are assumed to be rigid.

7. Knowing the values of the restraints $\{R\}$, the mode shapes of the continuous span bridge are obtained as the sum of the nodal line or generalized displacement parameters due to inertia forces which are calculated in step 4 and the nodal line or generalized displacement parameters due to the reactions of the internal restraints which are calculated in step 5. Thus

$$\{D\}^{k+1} = \sum_{j=1}^{NR}\{\delta_s\}_j R^k(j) + \{\delta_i\}^k \tag{4.2}$$

8. The frequency ω^{k+1} of the continuous span bridge is computed from Rayleigh quotient

$$\omega^{2(k+1)} = \frac{\{D\}^{T(k+1)}[K_b]\{D\}^{(k+1)}}{\{D\}^{T(k+1)}[M_b]\{D\}^{(k+1)}} \tag{4.3}$$

9. The mode shapes of the continuous span bridge are mass-orthonormalized as follows

$$\{D\}^{(k+1)} = \frac{\{D\}^{(k+1)}}{\left(\{D\}^{T(k+1)}[M_b]\{D\}^{(k+1)}\right)^{\frac{1}{2}}} \tag{4.4}$$

10. Convergence is then measured by comparing two successive values of ω. Therefore

$$\left|\frac{\omega^{2(k+1)} - \omega^{2(k)}}{\omega^{2(k+1)}}\right| < \in \tag{4.5}$$

where $\in$ is the specified tolerance.

11. If convergence is not within the specified tolerance, the iteration is restarted by using the frequency obtained in step 8 and the mode shape evaluated in step 9 as new assumed quantities.

12. The above iteration procedure leads to the first natural mode shape $\{\phi\}_1$ and also yields the fundamental (lowest) frequency ω_1. The higher modes and frequencies can be computed in ascending order by requiring that each trial vector $\{D\}^k$ to be orthogonal to all the previously computed mode shapes of the bridge. This procedure is known as Gram-Schmidt orthogonalization procedure . Suppose that the first s mode shapes have

already been obtained and are swept away from the trial vector, then the iteration on the constrained new trial vector $\{\dot{D}\}^k$ will converge to the $(s+1)^{th}$ mode shape. This constrained new trial vector is used in step 3 for mode iterations other the fundamental mode and is given by

$$\left\{\dot{D}\right\}^k = \{D\}^k - \sum_{p=1}^{s} \frac{\{\phi_p\}[M_b]\{D\}^k}{\{\phi_p\}[M_b]\{\phi_p\}^k}\{\phi_p\} \tag{4.6}$$

Since the mode shapes have been mass orthonormalized, equation (4.6) simplifies to:

$$\left\{\dot{D}\right\}^k = \{D\}^k - \sum_{p=1}^{s}\left(\{\phi_p\}[M_b]\{D\}^k\right)\{\phi_p\} \tag{4.7}$$

13. Form the modal matrix by arranging side by side all the mass-orthonormal mode shapes as follows:

$$[\Phi_b] = [\{\phi\}_1 \quad \{\phi\}_2 \quad \cdots \quad \{\phi\}_s \quad \cdots \quad \{\phi\}_{NM}] \tag{4.8}$$

where NM is the number of modes used in the analysis.

4.3 Forced Vibration Analysis of Beam Bridges

4.3.1 Displacement Function

The displacement function, w, at any point along the beam may be expressed as a product of a generalized coordinate, $\{q\}$, which is a function of time only, and a vibration mode shape, $[S_y][\Phi_b]$, which is a function of only the spatial coordinate y.

$$w(y,t) = [S_y][\Phi_b]\{q\} \tag{4.9}$$

where

$$[S_y] = \left[\sin\frac{\pi y}{l} \quad \sin\frac{2\pi y}{l} \quad . \quad . \quad . \quad \sin\frac{r\pi y}{l} \right]$$

and r is the number of harmonic terms used in the analysis.

4.3.2 Minimization of Total Potential Energy

The strain energy of the beam is given by

$$U = \frac{EI}{2}\int_0^l \left(\frac{\partial^2 w}{dy^2}\right) dy \tag{4.10}$$

where I and E are respectively the moment of inertia and elastic modulus of the beam. Substitutions of equation (4.9) into equation (4.10) gives the strain energy as

$$U = \frac{1}{2}\{q\}^T [K_b^*]\{q\} \tag{4.11}$$

where the stiffness matrix $[K_b^*]$ is given by

$$[K_b^*] = EI\int_0^l [\Phi_b]^T \left[\dot{S}_y\right]^T \left[\dot{S}_y\right][\Phi_b]dy \tag{4.12}$$

$$\text{in which } \left[\dot{S}_y\right] = \frac{\partial^2}{\partial y^2}[S_y]$$

Due to orthogonality properties of the mode shapes, the stiffness matrix becomes diagonal. Its diagonal elements are the square of frequencies of the bridge.

The potential energy due to the external distributed loads, p, can be written as

$$W_E = -\int_0^l pwdy \tag{4.13}$$

Substituting equation (4.9) into equation (4.13) gives

$$W_E = -\{q\}^T \{F^*\} \tag{4.14}$$

where $\{F^*\}$ is the load vector due to the external load and is given by the following integral

$$\{F^*\} = \int_0^l p[\Phi_b]^T [S_y]^T dy \tag{4.15}$$

For a concentrated force f, the above integral becomes the following simple expression.

$$\{F^*\} = f[\Phi_b]^T[S_y(y(t))]^T \tag{4.16}$$

where y represents the position of force which is a function of time for a moving force.

The inertia force per unit length of the beam is obtained from Newton's Second Law as follows:

$$p_I = -\rho A \frac{\partial^2 w}{\partial t^2} \tag{4.17}$$

where ρ is the mass per unit volume and A is the area of the cross-section.

The potential energy due to the inertia force p_I can be written as

$$W_I = -\int_0^l p_I w dy \tag{4.18}$$

After some substitutions, the potential energy due to the inertia force becomes

$$W_I = \{q\}^T[M_b^*]\{\ddot{q}\} \tag{4.19}$$

where the mass matrix $[M_b^*]$ is given by

$$[M_b^*] = \rho A \int_0^l \int_0^l [\Phi_b]^T [S_y]^T [S_y][\Phi_b] dy \tag{4.20}$$

Again because of orthogonality properties of the mode shapes, the mass matrix becomes diagonal. Furthermore, if the mode shapes are mass-orthonormal, the mass matrix becomes an identity matrix.

The distributed viscous damping force per unit length of the beam is obtained as follows:

$$p_D = -c\frac{\partial w}{\partial t} \tag{4.21}$$

where c is the distributed viscous damping coefficient.

The potential energy due to the damping force p_D can be written as:

$$W_D = -\int_0^l p_D w dy \tag{4.22}$$

After some substitutions, the potential energy due to the damping force becomes

$$W_D = \{q\}^T \left[C_b^*\right]\left\{\dot{q}\right\} \tag{4.23}$$

where the damping matrix $\left[C_b^*\right]$ is given by

$$\left[C_b^*\right] = c\int_0^l \left[\Phi_b\right]^T \left[S_y\right]^T \left[S_y\right]\left[\Phi_b\right] dy \tag{4.24}$$

The off-diagonal elements of the damping matrix vanish because of the orthogonality properties of the mode shapes.

The total potential energy of the beam, Π, is the sum of strain energy and potential energy. Thus

$$\Pi = U + W_E + W_I + W_D \tag{4.25}$$

According to the principle of minimum potential energy, the equilibrium configuration is defined by the NM algebraic equations.

$$\frac{\partial \Pi}{\partial q_p} = 0 \quad \text{for} \quad p = 1, 2, ..., NM \tag{4.26}$$

or in a compact form

$$\left\{\frac{\partial \Pi}{\partial \{q\}}\right\} = \{0\} \tag{4.27}$$

Substituting equation (4.25) into equation (4.27) and carrying out the partial differentiation produces a set of algebraic equations which can be written in the following matrix form:

$$[M_b^*]\{\ddot{q}\} + [C_b^*]\{\dot{q}\} + [K_b^*]\{q\} = \{F^*\} \tag{4.28}$$

4.3.3 Response Under a Two-axle Two-wheel Vehicle Model

Following the same procedure as in Chapter Two, the equilibrium equations of a multi-span beam bridge under a two-axle two-wheel vehicle can be written as follows:

$$\begin{bmatrix} ([M_b^*]+[M_I]) & [0] \\ [0] & [M_v] \end{bmatrix} \begin{Bmatrix} \{\ddot{q}\} \\ \{\ddot{d}\} \end{Bmatrix} + \begin{bmatrix} ([C_b^*]+[C_I]) & [C_{VI}] \\ [C_{HI}] & [C_v] \end{bmatrix} \begin{Bmatrix} \{\dot{q}\} \\ \{\dot{d}\} \end{Bmatrix}$$
$$+ \begin{bmatrix} ([K_b^*]+[K_I]) & [K_{VI}] \\ [K_{HI}] & [K_v] \end{bmatrix} \begin{Bmatrix} \{q\} \\ \{d\} \end{Bmatrix} = \begin{Bmatrix} \{F\} \\ \{0\} \end{Bmatrix} \tag{4.29}$$

where

$$[M_v]=\begin{bmatrix} m_s & 0 \\ 0 & \frac{i_{s1}}{s^2} \end{bmatrix}$$

$$[K_v]=\begin{bmatrix} k_f+k_r & a_f k_f - a_r k_r \\ a_f k_f - a_r k_r & a_f{}^2 k_f + a_r{}^2 k_r \end{bmatrix}$$

$$[C_v]=\begin{bmatrix} c_f+c_r & a_f c_f - a_r c_r \\ a_f c_f - a_r c_r & a_f{}^2 c_f + a_r{}^2 c_r \end{bmatrix}$$

$$[C_{HI}]=\left(\begin{bmatrix} -c_f \\ -a_f c_f \end{bmatrix}[S]_f+\begin{bmatrix} -c_r \\ a_r c_r \end{bmatrix}[S]_r\right)[\Phi_b]$$

$$[K_{HI}]=\left(\begin{bmatrix} -k_f \\ -a_f k_f \end{bmatrix}[S]_f+\begin{bmatrix} -c_f \\ -a_f c_f \end{bmatrix}[\dot{S}]_f+\begin{bmatrix} -k_r \\ a_r k_r \end{bmatrix}[S]_r+\begin{bmatrix} -c_r \\ a_r c_r \end{bmatrix}[\dot{S}]_r\right)[\Phi_b]$$

$$[M_t]=m_{uf}[\Phi_b]^T[S]_f^T[S]_f[\Phi_b]+m_{ur}[\Phi_b]^T[S]_r^T[S]_r[\Phi_b]$$

$$\begin{aligned}[C_t]=&[\Phi_b]^T[S]_f^T\left(c_f[S]_f+2m_{uf}[\dot{S}]_f\right)[\Phi_b]\\ &+[\Phi_b]^T[S]_r^T\left(c_r[S]_r+2m_{ur}[\dot{S}]_r\right)[\Phi_b]\end{aligned}$$

$$[K_I]=[\Phi_b]^T[S]_f^T\left(k_f[S]_f+c_f\left[\dot{S}\right]_f+m_{uf}\left[\ddot{S}\right]_f\right)[\Phi_b]$$
$$+[\Phi_b]^T[S]_r^T\left(k_r[S]_r+c_r\left[\dot{S}\right]_r+m_{ur}\left[\ddot{S}\right]_r\right)[\Phi_b]$$

$$[K_{VI}]=[\Phi_b]^T[S]_f^T[-k_f \quad -a_f k_f]+[\Phi_b]^T[S]_r^T[-k_r \quad a_r k_r]$$

$$[C_{VI}]=[\Phi_b]^T[S]_f^T[-c_f \quad -a_f c_f]+[\Phi_b]^T[S]_r^T[-c_r \quad a_r c_r]$$

$$\{F\}=[\Phi_b]^T[S]_f^T(m_{uf}+a_r m_s)+[\Phi_b]^T[S]_r^T(m_{ur}+a_f m_s)$$

The motion of the bridge and the vehicle are coupled through the matrices $[C_{VI}]$ and $[K_{VI}]$ and $[C_{HI}]$ and $[K_{HI}]$. The sub-matrices $[C_b^*]$, $[C_v]$, $[K_b^*]$, $[K_v]$, $[M_b^*]$ and $[M_v]$ are time invariant, while the sub-matrices $[C_{HI}]$, $[C_{VI}]$, $[K_{HI}]$, $[K_{VI}]$, $[C_I]$, $[K_I]$, $[M_I]$ and the vector $[F]$ vary with time as they contain the vectors $\{S\}_f$ and $\{S\}_r$ and their derivatives. To ensure that any wheel load outside the bridge will not be included in computing the response of the bridge, the terms that are associated with that wheel should not be included in the formation of the latter sub-matrices and the force vector.

4.4 Forced Vibration Analysis of Slab Bridges

4.4.1 Displacement Function

The displacement function, w, at any point on the bridge may be expressed as a product of a generalized coordinate, $\{z_b\}$, which is a function of time only, and a vibration mode shape,$[S_y][\Phi_b]$, which is a function of only the spatial coordinate y.

$$w(y,t) = [S_y][\Phi_b]\{z_b\} \tag{4.30}$$

where

$$[S_y] = \left[\sin\frac{\pi y}{l} \quad \sin\frac{2\pi y}{l} \quad . \quad . \quad . \quad \sin\frac{r\pi y}{l}\right]$$

and r is the number of harmonic terms used in the analysis.

The vertical displacements at contact point i is given by

$$w_i = [S][G]_i\{z_b\} \tag{4.31}$$

where

$$[S]=\left[\sin\frac{\pi(vt-s)}{l}\quad \sin\frac{2\pi(vt-s)}{l}\quad \sin\frac{3\pi(vt-s)}{l}\quad \cdots\quad \sin\frac{r\pi(vt-s)}{l}\right]$$

4.4.2 Response Under a Two-Axle Four-Wheel Vehicle Model

Following the same procedure as in Chapter Three, the equilibrium equations governing the response of a multi-span slab bridge under two-axle four-wheel vehicle model can be written as:

$$\begin{bmatrix}([M_b^*]+[M_I]) & [0]\\ [0] & [M_v]\end{bmatrix}\begin{Bmatrix}\{\ddot{z}_b\}\\ \{\ddot{d}\}\end{Bmatrix}+\begin{bmatrix}([C_b^*]+[C_I]) & [C_{VI}]\\ [C_{HI}] & [C_v]\end{bmatrix}\begin{Bmatrix}\{\dot{z}_b\}\\ \{\dot{d}\}\end{Bmatrix}$$
$$+\begin{bmatrix}([K_b^*]+[K_I]) & [K_{VI}]\\ K_{HI} & [K_v]\end{bmatrix}\begin{Bmatrix}\{z_b\}\\ \{d\}\end{Bmatrix}=\begin{Bmatrix}\{F\}\\ \{0\}\end{Bmatrix} \qquad (4.32)$$

where

$$[M_v]=\begin{bmatrix}m_s & 0 & 0\\ 0 & \frac{i_{s1}}{s^2} & 0\\ 0 & 0 & \frac{i_{s2}}{b^2}\end{bmatrix}$$

$$[K_v]=\begin{bmatrix} 2(k_f+k_r) & 2(a_f k_f - a_r k_r) & 0 \\ 2(a_f k_f - a_r k_r) & 2(a_f{}^2 k_f + a_r{}^2 k_r) & 0 \\ 0 & 0 & 2a_t{}^2(k_f+k_r) \end{bmatrix}$$

$$[C_v]=\begin{bmatrix} 2(c_f+c_r) & 2(a_f c_f - a_r c_r) & 0 \\ 2(a_f c_f - a_r c_r) & 2(a_f{}^2 c_f + a_r{}^2 c_r) & 0 \\ 0 & 0 & 2a_t{}^2(c_f+c_r) \end{bmatrix}$$

$$[C_{HI}]=\begin{bmatrix} -c_f \\ -a_f c_f \\ 2a_t{}^2 c_f \end{bmatrix}[S]_f[G]_i+\begin{bmatrix} -c_f \\ -a_f c_f \\ -2a_t{}^2 c_f \end{bmatrix}[S]_f[G]_j \\ \begin{bmatrix} -c_r \\ a_r c_r \\ 2a_t{}^2 c_r \end{bmatrix}[S]_r[G]_i+\begin{bmatrix} -c_r \\ a_r c_r \\ -2a_t{}^2 c_r \end{bmatrix}[S]_r[G]_j$$

$$[K_{HI}]=\begin{bmatrix} -k_f \\ -a_f k_f \\ 2a_t{}^2 k_f \end{bmatrix}[S]_f[G]_i+\begin{bmatrix} -k_f \\ -a_f k_f \\ -2a_t{}^2 k_f \end{bmatrix}[S]_f[G]_j+\begin{bmatrix} -c_f \\ -a_f c_f \\ 2a_t{}^2 c_f \end{bmatrix}[\dot{S}]_f[G]_i+\begin{bmatrix} -c_f \\ -a_f c_f \\ -2a_t{}^2 c_f \end{bmatrix}[\dot{S}]_f[G]_j \\ +\begin{bmatrix} -k_r \\ a_r k_r \\ 2a_t{}^2 k_r \end{bmatrix}[S]_r[G]_i+\begin{bmatrix} -k_r \\ a_r k_r \\ -2a_t{}^2 k_r \end{bmatrix}[S]_r[G]_j+\begin{bmatrix} -c_r \\ a_r c_r \\ 2a_t{}^2 c_r \end{bmatrix}[\dot{S}]_r[G]_i+\begin{bmatrix} -c_r \\ a_r c_r \\ -2a_t{}^2 c_r \end{bmatrix}[\dot{S}]_r[G]_j$$

$$
\begin{aligned}
[M_t] = [G]_i^T [S]_f^T \left(\left(\frac{m_{uf}}{4} + \frac{i_{uf2}}{b^2} \right) [S]_f [G]_i + \left(\frac{m_{uf}}{4} - \frac{i_{uf2}}{b^2} \right) [S]_f [G]_j \right) \\
+ [G]_j^T [S]_f^T \left(\left(\frac{m_{uf}}{4} - \frac{i_{uf2}}{b^2} \right) [S]_f [G]_i + \left(\frac{m_{uf}}{4} + \frac{i_{uf2}}{b^2} \right) [S]_f [G]_j \right) \\
+ [G]_i^T [S]_r^T \left(\left(\frac{m_{ur}}{4} + \frac{i_{ur2}}{b^2} \right) [S]_r [G]_i + \left(\frac{m_{ur}}{4} - \frac{i_{ur2}}{b^2} \right) [S]_r [G]_j \right) \\
+ [G]_j^T [S]_r^T \left(\left(\frac{m_{ur}}{4} - \frac{i_{ur2}}{b^2} \right) [S]_r [G]_i + \left(\frac{m_{ur}}{4} + \frac{i_{ur2}}{b^2} \right) [S]_r [G]_j \right)
\end{aligned}
$$

$$
\begin{aligned}
[C_t] = [G]_i^T [S]_f^T \left(\left(\left(\frac{1}{2} + 2a_t^2 \right) c_f [S]_f + 2 \left(\frac{m_{uf}}{4} + \frac{i_{uf2}}{b^2} \right) \left[\dot{S} \right]_f \right) [G]_i \right. \\
\left. + \left(\left(\frac{1}{2} - 2a_t^2 \right) c_f [S]_f + 2 \left(\frac{m_{uf}}{4} - \frac{i_{uf2}}{b^2} \right) \left[\dot{S} \right]_f \right) [G]_j \right) \\
+ [G]_j^T [S]_f^T \left(\left(\left(\frac{1}{2} - 2a_t^2 \right) c_f [S]_f + 2 \left(\frac{m_{uf}}{4} - \frac{i_{uf2}}{b^2} \right) \left[\dot{S} \right]_f \right) [G]_i \right. \\
\left. + \left(\left(\frac{1}{2} + 2a_t^2 \right) c_f [S]_f + 2 \left(\frac{m_{uf}}{4} + \frac{i_{uf2}}{b^2} \right) \left[\dot{S} \right]_f \right) [G]_j \right) \\
+ [G]_i^T [S]_r^T \left(+ \left(\left(\frac{1}{2} + 2a_t^2 \right) c_r [S]_r + 2 \left(\frac{m_{ur}}{4} + \frac{i_{ur2}}{b^2} \right) \left[\dot{S} \right]_r \right) [G]_i \right. \\
\left. \left. + \left(\left(\frac{1}{2} - 2a_t^2 \right) c_r [S]_r + 2 \left(\frac{m_{ur}}{4} - \frac{i_{ur2}}{b^2} \right)_r \left[\dot{S} \right]_r [G]_j \right) \right) \\
+ [G]_j^T [S]_r^T \left(\left(\left(\frac{1}{2} - 2a_t^2 \right) c_r [S]_r + 2 \left(\frac{m_{ur}}{4} - \frac{i_{ur2}}{b^2} \right) \left[\dot{S} \right]_r \right) [G]_i \right. \\
\left. \left(\left(\frac{1}{2} + 2a_t^2 \right) c_r [S]_r + 2 \left(\frac{m_{ur}}{4} + \frac{i_{ur2}}{b^2} \right)_r \left[\dot{S} \right]_r \right) [G]_j \right.
\end{aligned}
$$

$$
\begin{aligned}
[K_t] = [G]_i^T [S]_f^T \Bigg(& \left(\left(\frac{1}{2} + 2a_t^2 \right) \left(k_f [S]_f + c_f \left[\dot{S} \right]_f \right) + 2 \left(\frac{m_{uf}}{4} + \frac{i_{uf2}}{b^2} \right) \left[\ddot{S} \right]_f \right) [G]_i \\
& + \left(\left(\frac{1}{2} - 2a_t^2 \right) \left(k_f [S]_f + c_f \left[\dot{S} \right]_f \right) + 2 \left(\frac{m_{uf}}{4} - \frac{i_{uf2}}{b^2} \right) \left[\ddot{S} \right]_f \right) [G]_j \Bigg) \\
+ [G]_j^T [S]_f^T \Bigg(& \left(\left(\frac{1}{2} - 2a_t^2 \right) \left(k_f [S]_f + c_f \left[\dot{S} \right]_f \right) + 2 \left(\frac{m_{uf}}{4} - \frac{i_{uf2}}{b^2} \right) \left[\ddot{S} \right]_f \right) [G]_i \\
& + \left(\left(\frac{1}{2} + 2a_t^2 \right) \left(k_f [S]_f + c_f \left[\dot{S} \right]_f \right) + 2 \left(\frac{m_{uf}}{4} + \frac{i_{uf2}}{b^2} \right) \left[\ddot{S} \right]_f \right) [G]_j \Bigg) \\
+ [G]_i^T [S]_r^T \Bigg(& \left(\left(\frac{1}{2} + 2a_t^2 \right) \left(k_r [S]_r + c_f \left[\dot{S} \right]_r \right) + 2 \left(\frac{m_{ur}}{4} + \frac{i_{ur2}}{b^2} \right) \left[\ddot{S} \right]_r \right) [G]_i \\
& + \left(\left(\frac{1}{2} - 2a_t^2 \right) \left(k_r [S]_r + c_f \left[\dot{S} \right]_r \right) + 2 \left(\frac{m_{ur}}{4} - \frac{i_{ur2}}{b^2} \right)_r \left[\ddot{S} \right]_r \right) [G]_j \Bigg) \\
+ [G]_j^T [S]_r^T \Bigg(& \left(\left(\frac{1}{2} - 2a_t^2 \right) \left(k_r [S]_r + c_f \left[\dot{S} \right]_r \right) + 2 \left(\frac{m_{ur}}{4} - \frac{i_{ur2}}{b^2} \right) \left[\ddot{S} \right]_r \right) [G]_i \\
& \left(\left(\frac{1}{2} + 2a_t^2 \right) \left(\left(k_r [S]_r + c_r \left[\dot{S} \right]_r \right) + 2 \left(\frac{m_{ur}}{4} + \frac{i_{ur2}}{b^2} \right)_r \left[\ddot{S} \right]_r \right) [G]_j \right)
\end{aligned}
$$

$$[K_{VI}] = [G]_i^T [S]_f^T \begin{bmatrix} -k_f & -a_f k_f & 2a_t^2 k_f \end{bmatrix} + [G]_j^T [S]_f^T \begin{bmatrix} -k_f & -a_f k_f & -2a_t^2 k_f \end{bmatrix}$$
$$+ [G]_i^T [S]_r^T \begin{bmatrix} -k_r & a_r k_r & 2a_t^2 k_r \end{bmatrix} + [G]_j^T [S]_r^T \begin{bmatrix} -k_r & a_r k_r & -2a_t^2 k_r \end{bmatrix}$$

$$[C_{VI}] = [G]_i^T [S]_f^T \begin{bmatrix} -c_f & -a_f c_f & 2a_t^2 c_f \end{bmatrix} + [G]_j^T [S]_f^T \begin{bmatrix} -c_f & -a_f c_f & -2a_t^2 c_f \end{bmatrix}$$
$$+ [G]_i^T [S]_r^T \begin{bmatrix} -c_r & a_r c_r & 2a_t^2 c_r \end{bmatrix} + [G]_j^T [S]_r^T \begin{bmatrix} -c_r & a_r c_r & -2a_t^2 c_r \end{bmatrix}$$

$$\{F\} = \left(\frac{a_r m_s g}{2} + \frac{m_{uf} g}{2}\right)[G]_i^T \{S\}_f^T + \left(\frac{a_r m_s g}{2} + \frac{m_{uf} g}{2}\right)[G]_j^T \{S\}_f^T$$
$$+ \left(\frac{a_f m_s g}{2} + \frac{m_{ur} g}{2}\right)[G]_i^T \{S\}_r^T + \left(\frac{a_f m_s g}{2} + \frac{m_{ur} g}{2}\right)[G]_j^T \{S\}_r^T$$

Both the modal mass and stiffness matrices of the bridge are diagonal because of the orthogonality property of the mode shapes. The diagonal elements of the modal stiffness matrix contains the square of the frequencies. The modal mass matrix is an identity matrix since mass orthonormal mode shapes have been used. Furthermore, the modal damping matrix is assumed to be diagonal and its nth diagonal term is $2\xi_n\omega_n$, where ξ_n is interpreted as the damping ratio in the nth mode.

The motion of the bridge and the vehicle are coupled through the matrices $[C_{VI}]$ and $[K_{VI}]$ and $[C_{HI}]$ and $[K_{HI}]$. The sub-matrices $[C_b^*]$, $[C_v]$, $[K_b^*]$, $[K_v]$, $[M_b^*]$ and $[M_v]$ are time invariant, while the sub-matrices $[C_{HI}]$, $[C_{VI}]$, $[K_{HI}]$, $[K_{VI}]$, $[C_I]$, $[K_I]$, $[M_I]$ and the

vector $[F]$ vary with time as they contain the vectors $\{S\}_f$ and $\{S\}_r$ and their derivatives. To ensure that any wheel load outside the bridge will not be included in computing the response of the bridge, the terms that are associated with that wheel should not be included in the formation of the latter sub-matrices and the force vector.

4.5 Numerical Examples on Beam Bridges

4.5.1 Free Vibration Analysis of Multi-span Beam Bridges

A frequency analysis of four continuous bridges of two equal spans has been carried out . The geometry and material properties of the bridges are given in Table 4.1. Using my computer program, the lowest ten frequencies for each bridge are obtained. These frequencies are reported in Tables (4.2), (4.3), (4.4) and (4.5).

Table 4.1

Geometry and Material Properties

Bridge Number	span (l) (m)	Width (m)	Thickness (m)	E (kN/m^2)	ν	Mass density (Kg/m^3)
1	10.0	10.0	0.325	$2.65x10^7$	0.15	2446.5
2	15.0	10.0	0.400	$2.65x10^7$	0.15	2446.5
3	20.0	10.0	0.525	$2.65x10^7$	0.15	2446.5
4	25.0	10.0	0.675	$2.65x10^7$	0.15	2446.5

TABLE 4.2

Lowest Ten Frequencies for

a Continuous Beam Bridge

l = 10 m, B =10 m

Mode Number	Frequency (Hz)
1	4.85
2	7.58
3	19.40
4	24.55
5	43.65
6	51.23
7	77.60
8	87.60
9	121.26
10	133.69

TABLE 4.3

Lowest Ten Frequencies for

a Continuous Beam Bridge

l = 15 m, B =10 m

Mode Number	Frequency (Hz)
1	2.65
2	4.14
3	10.61
4	13.43
5	23.88
6	28.02
7	42.45
8	47.92
9	66.33
10	73.13

TABLE 4.4

Lowest Ten Frequencies for

a Continuous Beam Bridge

l = 20 m, B =10 m

Mode Number	Frequency (Hz)
1	1.96
2	3.06
3	7.84
4	9.92
5	17.63
6	20.69
7	31.34
8	35.38
9	48.97
10	53.99

TABLE 4.5

Lowest Ten Frequencies for

a Continuous Beam Bridge

l = 25 m, B =10 m

Mode Number	Frequency (Hz)
1	1.61
2	2.52
3	6.45
4	8.16
5	14.51
6	17.02
7	25.79
8	29.11
9	40.29
10	44.43

4.5.2 Forced Vibration Analysis of Multi-span Beam Bridges

Forced vibration analysis of the four bridges whose geometry and material properties are reported in Table 4.1 is carried out. The four vehicle models described in section 2.8 are used. The results of this part of analysis are reported in Tables (4.6), (4.7), (4.8), (4.9) and (4.10). Table (4.6) shows the maximum mid-span static deflections of the four bridges due to a single point load and a set of two point loads . Tables (4.7), (4.8), (4.9) and (4.10) show the maximum mid-span dynamic deflections and deflection amplification factors.

TABLE 4.6

Static Deflections at Mid-span of Continuous Bridges

Bridge Number	$W_{static}(mm)$ (One point load)	$W_{static}(mm)$ (Two point loads)
1	6.68	3.88
2	12.08	9.27
3	12.67	10.93
4	11.64	10.59

TABLE 4.7

Dynamic Deflections and Deflection Amplification Factor at Mid-span of a Continuous Beam Bridge

l = 10 m, B =10 m Bridge

Vehicle Model	$W_{dynamic}$	DAF
I	7.43	1.11
II	4.69	1.21
III	4.43	1.14
IV	4.43	1.14

TABLE 4.8

Dynamic Deflections and Deflection Amplification Factor at Mid-span of a Continuous Beam Bridge

l = 15 m, B =10 m Bridge

Vehicle Model	$W_{dynamic}$	DAF
I	16.83	1.39
II	10.08	1.09
III	11.34	1.22
IV	11.33	1.22

TABLE 4.9

Dynamic Deflections and Deflection Amplification Factor at Mid-span of a Continuous Beam Bridge

l = 20 m, B =10 m Bridge

Vehicle Model	$W_{dynamic}$	DAF
I	18.10	1.43
II	13.14	1.20
III	14.23	1.30
IV	14.21	1.30

TABLE 4.10

Dynamic Deflections and Deflection Amplification

Factor at Mid-span of a Continuous Beam Bridge

l = 25 m, B =10 m Bridge

Vehicle Model	$W_{dynamic}$	DAF
I	16.22	1.39
II	13.12	1.24
III	13.84	1.31
IV	13.80	1.30

4.6 Numerical Examples on Multi-span Slab Bridges

4.6.1 Free Vibration Analysis of Multi-span Slab Bridges

A frequency analysis of the four continuous slab bridges described in subsection 4.5.1 is carried out. A Poisson's ratio of 0.15 is used. The lowest ten frequencies for each bridge are obtained and are reported in Tables (4.11), (4.12), (4.13) and (4.14).

TABLE 4.11

Lowest Ten Frequencies for

a Continuous Slab Bridge

l = 10 m, B =10 m

Mode Number	Frequency (Hz)
1	4.88
2	7.64
3	8.51
4	10.68
5	18.91
6	19.57
7	20.41
8	23.92
9	24.78
10	28.62

TABLE 4.12

Lowest Ten Frequencies for

a Continuous Slab Bridge

l = 15m, B =10 m

Mode Number	Frequency (Hz)
1	2.66
2	4.17
3	6.34
4	7.41
5	10.69
6	13.54
7	15.61
8	17.98
9	18.37
10	19.00

TABLE 4.13

Lowest Ten Frequencies for

a Continuous Slab Bridge

l = 20 m, B =10 m

Mode Number	Frequency (Hz)
1	1.96
2	3.08
3	6.01
4	6.75
5	7.88
6	9.99
7	13.75
8	15.38
9	17.76
10	20.86

TABLE 4.14

Lowest Ten Frequencies for

a Continuous Slab Bridge

l = 25 m, B =10 m

Mode Number	Frequency (Hz)
1	1.62
2	2.53
3	6.06
4	6.48
5	6.65
6	8.21
7	13.31
8	14.58
9	14.60
10	17.15

4.6.2 Forced Vibration Analysis of Multi-span Slab Bridges

Forced vibration analysis of the four bridges whose geometry and material properties are reported in Table 4.1 is carried out. The four vehicle models described in section 3.10 are used. The results of this part of analysis are reported in Tables (4.15), (4.16), (4.17), (4.18) and (4.19). Table (4.15) shows the maximum mid-span static deflections of the four bridges due to a single point load and a set of two point loads . Tables (4.16), (4.17), (4.18) and (4.19) show the maximum mid-span dynamic deflections and deflection amplification factors.

TABLE 4.15

Static Deflections at Mid-span of Bridges

Bridge Number	$W_{static}(mm)$ (One point load)	$W_{static}(mm)$ (Two point loads)
1	7.61	4.25
2	12.40	9.28
3	12.66	10.80
4	11.56	10.46

TABLE 4.16

Dynamic Deflections and Deflection Amplification Factor at Mid-span of a Continuous slab Bridge

l = 10m, B =10 m Bridge

Vehicle Model	$W_{dynamic}$	DAF
I	8.18	1.07
II	4.92	1.16
III	4.65	1.09
IV	4.68	1.10

TABLE 4.17

Dynamic Deflections and Deflection Amplification Factor at Mid-span of a Continuous slab Bridge

l = 15 m, B =10 m Bridge

Vehicle Model	$W_{dynamic}$	DAF
I	16.89	1.36
II	10.03	1.08
III	11.30	1.22
IV	11.35	1.22

TABLE 4.18

Dynamic Deflections and Deflection Amplification Factor at Mid-span of a Continuous slab Bridge

l = 20 m, B =10 m Bridge

Vehicle Model	$W_{dynamic}$	DAF
I	17.82	1.41
II	12.99	1.20
III	14.01	1.30
IV	14.05	1.30

TABLE 4.19

Dynamic Deflections and Deflection Amplification Factor at Mid-span of a Continuous slab Bridge

l = 25 m, B =10 m Bridge

Vehicle Model	$W_{dynamic}$	DAF
I	15.91	1.38
II	12.94	1.24
III	13.62	1.30
IV	13.65	1.30

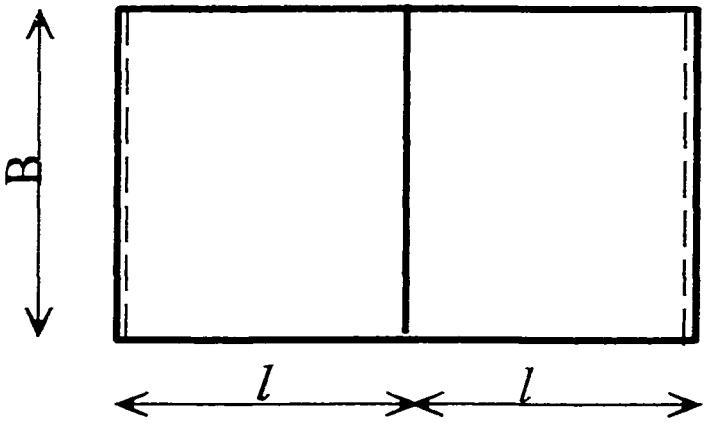

Figure 4.1 Two-span Bridge of Equal Spans

Chapter 5

SLAB-ON-GIRDER AND BOX GIRDER BRIDGES

5.1 Introduction

The finite strip analysis of slab bridges subjected to moving vehicle loads has been covered in Chapter Three. In this chapter the method is extended to dynamic analysis of box girder bridges and slab-on-girder bridges. Box girder bridges and slab-on-girder bridges are modeled in finite strip method as flat shell strip. Each flat shell element is subject to in-plane stresses and out-of-plane bending stresses (plate strip stresses). Since there is no interaction between the in-plane stresses and out-of-plane bending stresses; the mass, stiffness and damping matrices and the load vector of the strip due to the two stresses are established separately and then combined. The plate strip was formulated in Chapter Three, and plane stress relations are reviewed in the following sections.

5.2 Plane Stress

In plane stress problems, all the external forces act in the plane of the plate. These external forces are uniform through the thickness and are thus functions of only x and y. The displacements of the strip also vary with x and y only and can be resolved into two components (u and v) along x and y. If the displacements u and v along the transverse and the longitudinal directions are taken as degrees of freedom at each nodal lines across the width, a suitable displacement function for each of the displacement components that satisfies the compatibility between the adjoining strips and the boundary conditions can be represented by the product of a linear polynomial function which represents the variations of u and v in the transverse direction and an harmonic series which represent their variation along the longitudinal direction. The nodal displacement parameters and the nodal force vector of each in-plane stress strip corresponding to the m^{th} series term are:

$$\{\delta^P\}_m = \begin{Bmatrix} u_i \\ v_i \\ u_j \\ v_j \end{Bmatrix}_m \tag{5.1}$$

$$\{F^P\}_m = \begin{Bmatrix} U_i \\ V_i \\ U_j \\ V_j \end{Bmatrix}_m \tag{5.2}$$

where the superscript p refers to plane stress quantites.

For a rectangular plate with two simply supported ends, the boundary conditions become

$$u = 0 \quad \text{and} \quad \sigma_y = 0 \quad \text{at} \quad y = 0 \quad \text{and} \quad y = l$$

The displacement components at any point in the strip can then be represented as

$$u(x,y) = \sum_{m=1}^{r} (N_1^p(x)u_{1m} + N_2^p(x)u_{2m}) \sin\frac{m\pi y}{l} \tag{5.3}$$

$$v(x,y) = \sum_{m=1}^{r} (N_1^p(x)v_{1m} + N_2^p(x)v_{2m}) \cos\frac{m\pi y}{l} \tag{5.4}$$

where,

$$N_1^p(x) = (1 - X)$$

$$N_2^p(x) = X$$

$$X = \frac{x}{b}$$

and r is the total number of terms considered in the analysis

These expressions can be written in the following more compact form

$$\begin{Bmatrix} u \\ v \end{Bmatrix} = \sum_{m=1}^{r} [C]_m \{\delta^p\}_m \tag{5.5}$$

where $[C]$ is a matrix of shape functions and is given by

$$[C]_m = \begin{bmatrix} N_1^p \sin\dfrac{m\pi y}{l} & 0 & N_2^p \sin\dfrac{m\pi y}{l} & 0 \\ 0 & N_1^p \cos\dfrac{m\pi y}{l} & 0 & N_2^p \cos\dfrac{m\pi y}{l} \end{bmatrix} \tag{5.6}$$

5.3 Strains

Once the displacement functions are known, the strains are obtained by appropriately differentiating the displacement function with respect to the coordinates x and y in the following manner:

$$\{\varepsilon\} = \begin{Bmatrix} \varepsilon_x \\ \varepsilon_y \\ \gamma_{xy} \end{Bmatrix} = \begin{Bmatrix} \dfrac{\partial u}{\partial x} \\ \dfrac{\partial v}{\partial y} \\ \dfrac{\partial u}{\partial y} + \dfrac{\partial v}{\partial x} \end{Bmatrix} = \sum_{m=1}^{r} \left[B^p\right]_m \left\{\delta^p\right\}_m \tag{5.7}$$

where $[B^p]_m$ is the strain matrix and is explicitly in the form

$$[B^p]_m = \begin{bmatrix} N_1^{p'} \sin k_m y & 0 & N_2^{p'} \sin k_m y & 0 \\ 0 & k_m C_1 \sin k_m y & 0 & k_m C_2 \sin k_m y \\ k_m C_1 \cos k_m y & N_1^{p'} \cos k_m y & k_m C_2 \cos k_m y & N_2^{p'} \cos k_m y \end{bmatrix} \quad (5.8)$$

in which $N_i^{p'} = \dfrac{dN_i^p}{dx}$ $i = 1,2$ and $k_m = \dfrac{m\pi}{l}$

5.4 Stresses

The stresses at any point in a strip are related to the curvatures as

$$\begin{aligned} \sigma_x &= \frac{1}{1 - \nu_x \nu_y}(E_x \varepsilon_x + \nu_x E_y \varepsilon_y) \\ \sigma_y &= \frac{1}{1 - \nu_x \nu_y}(\nu_y E_y \varepsilon_x + E_y \varepsilon_y) \\ \tau_{xy} &= E_{xy} \gamma_{xy} \end{aligned} \quad (5.9)$$

in which ν_x and ν_y are Poisson's ratio in the x and y directions respectively, E_x and E_y are moduli

of elasticity in the x and y directions respectively, E_{xy} is the shear rigidity and h is the thickness of the plate strip.

In matrix form, equation (5.9) becomes

$$\{\sigma\} == [D^p]\{\varepsilon\} \tag{5.10}$$

where $[D^p]$ is the elasticity matrix for the in-plane stress analysis defined in equation (5.9).

$$[D^p] = \frac{1}{1-\nu_x\nu_y}\begin{bmatrix} E_x & \nu_x E_y & 0 \\ \nu_y E_y & E_y & 0 \\ 0 & 0 & 1-\nu_x\nu_y E_{xy} \end{bmatrix} \tag{5.11}$$

For in-plane stress analysis of an isotropic plate,

$$[D^p] = \frac{E}{(1-\nu^2)}\begin{bmatrix} 1 & \nu & 0 \\ \nu & 1 & 0 \\ 0 & 0 & \frac{1-\nu}{2} \end{bmatrix} \tag{5.12}$$

where E is the elastic modulus and ν is the Poisson's ratio.

Substitution of equation (5.7) into (5.10) yields

$$\{\sigma\} = \sum_{m=1}^{r} [D^p][B^p]_m \{\delta^p\}_m \tag{5.13}$$

5.5 Minimization of Total Potential Energy

The strain energy of a plane stress strip is given by

$$U = \frac{1}{2}\int_0^l \int_0^b \{\sigma\}^T \{\varepsilon\} dxdy \tag{5.14}$$

The transpose of $\{\sigma\}$ is

$$\{\sigma\}^T = \sum_{m=1}^{r} \{\delta^p\}_m^T [B^p]_m^T [D^p] \tag{5.15}$$

Substituting equations (5.7) and (5.15) into equation (5.14) yields

$$U = \frac{1}{2}\sum_{m=1}^{r}\sum_{n=1}^{r} \{\delta^p\}_m^T \int_0^l \int_0^b [B^p]_m^T [D^p][B^p]_n dxdy \{\delta^p\}_n \tag{5.16}$$

The product of the three matrices to be integrated in this equation contains products of functions that are orthogonal to each other, and as a result of orthogonality properties of these functions, the summation in equation (5.16) requires to be carried out once only. Thus equation (5.16)

becomes

$$U = \frac{1}{2}\sum_{m=1}^{r} \{\delta^p\}_m^T \int_0^l \int_0^b [B^p]_m^T [D^p][B^p]_m dxdy \{\delta^p\}_m \tag{5.17}$$

After integration, equation (5.17) is reduced to

$$U = \frac{1}{2}\sum_{m=1}^{r} \{\delta^p\}_m^T [k^p]_m \{\delta^p\}_m \tag{5.18}$$

where $[k]_m$ (a 4 x 4 matrix) is the stiffness matrix and is given by the following integral.

$$[k^p]_m = \int_0^l \int_0^b [B^p]_m^T [D^p][B^p]_m dxdy \tag{5.19}$$

The potential energy of external loads acting on the plane stress strip can also be expressed in terms of the displacement parameters

$$W_e = -\int_0^l \int_0^b \begin{Bmatrix} u \\ v \end{Bmatrix}^T \begin{Bmatrix} p_x \\ p_y \end{Bmatrix} dxdy \tag{5.20}$$

By substituting the displacement function in equation (5.5) into equation (5.20), the potential energy of external loading can also be expressed in terms of the displacement parameters:

$$W_e = -\sum_{m=1}^{r} \{\delta^p\}_m^T \int_0^l \int_0^b [C]^T \begin{Bmatrix} p_x \\ p_y \end{Bmatrix} dxdy \tag{5.21}$$

The integration of equation (5.21) produces

$$W_e = -\sum_{m=1}^{r} \{\delta^p\}_m^T \{p\}_m \tag{5.22}$$

where $\{p\}_m$ (a 4 x 1 vector) is the equivalent nodal force vector of the external load and is given by the following integral:

$$\{p\}_m = \int_0^l \int_0^b [C]^T \begin{Bmatrix} p_x \\ p_y \end{Bmatrix} dxdy \tag{5.23}$$

For a concentrated load at (x_p, y_p) the above integral is reduced to the following simple expression.

$$\{p\}_m = \left[C_{\substack{(x=x_p) \\ (y=y_p)}} \right]^T \begin{Bmatrix} p_x \\ p_y \end{Bmatrix} \tag{5.24}$$

where x_p and y_p is the position of the load and p_x and p_y are its magnitude.

The inertia force acting on an infinitesimal area dA of mid-plane of a plane stress strip is

$$\{q_i\} = -\rho h \frac{\partial^2 \begin{Bmatrix} u \\ v \end{Bmatrix}}{\partial t^2} \tag{5.25}$$

where ρ is the mass per unit volume .

Substituting equation (5.5) into equation (5.25) gives

$$\{q_i\} = -\rho h \sum_{m=1}^{r} [C] \left\{ \ddot{\delta}^p \right\}_m \tag{5.26}$$

The potential energy of distributed inertia forces can be calculated as

$$W_i = \sum_{m=1}^{r} \sum_{n}^{r} \{\delta^p\}_m^T \int_0^l \int_0^b \rho h [C]_m^T [C]_n^T dxdy \left\{ \ddot{\delta}^p \right\}_n \tag{5.27}$$

After integration, equation (5.27) is reduced to

$$W_i = \sum_{m=1}^{r} \{\delta^p\}_m^T [m^p] \left\{ \ddot{\delta}^p \right\}_m \tag{5.28}$$

where $[m]$ (a 4 x 4 matrix) is the consistent mass matrix and is given by the following integral.

$$[m^p] = \int_0^l \int_0^b \rho h [C]_m^T [C]_m dxdy \tag{5.29}$$

5.6 Flat Shell Strip

The flat shell strip is the combination of a plate strip and a plane stress strip. Consider a flat shell element subjected simultaneously to in-plane and bending forces. For in-plane action, the nodal line displacement parameters are related to the nodal line force vectors through the relation

$$\{F^p\}_m = [k^p]_m \{\delta^p\}_m \tag{5.30}$$

where

$$\{\delta^p\}_m = \begin{Bmatrix} u_i \\ v_i \\ u_j \\ v_j \end{Bmatrix}_m \tag{5.31}$$

and

$$\{F^p\}_m = \begin{Bmatrix} U_i \\ V_i \\ U_j \\ V_j \end{Bmatrix}_m \tag{5.32}$$

Similarly, for the bending action, the nodal line displacement parameters are related to the nodal line force vectors through the relation

$$\{F^b\} = [k^b]_m \{\delta^b\}_m \tag{5.33}$$

where the superscript b refers to the bending action,

$$\{\delta^b\}_m = \begin{Bmatrix} w_i \\ \theta_i \\ w_j \\ \theta_j \end{Bmatrix}_m \tag{5.34}$$

and

$$\{F^b\}_m = \begin{Bmatrix} W_i \\ M_i \\ W_j \\ M_j \end{Bmatrix}_m \tag{5.35}$$

By combining the nodal line displacement parameters and forces for both actions, the strain energy of a flat shell strip can be written as:

$$U = \frac{1}{2}\sum_{m=1}^{r} \{\delta\}_m^T [k]_m \{\delta\}_m \tag{5.36}$$

where

$$\{\delta\}_m = \begin{Bmatrix} u_i & v_i & w_i & \theta_i & u_j & v_j & w_j & \theta_j \end{Bmatrix}^T \tag{5.37}$$

and

$$[k]_m = \begin{bmatrix} [k_{ii}^p] & 0 & [k_{ij}^p] & 0 \\ 0 & [k_{ii}^b] & 0 & [k_{ij}^b] \\ [k_{ij}^p] & 0 & [k_{jj}^p] & 0 \\ 0 & [k_{ij}^b] & 0 & [k_{jj}^b] \end{bmatrix}_m \tag{5.38}$$

Similarly, its potential energy due to inertia forces can be written as follows:

$$W_i = -\sum_{m=1}^{r} \{\delta\}_m^T [m] \{\ddot{\delta}\}_m \tag{5.39}$$

where

$$[m] = \begin{bmatrix} [m_{ii}^p] & 0 & [m_{ij}^p] & 0 \\ 0 & [m_{ii}^b] & 0 & [m_{ij}^b] \\ [m_{ij}^p] & 0 & [m_{jj}^p] & 0 \\ 0 & [m_{ij}^b] & 0 & [m_{jj}^b] \end{bmatrix} \tag{5.40}$$

and

$$\{\ddot{\delta}\}_m = \{\ddot{u}_i \quad \ddot{v}_i \quad \ddot{w}_i \quad \ddot{\theta}_i \quad \ddot{u}_j \quad \ddot{v}_j \quad \ddot{w}_j \quad \ddot{\theta}_j\}^T \tag{5.41}$$

Finally the potential energy of the external loads of the flat shell strip is given by

$$W_e = -\sum_{m=1}^{r} \{\delta\}_m^T \{F^i\}_m \tag{5.42}$$

where

$$\{F^t\}_m = \{U_i \quad V_i \quad W_i \quad M_i \quad U_j \quad V_j \quad W_j \quad M_j\}^T \tag{5.43}$$

All of the above derivations are carried out in a local coordinate system whose x and y axes coincide with the mid-surface of a strip. Since box girder bridges and slab-on-girder bridges have strips that may in general meet at an angle, it is convenient to carry out the assembling procedure of the system matrices and vectors of non-coplanar strips in a global coordinate system common to all the strips. This is done by transforming displacements and forces vectors from local coordinates to global coordinates.

Transformations of displacements and force vectors from local coordinates x, y, z to the global coordinates x', y', z' is carried out as follows:

$$\{\delta\}_m = [T]\{\delta_G\}_m \tag{5.44}$$

in which [T] is a transformation matrix and the subscript G refers to global coordinates

$$[T] = \begin{bmatrix} [t] & 0 \\ 0 & [t] \end{bmatrix} \tag{5.45}$$

where

$$[t] = \begin{bmatrix} \cos\theta & 0 & \sin\theta & 0 \\ 0 & 1 & 0 & 0 \\ -\sin\theta & 0 & \cos\theta & 0 \\ 0 & 0 & 0 & 1 \end{bmatrix} \tag{5.46}$$

with θ being the angle between the x and x' axes

Substituting equation (5.44) into equations (5.36), (5.39), and (5.42) leads to the following results:

$$U = \frac{1}{2}\sum_{m=1}^{r}\{\delta_G\}_m^T[T]^T[k]_m[T]\{\delta_G\}_m \tag{5.47}$$

$$W_i = \sum_{m=1}^{r}\{\delta_G\}_m^T[T]^T[m][T]\{\ddot{\delta}_G\}_m \tag{5.48}$$

$$W_e = -\sum_{m=1}^{r}\{\delta_G\}_m^T[T]^T\{F^t\}_m \tag{5.49}$$

The total potential energy of the entire structure, Π, is the sum of U and W contributions from all the strips comprising the slab deck. Thus

$$\Pi = \sum_{s=1}^{NS}(U + W_i + W_e) \tag{5.50}$$

in which NS is the total number of strips.

Substituting equations. (5.47), (5.48), and (5.49) into equation (5.50) produces

$$\Pi = \sum_{S=1}^{NS}(\frac{1}{2}\sum_{m=1}^{r}\{\delta_G\}_m^T[k_G]_{Sm}\{\delta_G\}_m + \sum_{m=1}^{r}\{\delta_G\}_m^T[m_G]_S\{\ddot{\delta}_G\}_m - \sum_{m=1}^{r}\{\delta_G\}_m^T\{F_G^t\}_{Sm}) \tag{5.51}$$

where

$$[k_G]_m = [T]^T[k]_m[T] \tag{5.52}$$

$$[m_G] = [T]^T[m][T] \tag{5.53}$$

$$\left\{F_G^t\right\}_m = [T]^T[F^t]_m \tag{5.54}$$

The equations of dynamic equilibrium is obtained by minimizing the total potential energy Π with respect to each of the displacement parameters $\{\delta\}_{tm}$ of the whole bridge, as follows:

$$\left\{\frac{\partial \Pi}{\partial\{\delta\}_{tm}}\right\} = \{0\} \tag{5.55}$$

where *tm* is equal *r* times the total number of degrees of freedom of the whole structure. Substituting equation (5.51) into equation (5.55) and performing the partial differentiation produces a system of linear algebraic equations which after damping is included and the subscript G dropped for convenience can be written in the following matrix form:

$$[M_b]\left\{\ddot{\delta}\right\}_m + [C_b]\left\{\dot{\delta}\right\}_m + [K_b]_m\{\delta\}_m = \{F^t\}_m \tag{5.56}$$

in which $[K_b]_m$, $[C_b]$, $[M_b]$,$\{\delta\}_m$, $\{\dot{\delta}\}_m$, $\{\ddot{\delta}\}_m$ and $\{F^t\}$ are the stiffness matrix, the damping matrix, the mass matrix, the nodal displacement vector, the nodal velocity vector, the nodal acceleration vector and the force vector of the whole bridge respectively.

After the system matrices are derived, the solution procedure explained in Chapter Three is followed by using the relevant system matrices and vectors of slab-on-girder and box girder bridges.

5.7 Numerical Examples

5.7.1 Free Vibration Analysis of Slab-on Girder and Box Girder Bridges

The simply supported concrete slab-on-girder bridge shown in Figure (5.1) and the box-girder bridge shown in Figure (5.2) are analyzed as examples. The material properties of the two bridges are given below

$$E = 2.65\text{x}10^{10}\ \text{N/m}^2$$

$$\rho = 2446.5\ \text{Kg/m}^3$$

$$\nu = 0.15$$

The lowest twenty natural frequencies and their mode shapes were calculated and arranged in order of increasing magnitude. The harmonic term corresponding to each mode shape is also recorded. The results of this part of analysis are reported in Tables 6.1 and 6.2.

TABLE 5.1

Free Vibration Characteristics of Slab-on-Girder Bridge (Figure 5.1)

Mode number (j)	Natural frequency (Hz)	Series term (m_j)
1	4.58	1
2	7.72	1
3	12.77	1
4	17.38	2
5	20.36	2
6	36.17	3
7	37.54	3
8	37.85	1
9	38.73	2
10	44.83	2
11	54.87	3
12	57.24	4
13	58.64	4
14	64.91	3
15	65.80	1
16	67.09	4
17	76.35	1
18	77.09	5
19	81.07	5
20	82.90	2

TABLE 5.2

Free Vibration Characteristics of Box-Girder Bridge (Figure 5.2)

Mode number (j)	Natural frequency (Hz)	Series term (m_j)
1	4.39	1
2	7.33	1
3	16.15	2
4	23.55	1
5	26.15	2
6	32.39	3
7	45.15	2
8	50.67	3
9	50.71	4
10	54.84	1
11	63.05	3
12	69.68	5
13	73.51	4
14	78.46	1
15	82.62	4
16	83.70	2
17	88.63	6
18	90.82	5
19	96.70	3
20	101.80	1

5.7.2 Forced Vibration Analysis of Slab-on-girder and Box Girder Bridges

For the dynamic response analysis a vehicle with the following properties were chosen:

Sprung mass = 30189 Kg

Unsprung mass = 4209 Kg

Natural frequency = 2.2 Hz

Damping = 0.0

A vehicle velocity of120 km/ hr is used and bridge damping is not included in the analysis. The static and dynamic deflections at center of mid-span of the bridges and the deflection magnification factor are reported in Tables 5.3 and 5.4.

TABLE 5.3

Static and Dynamic Deflections and Deflection Magnification Factor at Center of Mid-span of Slab-on-girder Bridge (Figure 5.1)

W_{static} (mm)	$W_{dynamicc}$ (mm)	$W_{dynamic}/W_{static}$
3.17	3.68	1.16

TABLE 5.4

Static and Dynamic Deflections and Deflection Magnification Factor at Center of Mid-span of Box Girder Bridge (Figure 5.2)

W_{static} (mm)	$W_{dynamicc}$ (mm)	$W_{dynamic}/W_{static}$
2.21	2.42	1.10

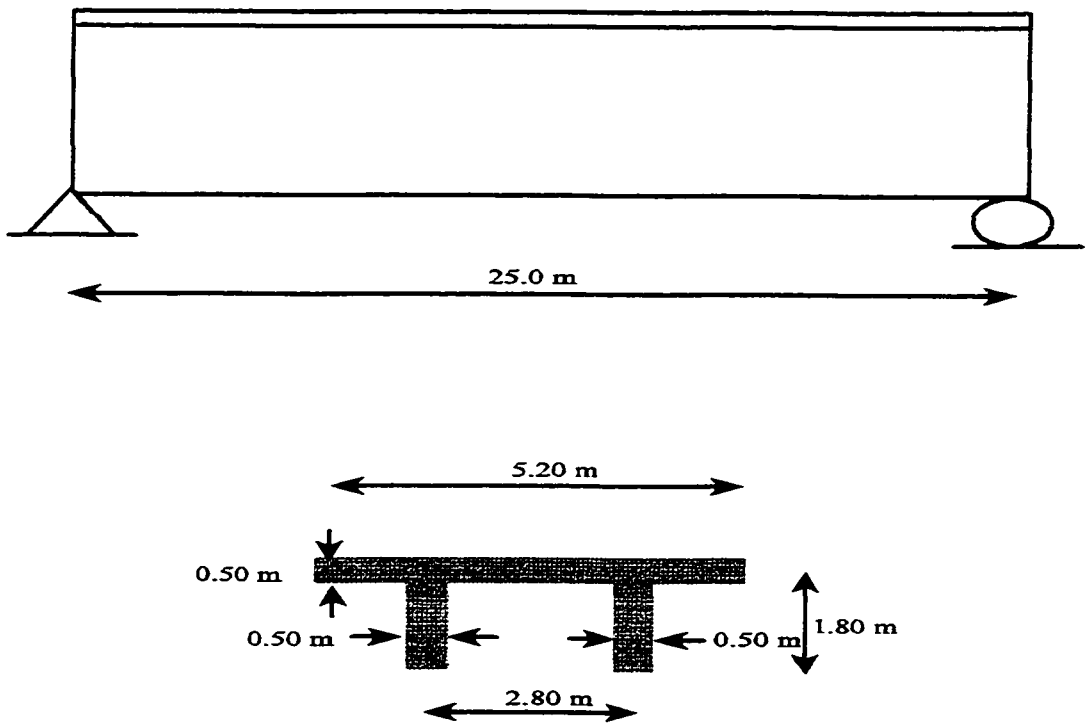

Figure 5.1 Slab-on-Girder Bridge

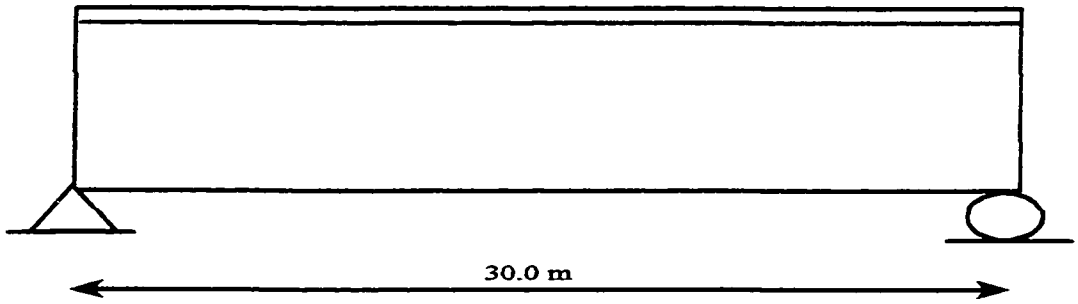

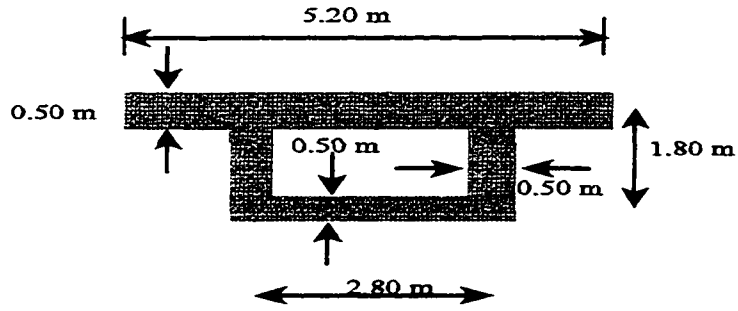

Figure 5.2 Box-Girder Bridge

Chapter 6

CONCLUSIONS AND RECOMMENDATIONS

6.1 Conclusions

The finite strip has been applied to dynamic analysis of slab bridges, slab-on-girder bridges, box girder bridges and multi-span beam and slab bridges. Some beam and plate examples were carried out to compare them with some existing in the literature and in all cases very good agreements were observed.

Four different vehicle models were used in this study to illustrate the impact of vehicle model on bridge response and by following the same procedure more complex vehicle models can readily be adopted. Single axle vehicle models generally produce higher deflection magnification factors than two-axle vehicle models. So multi-axle vehicles cannot be idealized as single axle vehicle models. Multi-axle vehicles can be modeled by multi sprung masses traveling in sequence without compromising the accuracy of the results. The deflection magnification factor of multi-span bridges is usually lower than that of single span bridges.

The accuracy of the solution depends on the number of modes used in the analysis. More modes are required for convergence of moments than deflections. The number of modes sufficient for accurate solution should at least include the third harmonic. Bridges that have very large ratios of longitudinal to transverse bending rigidities require more vibration modes to include higher harmonic terms. When many modes are required in the analysis subspace vector iteration is superior to inverse vector iteration with Gramm-Schmidt orthogonalization. Since the later introduce an accumulation of round-of errors which leads to a progressive deterioration of the accuracy in computed modes. Oscillatory convergence has been observed during mode iteration of multi-span bridges.

6.2 Recommendations

The finite strip method may be extended to dynamic analysis of bridges that have boundary conditions other than simple supports.

The finite strip method may be extended to dynamic analysis of skew bridges, curved bridges and cable-stayed bridges.

The compound finite strip method may be employed for dynamic analysis of bridges with discrete internal supports, attached beams and columns.

Parametric study of bridge responses may be carried out by employing finite strip method or

compound finite strip method. Different vehicle load models may be adopted and their effect on the responses of bridges with various span lengths may be explored.

REFERENCES

1. Cheung, Y. K. The Finite Strip Method in the Analysis of Elastic Plates with Two Opposite Simply Supported Ends. Proc. Inst. Civ. Engrs., Vol. 40, pp. 1-7. Dec.1968.
2. G. H. Powell and D. W. Ogden, Analysis of Orthotropic steel plate bridge decks. Proc. ASCE, Vol. 95, No. ST5, pp. 909-922, May, 1969.
3. J. W. Smith, Finite Strip Analysis of the Dynamic Response of Beam and Slab Highway Bridges, Earthq. Eng. Struct. Dyn., 1, pp. 357-370, 1973.
4. Y. K. Cheung, Analysis of Box Girder Bridges by Finite Strip Method. Proc. Second Int. Symposium on concrete Bridge Design, Chicago, ACI Publications Sp 26, pp. 357-378, April, 1969
5. Y. K. Cheung, Finite Strip Method Analysis of Elastic Slabs. Proc. ASCE, Vol. 94, No. EM6, pp. 1365-1378, Dec., 1968.
6. Y. K. Cheung and M. S. Cheung, Analysis of Curved Box Girder Bridge by Finite Strip Method. IABSE Publications. Vol. 31 / I, pp. 1-19, 1971.
7. M.S. Cheung, Y. K. Cheung and A. Ghali, Analysis of Slab and Girder Bridges by the Finite Strip Method. Building Science, Vol. 5, No. 2, pp. 95-105, Oct. 1970.
8. Y. C. Loo, Analysis of Continuous Highway Box Bridge with Intermediate Stiffening, Eighth Aust. Road Res. Board Conf. pp. 13-20, 1976.
9. M. S. Cheung, Y. K. Cheung and D. V. Reddy, Frequency Analysis of Certain Single and Continuous Span Bridges, Development in Bridge Design and Construction, pp. 188-199,

Crosby Lockwood, 1971.

10. M. S. Cheung and Y. K. Cheung, Flexural Vibrations of Rectangular and other polygonal Plates , proc. ASCE, Eng. Mech. Div., 97 (EM2), pp. 391-411, 1971.
11. T.G. Brown and A. Ghali, Finite Strip Analysis of Skew Slabs, Proc. McGill-EIC Conference in Finite Element Method in Civil Engineering, pp. 1141-1151, 1972.
12. C. Delcourt and Y. K. Cheung, Finite Strip Analysis of Continuous Folded Plates, Proceedings, International Association of Bridge and Structural Engineers, pp. 1-16, May, 1978.
13. C.I. Wu and Y. K. Cheung, Frequency Analysis of Rectangular Plates Continuous in One or Two Directions, Earthquake Engineering and Structural Dynamics, Vol.3, 1974.
14. M. S. Cheung and Wenchang Li, Analysis of Haunched, Continuous bridges by Finite Strips, Computers, Vol. 28, No. 5, pp. 621-626,1988.
15. M. S. Cheung and Wenchang Li and L. G. Jaeger, Nonlinear Analysis of Cable-stayed Bridge by Finite Strip Method, Computers and Structures, Vol. 29, 1990.
16. M. S. Cheung and Wenchang Li, Analysis of Haunched, Continuous bridges by Finite Strips, Journal of Structural Engineering, ASCE, Vol. 115, No. 5, pp. 1076-1087, May, 1989.
17. M. S. Cheung, W. Li and S. E. Chidiac, Finite Strip Analysis of Bridges, E & FN SPON, London, 1996.
18. Y. K. Cheung, Finite Strip Method in Structural Analysis, Pergaman Press, 1976.
19. Y. C. Loo and A. R. Cusens, The Finite Strip Method in Bridge Engineering, A Viewpoint Publication, 1978.
20. M. S. Troitsky and A. K. Azad, Analysis of Orthotropic steel bridge decks by a stiffness method. Proc. Inst. Engrs., Part 2, Vol. 55, pp. 447-462, June, 1973.
21. R. D. Cook, D. S. Malkus and M. E. Plesha, Concepts and Applications of Finite Element

Analysis, 3rd edn., John Wiley & Sons, New York, 1989.

22. Klaus-Jurgen Bathe, Finite Element Procedures, 2nd edn., Prentice Hall, New Jersey, 1996.

23. J. L. Humar, Dynamics of Structures, Prentice Hall, New Jersey, 1990.

24. S. Timoshenko and S. Woinowsky-Krieger, Theory of Plates and Shells, 2nd edn., McGraw-Hill Book Company Inc., 1959.

25. S. Timoshenko and J. N. Goodier, Theory of Elasticity, 3rd edn., McGraw-Hill Book Company Inc., 1970.

26. R. Jategaonkar, L. G. Jaeger and M. S. Cheung, Bridge Analysis Using Finite Elements, The Canadian Society for Civil Engineering, Desktop Monograph Series, 1985.

27. Biggs, J. M., Suer, H. S. and Louw, J. M., "Vibration of Simple-span Highway Bridges", ASCE Trans., 124, (2979), 1959, pp. 291-318.

28. R. W. Clough and J. Penzien, Dynamics of Structures, McGraw-Hill Book Company Inc., 1970.

29. D. J. Gorman, Free Vibration Analysis of Rectangular Plates, Elsevier North Holland Inc, 1982.

30. A. C. Scordelis, Analytical Solution for box girder bridges. Development in bridge design and construction, pp.200-216, Crosby Lockwood, 1971.

31. A. R. Cusens and R. P. Pama, Distribution of Concentrated Loads on Orthotropic Steel Bridge Decks. The Structural Engineer, Vol. 47(9), pp. 277-285, Sept., 1969.

32. E. S. Eichman, Note on the Auxiliary Effect of a Moving Force on a Simple Beam, Journal of Applied Mechanics, December, 1953, p. 562.

33. R. S. Ayre, F. Ford and L. S. Jacobsen, Transverse Vibration of a Two-span Beam under Action of a Moving Constant Force, J. Appl. Mech., Trans. ASME, 17 (1), 1950, pp.1-12

34. J. F. Fleming and J. P Romualdi, Dynamic Response of Highway Bridges, ASCE J. Struc.

Div, 87(ST), 1961, pp. 31-61

35. F. V. Filho, Finite Element Analysis of Structures Under Moving Loads, ShViDi, Vol. 10, No. 8, 1978, pp. 27-35.

36. D. M. Yoshida, Dynamic Response of Beams and Plates to Moving Loads, Ph. D. Thesis, Standford University, Standford, 1970.

37. W. Li, Linear and Nonlinear Finite Strip Analysis of Bridges, Ph. D. Thesis, University of Ottawa, Ottawa, 1991.

38. A. Megnounif, Parametric Study on Human Response to Vibrations of Box Girder Bridges, M. Eng. Thesis, University of Ottawa, Ottawa, 1988.

39. A. M. Kashif, Dynamic Response of Highway Bridges to Moving Vehicles, Ph. D. Thesis, Carleton University, Ottawa, 1992.

40. N. M. Newmark, A method of Computation of Structural dynamics, Journal Eng. Mech. Div., ASCE, No. EM3, proc. Paper, 2094, July, 1959, pp. 67-94.

41. K. T. Sundara Raja Iyengar and K. S. Jagadish, Dynamic Response of Beam and Slab Bridges to Moving Forces, Intl. Assoc. Bridge Struc. Eng., Vol. 28 (II), 1968, pp. 69-86.

42. K T Sundara Raja Iyengar and K. S. Jagadish, Dynamic Response of Highway Bridges to Moving Loads, Intl. Assoc. Bridge Struc. Eng., Vol. 20 (II), 1970, pp. 57-76.

43. A. S. Velestos and T. Huang, Analysis of Dynamic Response of Highway Bridges to Moving Loads, ASCE J. Eng. Mech. Div. 96 (EM5), 1970, pp. 593-620.

44. Chaudhuri, S. K., "Dynamic Response of Horizontally Curved I-Girder Highway Bridges Due to a Moving Vehicle", A Dissertation presented to University of Pennsylvania in Partial Fulfillment of the requirements for the degree of Doctor of Philosophy, 1975.

45. Wills, R., "Report on the commissioners Appointed to Inquire the Application of Iron to Railway Structural Appendix", H. M. Stationery Office, London, 1849.

46. Stokes, G. G., "Discussion of a Differential Equation Related to the Breaking of Railway

Bridges", Trans. Cambridge Phil. Soc., Vol. 8, Part 5, 1887, pp. 707-735.

47. Tung, T. P., Goodman, L. E., Chen, T. Y., and Newmark, N. M., "Highway Bridge Impact Problems", International Journal for Numerical Methods in Engineering, Vol. 7, 1973, pp. 175-183.

48. Hillerborg, A., "A study of Dynamic Influence of moving loads on Girders", 3rd Congress, Intl. Assoc. Bridge Struct. Engr., Prelim. Publ., 1948, pp. 661-667.

49. Jeffcot, H. H, "On the Vibration of Beams under the Action of Moving Loads", Philosophical Magazine, 8 (48), 1929, pp. 66-97.

50. Raizadeh, R. and Shore, S., "Dynamic Analysis of Curved Box Girder Bridges", ASCE Journal of Structural Division, September 1975, pp. 1898-1912.